Development of Modified Cuckoo Search Algorithm to Optimize WEDM Process and Prediction of Geometrical Errors and Surface Integrity while Machining Nickel based Super Alloys

Submitted in partial fulfillment of the requirements

for the award of the degree of

Doctor of Philosophy

by

M. Sreenivasa Rao

Roll No. 701241

Under the Guidance of

Dr. N. Venkaiah

DEPARTMENT OF MECHANICAL ENGINEERING

NATIONAL INSTITUTE OF TECHNOLOGY WARANGAL

April 2016

Dedicated to my wife Priyadarsini,

my daughter Joshitha, my son Rohan

and my parents

THESIS APPROVAL FOR Ph.D.

This thesis entitled **"Development of Modified Cuckoo Search Algorithm to Optimize WEDM Process and Prediction of Geometrical Errors and Surface Integrity while Machining Nickel based Super Alloys"** by **Mr. M. Sreenivasa Rao** is approved for the degree of Doctor of Philosophy.

Examiners

_____

_____

_____

Supervisor

Dr. N. Venkaiah

Assistant Professor, Mechanical Engineering Department, NIT Warangal

Chairman

Prof. C. S. P. Rao

Head, Mechanical Engineering Department, NIT Warangal

DEPARTMENT OF MECHANICAL ENGINEERING
NATIONAL INSTITUTE OF TECHNOLOGY
WARANGAL

CERTIFICATE

This is to certify that the thesis entitled "**Development of Modified Cuckoo Search Algorithm to Optimize WEDM Process and Prediction of Geometrical Errors and Surface Integrity while Machining Nickel based Super Alloys**" submitted by **Mr. M. Sreenivasa Rao**, Roll No. 701241, to **National Institute of Technology, Warangal** in partial fulfillment of the requirements for the award of the degree of **Doctor of Philosophy in Mechanical Engineering** is a record of bonafide research work carried out by him under my supervision and guidance. This work has not been submitted elsewhere for the award of any degree.

Dr. N. VENKAIAH
(Supervisor)
Assistant Professor
Department of Mechanical Engineering
National Institute of Technology
Warangal-506004

DECLARATION

This is to certify that the work presented in the thesis entitled "**Development of Modified Cuckoo Search Algorithm to Optimize WEDM Process and Prediction of Geometrical Errors and Surface Integrity while Machining Nickel based Super Alloys**", is a bonafide work done by me under the supervision of **Dr. N. Venkaiah**, Assistant Professor, Department of Mechanical Engineering, NIT Warangal, India and has not been submitted for the award of any degree to any other University or Institute.

I declare that this written submission represents my ideas in my own words and where ever others ideas or words are included have been adequately cited and referenced with the original sources. I also declare that I have adhered to all principles of academic honesty and integrity and have not misrepresented or fabricated or falsified any idea/data/fact/source in my submission. I understand that any violation of the above will cause for disciplinary action by the institute and can also evoke penal action from the sources which have thus not been properly cited or from whom proper permission has not been taken when needed.

M. SREENIVASA RAO

(Roll No. 701241)

Acknowledgements

To begin with most influencing factor of this piece of work, it is my proud privilege to express my deep sense of reverence and gratitude to my supervisor, **Dr. N. Venkaiah** for his excellent supervision, skilled guidance, unfailing support, stimulating discussions, critical evaluation and constant encouragement during this dissertation work. I have learned a lot and improved my skills under his valuable guidance. I thank him for his time and efforts for making me a better researcher. During my Ph.D. tenure he has been more than a guide and a source of inspiration. I am extremely thankful to him for spending his valuable time in spite of his busy schedule.

I am very much thankful to **Prof. C.S.P. Rao**, Head, Mechanical Engineering Department for his support and also valuable suggestions in the area of optimization. I also express my deep sense of gratitude to my doctorial scrutiny committee members, **Prof. A. Venu Gopal**, Mechanical Engineering Department, **Dr. A. Kumar**, Mechanical Engineering Department and **Dr. N. Narasaiah**, Metallurgy and Materials Engineering Department for their constructive and encouraging suggestions during my research work. I express my sincere thanks to **Prof. T. Srinivasa Rao,** Director NIT Warangal, for providing me the facilities and supporting the research work by providing Research Seed Money.

Portion of this research was funded by MHRD, Government of India, Department of Science & Technology under fast track scheme for young scientists. I am thankful for funding this research for procuring WEDM machine which helped me to carry-out experimental investigations within the campus.

My special thanks to everyone who assisted me in my research work especially:

- **Prof. L. Krishnanand**, Mechanical Department, NITW for all his support and encouragement.
- **Dr. A. V. Naresh Babu,** Electrical Department, DVR & Dr. HS MIC College of Technology, Kanchikacherla, Krishna district, A.P., for his help in programming using MATLAB.
- **Dr. R. Satish Babu**, Biotechnology Department, NITW for providing me guidance in Neural network.

I would like to express my sincere thanks to the management of my parent institute **DVR & Dr. HS MIC College of Technology**, Kanchikacherla, Krishna district, A.P., for their encouragement by giving me an opportunity to do this work.

I always remember the advices and help offered by my senior research scholar Dr. A. Varun. I also express my sincere thanks to all my fellow scholar friends N. Shiva Kumar, K. Kishore Kumar, M. Sandeep Kumar, A. Manmadha Chary, P.Naresh, B. Durga Hari Kiran, M. Vishnu Prasad, Koteswara Rao, T. Kiran Kumar and D. Sarathchandra with whom I laughed my heart out during my stay at NIT Warangal. I am also greatly thankful to foreman Mr. Yellaswami for his helping hand at workshop. I also wish to thank Mr. Ilaiah and Mr. Raju lab technicians in production engineering section for their help.

Lastly, I owe a special thanks to my wife, daughter, son, parents, brothers and sisters for their love and encouragement without which I never would have imagined myself to pull it this far.

- M. Sreenivasa Rao

ABSTRACT

Machining is the process of removal of unwanted material to give a desired size and shape to the components. Usage of super alloys are increasing day-by-day in various engineering applications such as aircraft, power-generation turbines, rocket engines, automobiles, nuclear power, and chemical processing plants etc. Machining of Nickel based super alloys using conventional machining processes is very difficult due to their high hardness even at elevated temperatures and also low thermal conductivity. Wire cut electrical discharge machining (WEDM) is one of the widely used advanced machining processes to machine any electrically conductive material, irrespective of its hardness. Due to its stochastic nature, WEDM process is difficult to understand and analyze. Hence some specific aspects of the process such as modeling of material removal rate, surface roughness, geometrical errors, recast-layer thickness and micro hardness and influence of various process parameters on these responses need to be studied thoroughly.

Identification of optimal values for material removal rate and surface roughness is essential from productivity and quality viewpoints. Cuckoo search (CS) algorithm was found to be efficient in yielding the global optimal value and this algorithm was found to outperform genetic algorithm (GA) and particle swarm optimization (PSO) techniques. In order to improve the performance of cuckoo search further, an attempt has been made in the present work to propose a modified cuckoo search involving two-stage initialization. Benchmark functions have been used to test the performance of the proposed method. Furthermore, the proposed method has been applied to WEDM process and was found to be accurate and fast as compared to the existing cuckoo search. The machining data generated in this work for Inconel-690 and Nimonic-263 materialswill also be useful to the industry.Further, in order to optimize material removal rate and surface roughness simultaneously, a non-dominated sorting principle has been applied to the proposed algorithm and pareto-optimal sets are also generated.

Machining of axi-symmetrical components of desired quality using WEDM on materials such as Inconel-690 and Nimonic-263 is a challenging task. Prediction of geometrical errors such as circularity and cylindricity in WEDM is difficult due to stochastic nature of the process. Hence, a study on influence of process parameters and accurate prediction of geometrical errors is very much essential for the manufacturer in order to reduce the rejection rate of the parts during inspection. Investigations on the influence of process

parameters on the geometrical errors are carried out in this work. In order to predict geometrical errors accurately, modelsare also developed for the first time to estimate these errors using a feed forward back propagated neural network. Predicted results of the models are validated against the experimental values. It has been found that the developed modelsare predicting the geometrical errors with acceptable deviation.

Though the WEDM is used to cut hard materials, one of themajor disadvantages of this process is formation of recast layeras it affects the properties of the machined surfaces. In the present study experimental investigation has been carried out to study the effect of process parameters on micro-hardness and recast layer while machining Inconel-690 and Nimonic-263 materials.Interestingly, hardness of the machined surface was found to be lower than that of the bulk material. The micro-hardness and recast layer thickness are inversely related to the variation of process parameters. The research findings and the data generated for the first time on hardness and recast layer thicknessfor Inconel-690 and Nimonic-263 will be useful to the industry.

Keywords: Wire Electrical Discharge Machining, Modified cuckoo search algorithm, Neural networks, Geometrical errors, Recast-layer thickness, Micro-hardness.

CONTENTS

LIST OF FIGURES

LIST OF TABLES

ABBREVIATIONS

ANOVA	Analysis of variance
ABC	Artificial bee colony
ANN	Artificial neural network
BPNN	Back propagated neural network
CCD	Central composite design
CMM	Coordinate measuring machine
CS	Cuckoo search
DE	Differential evolution
EDS	Energy-dispersive X-ray spectroscopy
GA	Genetic algorithm
GP	Genetic programming
GRA	Grey relational analysis
LSC	Least squares circle
MRR	Material removal rate
MIC	Maximum inscribed circle
MMC	Metal matrix composites
MH	Micro-hardness
MCC	Minimum circumscribed circle
MZC	Minimum zone circles
MCS	Modified cuckoo search
MRSN	Multi response signal to noise ratio

NSMCS	Non dominated sorting modified cuckoo search
NSGA	Non-dominated sorting genetic algorithm
PSO	Particle swarm optimization
RLT	Re-cast layer thickness
RSM	Response surface methodology
SEM	Scanning electron microscopy
SFL	Shuffled frog leaping algorithm
SA	Simulated annealing
SR	Surface roughness
TWR	Tool wear rate
WPC	Weighted principle component
WEDM	Wire cut electrical discharge machine

NOMENCLATURE

α	Constant generated randomly between -1 and 1
(x_0, y_0, r_0)	Least squares circle parameters
D	Diameter of the hole
d	Diameter of the boss
Δ	Cylindricity/ Circularity error
ΔV	Vector of adjustments
e_i	Deviation between the measured point and the reference circle
e_k	Deviation of k^{th} point from assessment cylinder
e_{max}	Maximum deviation
e_{min}	Minimum deviation
Fit_p	Fitness value of an individual particle
I_p	Peak current
J	Jacobian matrix
K	Index for data points
K	Vector of residuals
l_0, m_0	Slope values
N	Number of data points
Ncv	Number of control variables
Nhn	Number of host nests
p, f	Particle or host nest numbers
p_a	Probability for an egg to be identified by host bird
$P_i\ (x_i, y_i, z_i)$	Coordinates of i^{th} point
Ps	Population size
Pv	Population vector
r_0	Radius of the assessment cylinder/circle
s_{pq}	Step size of q^{th} variable for p^{th} particle
S_v	Servo voltage
T	Machining time
T_{off}	Pulse off time
T_{on}	Pulse on time
W_t	Thickness of work piece

x_0, y_0	Trace coordinates of axis of the assessment cylinder
x_{ij}	Value of j^{th} variable in i^{th} particle
x_j^{max}	Upper bound for j^{th} variable
x_j^{min}	Lower bound for j^{th} variable
$x_{pq}(t)$	Value of q^{th} variable in p^{th} host nest at current generation, t
$x_{pq}(t+1)$	Value of q^{th} variable in p^{th} host nest at next generation
Z	Interval between sections
z_j	Height of j^{th} section
λ	Constant generated randomly between 1 and 3

CHAPTER 1

INTRODUCTION

1.1. General

Owing to increase in the usage of nickel based alloys due to their superior properties such as high temperature hardness and resistance to oxidation and corrosion, it is essential to know the machining behavior of these materials. They have great demand in nuclear and aerospace applications as they retain their mechanical and physical properties at temperature over 700 °C. They are difficult to machine because, of their high shear strength, work hardening and precipitation hardening. High abrasive particles in their microstructure and tendency to form built up edge (BUE) make them more difficult to machine. Friction between tool and material and its low thermal conductivity results in high temperature generation. Cutting tool material undergoes severe thermal and mechanical changes because of high heat generation. The temperature produced at tool tip results in rapid tool wear; reduce the life of the tool. Dimensional variations of the product cause due to tool wear. Tool failure occur mainly because of combination of problems like high temperature produced, high material strength, work hardening of alloys, abrasive chips formation and very large amount of heat generation. Due to these reasons a search for an alternative machining process led to find the pathway for a new advanced machining processes.

Wire-cut electrical discharge machining (WEDM) is one of the most emerging non conventional manufacturing processes for machining hard to cut materials and intricate shapes which are very difficult to machine with conventional machining methods. The ability to produce intricate profiles on materials irrespective of the mechanical properties made this process to be widely used in industries. WEDM process is generally used in tool and dies industry where accuracy and surface finish is of great importance. WEDM has the capability to impart production accuracy in the range of ± 2.5 µm. WEDM is used for machining of newer and difficult to machine materials, such as hardened steel, high-strength, temperature-resistant alloys and fiber-reinforced composites in aerospace, nuclear, missile, turbine, automobile, and tool and die making industries. This process enables machining of any type of feature such as deep, blind, inclined and micro holes and complicated profiles. The important WEDM responses are material

removal rate, surface roughness, kerf, crater size, wire wear rate, recast layer thickness and micro hardness. In the present work experiments are carried out on super alloys such as Inconel-690 and Nimonic-263 using WEDM to study and develop the mathematical models for various WEDM responses such as material removal rate (MRR), surface roughness (SR), geometrical errors, re-cast layer thickness (RLT) and micro-hardness (MH).

This chapter introduces the super alloys with their applications, chemical compositions and properties, advanced machining processes and principle of WEDM. This chapter also describes the design of experiments and lastly organization of the thesis is presented.

1.2. Super alloys

The term "super alloy" is applied to alloys, which can have very high temperature strength and oxidation resistance. Nickel-based super alloys are a special class of materials with an exceptional combination of high temperature strength, toughness, and resistance to degradation in corrosive or oxidizing environments. Super alloys are the primary materials used in the hot portions of jet turbine engines, such as the blades, vanes, and combustion chambers, constituting over 50% of the engine weight as shown in Figure 1.1. Super alloys are also used in other industrial applications where their high temperature strength and/or corrosion resistance is required. These applications include rocket engines, steam turbine power plants, reciprocating engines, metal processing equipment, heat treating equipment, chemical and petrochemical plants, pollution control equipment, coal gasification and liquification systems, and medical applications. The Nickel based super alloys can be used up to an operating temperature of 1230 ^{0}C and is shown in Figure 1.2.

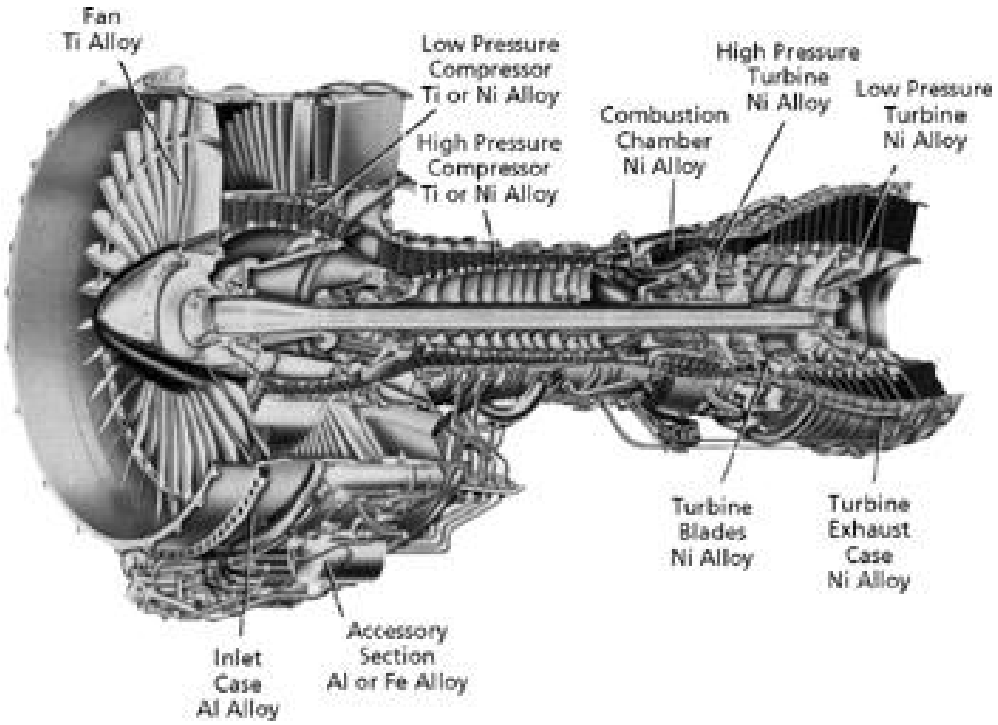

Figure 1.1 Typical material distributions in jet engine

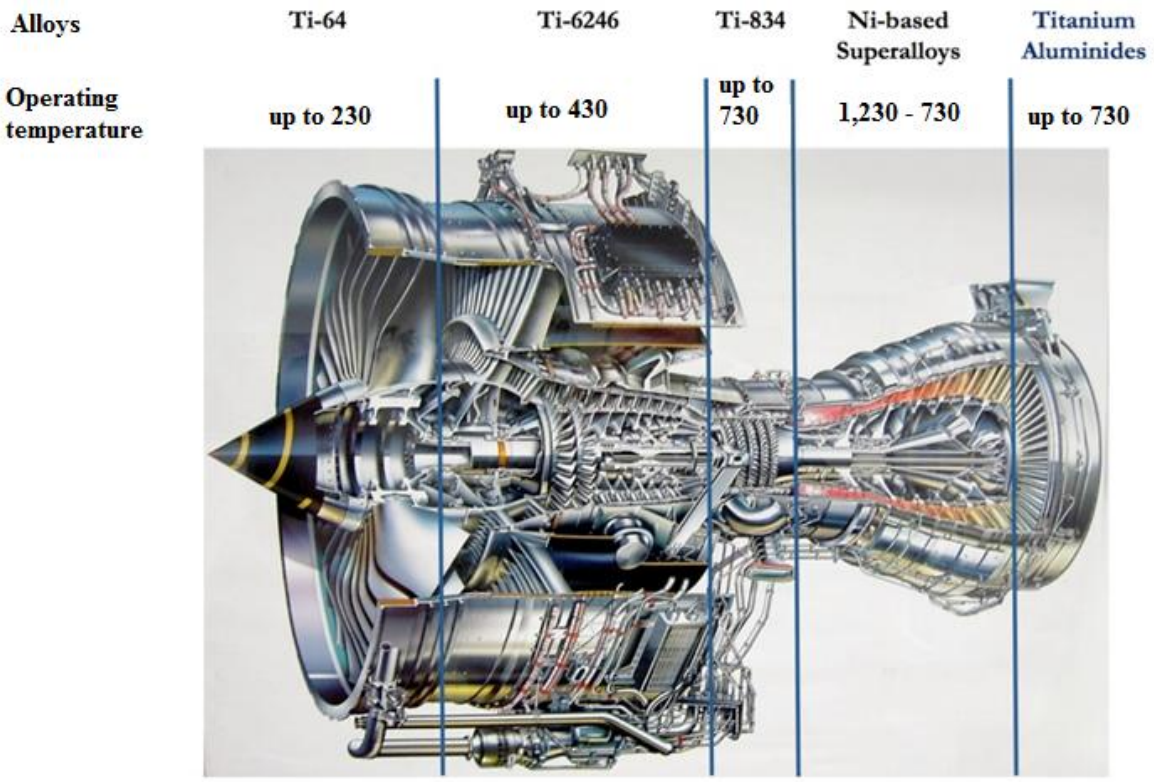

Figure 1.2 Operating temperatures of super-alloys

Machining of these materials using conventional machine tools is very difficult due to their high hardness and low thermal conductivity. A large amount of cutting force is required for these materials due to their high hardness; a reasonable amount of heat is generated. Due to low thermal conductivity, accumulation of temperature at tool and work, and tool and chip interface leads to increase of tool wear and surface roughness. Due to these reasons conventional machines are not encouraged to machine super alloys. Wire-cut EDM, one of the advanced machining processes, is an alternative process to machine this kind of materials and produce intricate shapes which are not possible with conventional machining methods.

1.2.1. Inconel-690

It is a high-chromium nickel based super alloy having excellent properties such as hardness and corrosive resistance at high temperature atmospheres. Due to its superior properties it is widely used for steam generator tubes, baffles, tube sheets, and hardware in nuclear power generation. The chemical composition in % of weight has been given in Table 1.1. Physical and thermal properties of the Inconel-690 are given in the Table 1.2

Table 1.1 Chemical composition of Inconel-690 in % of weight

Element	**% of weight**	**Element**	**% of weight**
Nickel	60.0	Chromium	29.58
Ferrous	9.05	Carbon	0.017
Silicon	0.25	Manganese	0.21
Sulphur	0.0013	Copper	0. 01
Titanium	0.2	Niobium	0.02

Table 1.2 Properties of Inconel-690 alloy

Density	8.19 g/cm^3
Melting range	1343-1377 ^0C
Electrical resistivity	1.15 μΩ-m
Specific heat capacity	0.450 J/g- ^0C
Thermal conductivity	13.5 W/m-K
Hardness	221 HV

1.2.2. Nimonic-263

It is a nickel-chromium-cobalt-molybdenum alloy specially meant for use in high temperature and high strength applications. This material is mainly used in gas turbine hot section components. The chemical composition in % of weight has been given in Table 1.3. Physical and thermal properties of the Inconel-690 are given in the Table1.4

Table 1.3 Chemical composition of Nimonic-263, in % of weight

Element	**% of weight**	**Element**	**% of weight**
Nickel	51.44	Chromium	20.0
Ferrous	0.25	Carbon	0.043
Silicon	0.04	Manganese	0.43
Sulphur	0.005	Copper	0.002
Titanium	2.2	Niobium	0.02
Aluminum	0.48	Cobalt	19.5
Molybdenum	5.6	Oxygen	0.0022
Nitrogen	0.0031	Phosphorous	0.005

Table 1.4 Properties of Nimonic-263 alloy

Density	8.36 g/cm^3
Melting range	1300-1355 ^0C
Electrical resistivity	1.148 μΩ-m
Specific heat capacity	0.461 J/g - ^0C
Thermal conductivity	11.7 W/m-k
Hardness	350 HV

1.3. Machining process – EDM

Machining is simply a process of removing unwanted material to provide the required shape and size to an object using a machine tool. The machining processes are broadly divided into two groups and they are conventional machining processes and advanced machining processes. In conventional machining process, there is a direct contact between tool and work material, and a large force is applied to remove the material in the form of chips. To meet this, cutting tool required is harder than that of workpiece and also a firm fixing of both material and tool are required in conventional machining. Huge amount of heat is generated at cutting tool and work material and also at tool and chip interface. This leads to decrease in tool life, and surface finish.

Now a days, different materials are emerging in the industry to meet special applications such as high hardness at elevated temperatures, high resistance to corrosion, oxidation and friction. Nickel based super alloys come under this category and are used extensively in automobile, aeronautics and nuclear power generation applications. Machining of these materials with conventional machining processes like turning, milling, drilling etc. is very difficult due to their superior properties such as high hardness and low thermal conductivity. Further, these

conventional methods cannot be used where complex shapes, low tolerances and good surface finish are required. Therefore to machine these hard to cut materials, advanced machining processes are developed. There are different advanced machining processes and are grouped into three basic categories based on type of energy required as shown in Figure 1.3.

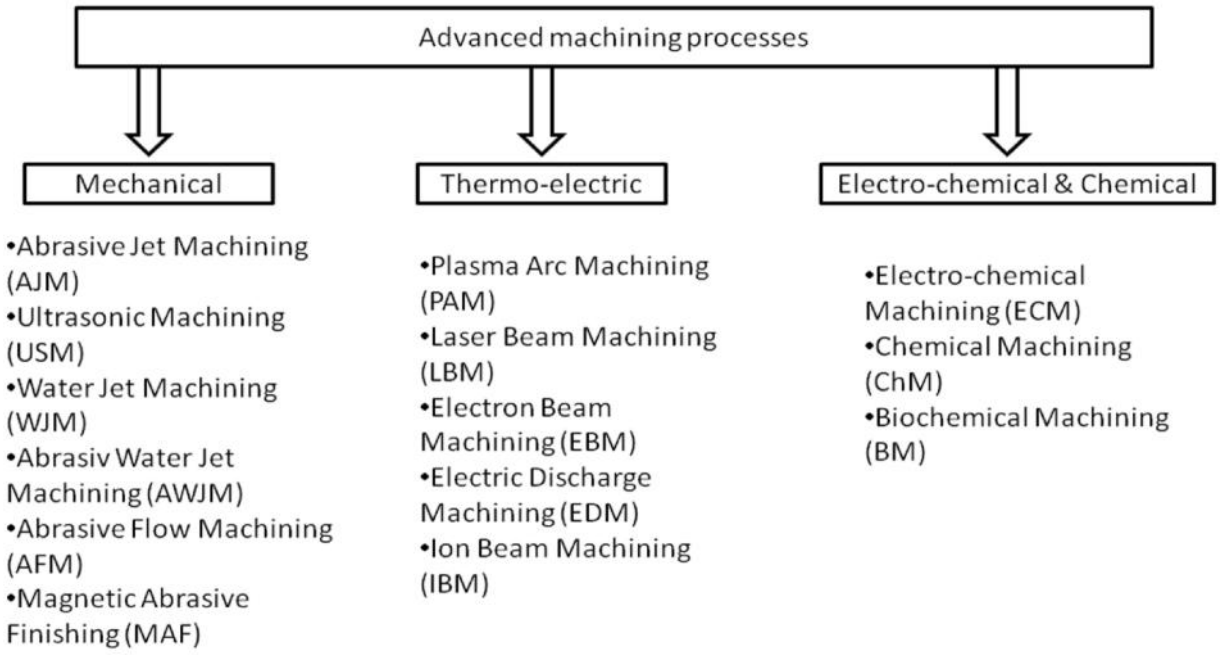

Figure 1.3 Classification of advanced machining processes

At all machining situations, none of these processes is the best. Therefore, selection appropriate machining process is important for a given situation. The comparative study of various advanced machining processes, in terms of material removal rate with respect to power consumption are presented, in Figure 1.4. It can be found that the power consumption rates of EDM, MCG and PAM are less as compared to other advanced machining processes. The EDM has the capability to machine electrically conductive materials irrespective of their hardness. EDM has the lower capital cost and produces components with higher surface finish. Further WEDM can be used to produce intricate shapes and also WEDM can cut up to 300 mm thick plates. Due to these reasons WEDM has been selected in the present work to machine super alloys.

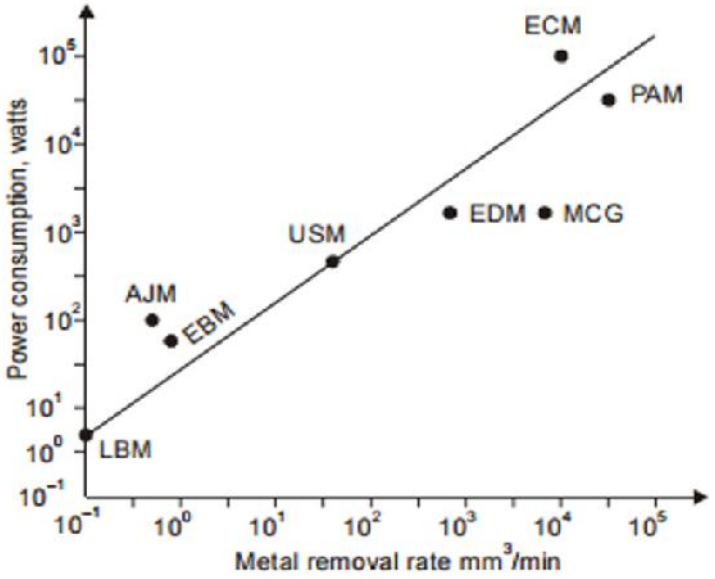

Figure 1.4 Comparison of various machining processes on mean power consumption with MRR (Singh, 2010)

There are two types of EDM processes and are differentiated by usage of electrode.

1. Die-sinking EDM and
2. Wire-cut EDM

1.3.1. Die-sinking EDM

The die-sinking EDM is widely used in mould and die making industry in machining complex die cavities for producing plastic injection-molded parts and die-cast parts. A copper or graphite tool electrode is normally used in the process and the workpiece (normally a mould or die) to be machined is immersed in dielectric fluid. Electrode of die-sinking EDM is the replica of the part to be machined. By switching DC voltage supply to the tool electrode and workpiece, high frequency electrical sparks will be generated (Guitrau, 1997) such that very high temperatures of the order of 12000^0 C developed locally will melt and vaporize (DiBitonto et al., 1989; Patel et al., 1989) the workpiece to form the required cavity.

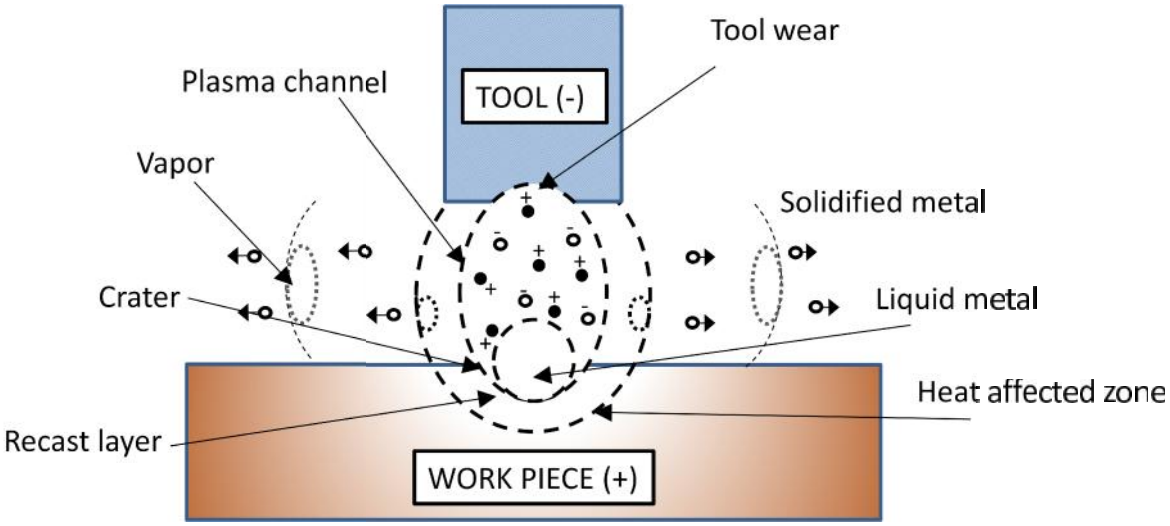

Figure 1.5 EDM working principle

1.3.2. Wire - EDM

WEDM is a thermo- electrical process in which material is removed by a series of sparks between workpiece and wire electrode (tool). The workpiece and wire are immersed in a dielectric (electrically non-conductive) fluid, usually de-ionized water, which also acts as a coolant and flushes the debris away. The material to be cut must be electrically conductive. In WEDM, there is no direct contact between workpiece and tool (wire) as in conventional machining process, therefore materials of any hardness can be machined and minimum clamping pressure is required to hold the workpiece (Kuriakose and Shanmugam, 2004). In this process, the material is eroded by a series of discrete electrical discharges between the workpiece and tool. When the material approaches the electrode and the gap reaches a certain threshold value, the insulating liquid breaks down and discharging channel forms thereby sparks are generated resulting in high temperature instantaneously up to about 10000º C. These temperatures are huge enough to melt and vaporize the workpiece metal and the eroded debris cool down swiftly in working liquid and flushed away. The working principle is shown in the figure 1.6. In 1969, the Swiss firm Agie produced the world's first wire EDM machine. These early machines were extremely slow but today, machines are equipped with automatic wire threading and can cut over 20 times faster, (Carl and Steev, 2005).

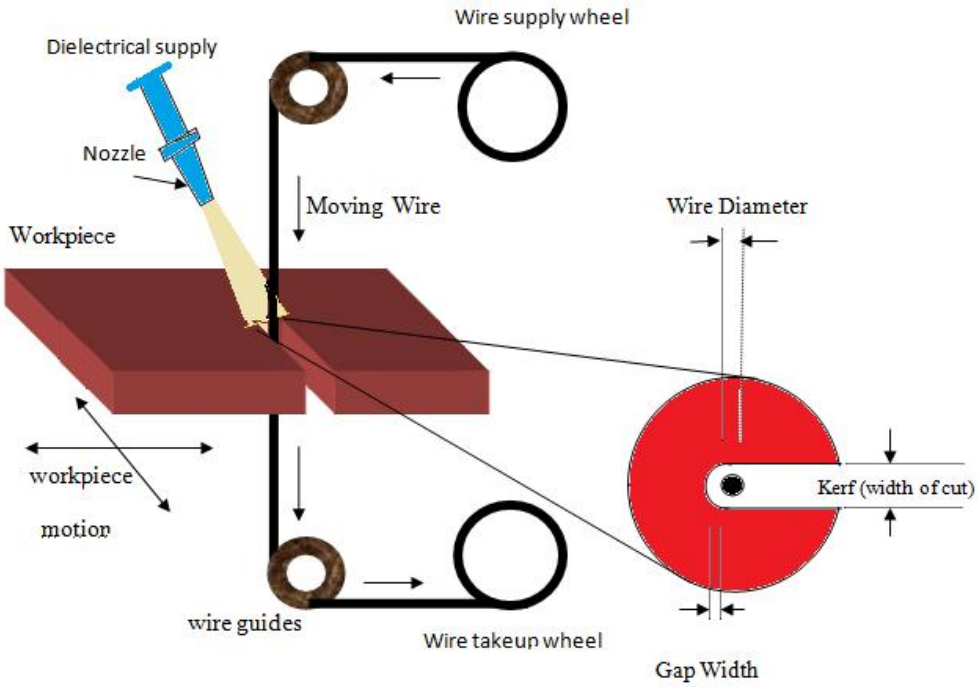

Figure 1.6 Working principle of WEDM

The effectiveness of the whole process depends on number of process parameters such as pulse on time, pulse off time, servo voltage, peak current, dielectric flow rate, wire feed, and wire tension. Wire EDM has its own particular advantages; this machining process is capable of cutting materials regardless of its hardness. It can cut intricate shapes and narrow slots. Furthermore, no burrs are generated during the process. Wire EDM is able to cut taper shaped products and can cut multiple parts in a stack. It is a highly accurate method of part production and its technology is essential for narrow tolerance parts and repeatable tooling as achieving high accuracy and tighter tolerances is essential in many industries. This process can produce and repeat the required specifications with ease. Besides that, wire EDM also has disadvantages; this is more expensive than conventional machines and high skills are required to handle the machine. Wire EDM gives low material removal rate (MRR) and is less flexible on workpiece material when compared to other machines. The workpiece to be machined should be a conductor and leaves white layer and HAZ on the machined component. Prototypes are expensive to produce using WEDM. Wire EDM has a broad range of applications that are continuing to grow in many

industries such as aerospace for complex geometries, in medical and dental for instrumentation, tooling for forging or injection molding operations and for manufacturing of progressive, blanking and trimming dies. This process is suitable for thin or delicate parts that are susceptible to tool pressure in conventional manufacturing processes. Recently, WEDM process is also being used to machine a wide variety of miniature and micro-parts in metals, alloys, sintered materials, cemented carbides, ceramics and silicon (Mukherjee et al., 2012) The above list of applications represents only a few of areas where wire EDM is being used.

1.4. Optimization

Optimization is the process used to select an optimal (best) choice from a set of alternatives. The technique used for optimization is termed as optimization technique. An optimization problem consists of maximizing or minimizing a real function (objective function) systematically. A feasible solution that minimizes or maximizes the objective function is a candidate solution. Fermat and Lagrange found calculus-based formulas for identifying optima, while Newton and Gauss proposed iterative methods for moving towards an optimum. Classification of optimization techniques is shown in Figure 1.7.

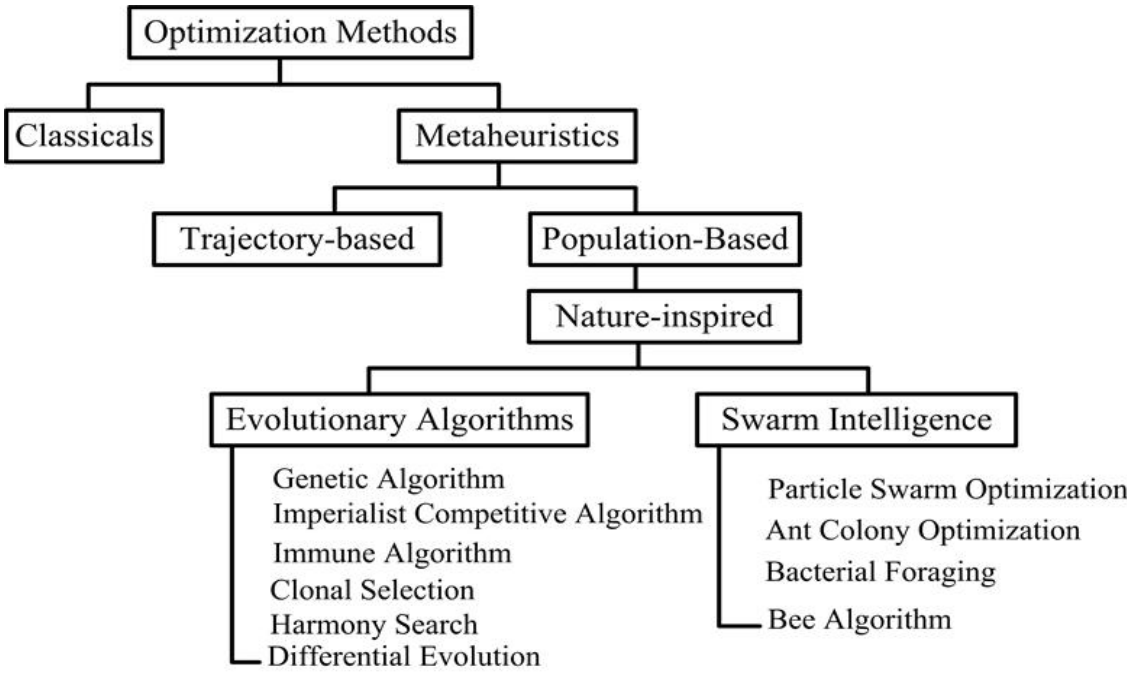

Figure 1.7 Classification of optimization methods

Techniques shown in Figure 1.7, fall under the metaheuristic techniques. The Traditional or classical methods include linear programming, non-linear programming, quadratic programming, gradient method, Newton's method, interior point methods etc. However, these techniques suffer from drawbacks in addressing multi-modal problems and handling discrete control variables. Since the WEDM process, being a stochastic in nature, and the responses involve number of discrete variables, metaheuristic techniques are employed in the present work.

1.5. Design of experiments: RSM

For analyzing of any system or process effectively, efficiently and economically, experiments are to be designed and conducted systematically. In any experiment, the results and conclusions that can be drawn depend to a large extent on the manner in which the data were collected. The aim of any experimental design is to provide an insight into the relationship between process parameters with their responses, the influence of various process parameters and also their percentage contributions. One-Variable-At-a-Time (OVAT) approach is used in manufacturing industries, where one variable is varied at a time keeping all other variables in the experiments fixed. This type of experimentation requires large resources to be obtained and also involves many constraints such as it depends upon guesswork, luck, experience and instinct for its success. Therefore, these are often considered as unreliable, inefficient, time consuming and may yield false optimum conditions for the process.

Factorial design of experiments is mostly used to simultaneously determine the significance of multiple independent variables and their interactions. In a full factorial design of experiments two or more factors with discrete values or levels are considered with all the possible combinations. However, it is costly to perform full factorial experiments. Instead, a fractional factorial design, which is a subset of full factorial design, is generally used which requires fewer runs. Factorial design is less preferable when more than two levels are considered. This is needed, as the number of experiments required for such designs will be considerably greater than their two level counterparts. Generally, factors in real engineering problems are continuous, but the two-level factorial design assumes that the effect is linear. In order to consider a quadratic effect, a more complicated experiment is to be selected such as central composite design.

Response surface methodology (RSM) is mostly used while optimizing factors that could have quadratic effects (Rao, 2011).

RSM is a collection of statistical and mathematical techniques useful for the modeling and analysis of problems (Montgomery, 2005). They can be applied for modeling and optimization of any engineering problems. In RSM, the objective is to optimize the responses that are influenced by the input process parameters. Sufficient data is gathered through the designed experimental layout and a second-order regression equation is developed. A multi-variable regression analysis has been developed between the input process parameters and responses. The general second order regression equation is given by equation 1.1.

$$Y_r = b_0 + \sum_{i=1}^{n} b_i X_{ir} + \sum_{i=1}^{n} b_{ii} X_{ir}^2 + \sum_{j>i}^{n} b_{ij} X_{ir} X_{ju} + e_r \qquad 1.1$$

where, Y_r is response, X_{ir} is the value for i^{th} input process parameter of r^{th} experiment; n is the number of process parameters; b_i, b_{ii}, b_{ij} are the regression coefficients; and e_r is the experimental error of the r^{th} observation. This regression modeling is done to generate the fitness equations for the output responses.

Optimization study in RSM is carried out in three stages. First stage is to determine the independent input parameters and their levels for experimentation. In the second stage, selection of experimental design, prediction and verification of the model equation is performed. Lastly, the response surface plots and contour plots of these response functions are used to determine the optimum points. RSM has several advantages as compared to classical experimental methods as listed below.

- RSM delivers more information from less number of experiments. Whereas, classical methods are more time consuming with large number of experiments to explain the behavior of a system.
- It is possible to determine the interaction effect of the parameters on the responses. RSM model can easily clarify theses interaction effects for binary combination of the independent parameters.
- Empirical model is also developed which helps to obtain the nature or trend of the response with respect to the input parameters in the given process.

On the contrary, the major drawback of RSM is to fit the data to a second order polynomial. It cannot be said that all systems containing curvature are well accommodated by the second order polynomial. Therefore, preliminary experiments are required to be carried out to determine the range of independent input parameter.

1.6. Organization of thesis

The thesis is organized into seven chapters.

Chapter-1: Introduction

A brief background of the work has been reported in this chapter and insight into super alloys and their applications are introduced. Different EDM processes are also introduced here. At the end of the chapter design of experiments is also explained briefly.

Chapter-2: Literature review

The literature on the topics related to optimization of MRR, SR, evolutionary algorithms, circularity and cylindricity errors, neural networks, recast layer thickness and micro hardness are presented in this chapter. Based on literature survey, research gaps are identified and objectives are formulated at the end of this chapter.

Chapter-3: Experimental setup and measurement of responses

A description on the experimental set-up, selection of process parameters with their ranges and levels, working conditions and procedures adopted while conducting the experiments to fulfill the objectives of the present work on super alloys are given in this chapter. Different equipments used in the present study to measure the responses are also described in this chapter.

Chapter-4: A modified cuckoo search algorithm for optimization of MRR and SR

Introducing cuckoo search algorithm and its procedural steps, proposed modified cuckoo search and application of modified method to bench mark problems for validation are explained in this chapter. Application of MCS to optimize MRR and SR of Inconel-690 and Nimonic-263, ANOVA analysis, combinations for desired responses, optimal results from different methods and optimization of wire EDM parameters for simultaneous improvement of surface roughness and MRR by applying non-dominated sorting principle are also presented in this chapter.

Chapter-5: Geometrical errors

This chapter reports introduction to geometrical errors. Application of neural network method in modeling of geometrical errors such as circularity and cylindricity errors is presented. Methods to evaluate circularity and cylindricity errors also presented. The influence of various process parameters on circularity and cylindricity, mathematical models to predict these errors are also given in this chapter.

Chapter-6: Experimental investigation on re-cast layer thickness and micro-hardness of WEDMed surfaces of Inconel-690 and Nimonic-263

This chapter presents introduction on re-cast layer thickness and micro-hardness. Modeling of RCLT and MH for Inconel-690 and Nimonic-263 super alloys, influence of WEDM process parameters on RCLT and MH through ANOVA are also presented. It also reports EDS analysis to check the chemical composition after the process.

Chapter-7: Conclusions and future scope

The conclusions drawn from the results obtained by conducting experimental investigations, modeling and optimization of WEDM process while machining Nickel based super alloys are presented in this chapter. All the limitations encountered during conduct of research and possible extension to the present work is given in the form of future scope.

References

The published research work reported by earlier authors in the related area in the form of journal papers, conference papers, text books, manuals and hand books which are referred in the thesis have been listed under the heading “References”.

CHAPTER 2

LITERATURE

2.1. Introduction

Nowadays WEDM is being used due to its wide applications such as aerospace, nuclear and automobiles (Jain, 2005). And also it can be used to machine any electrically conductive materials, irrespective of their hardness. The reason for extensive use of WEDM is due to its ability to machine precise, complex and irregular shapes (Ho et al. 2004; Su 2012). Due to these reasons research on WEDM is gaining importance day by day. Hence it is required to study the behavior of WEDM process parameters in machining of different materials and also to develop mathematical models to predict different responses of WEDM. In the recent past several researchers conducted experiments to investigate the influence of different process parameters such as pulse-on time, pulse-off time, peak current, servo voltage, wire tension, di-electric fluid pressure and wire speed on different response parameters such as MRR, SR, kerf, WWR and white layer thickness.

The effectiveness of the WEDM process depends on number of input process parameters such as pulse on time, pulse off time, servo voltage, peak current, dielectric flow rate, wire feed, and wire tension. Pulse-on time, also called pulse duration, is expressed in micro seconds. During the pulse-on time, the voltage is applied in the gap between workpiece and the electrode thereby producing discharge. Higher the pulse on time, higher will be the energy applied thereby generating more amount of heat energy during this period. Material removal rate depends upon the amount of energy applied during the pulse on time (Kansal et al., 2005). Pulse-off time, also known as pulse interval, is also expressed in micro seconds. This is the time between discharges. Off time is the pause between discharges that allows the debris to solidify and be flushed away by the dielectric fluid prior to the next discharge. Reducing pulse-off time can increase cutting speed, by allowing more productive discharges per unit time. However, reducing off time can overload the wire, causing wire breakage and instability of the cut by not allowing enough time to evacuate the debris before the next discharge (Fuller, 1996). Peak current is the amount of power

used in machining and is measured amperes. The current increases until it reaches a preset value during each pulse-on time, which is known as peak current. The metal removal rate is directly proportional to peak current (Singh and Garg, 2009)

Servo voltage acts as the reference voltage to control the wire advances and retracts. If the mean machining voltage is higher than the set servo voltage level, the wire advances, and if it is lower, the wire retracts. When a smaller value is set, the mean gap becomes narrow, which leads to an increase in spark intensity, resulting in higher machining rate. However, the state of machining at the gap may become unstable, causing wire breakage (Ghodsiyeh et al., 2013). Dielectric flow rate is the rate at which the dielectric fluid is circulated. Flushing is important for efficient machining to flush the debris from the machining area and to act as a coolant. Flushing pressure is produced from both the top and bottom nozzles. As the wire feed rate increases, the consumption of wire as well as cost of machining will increase. Low wire speed will cause wire breakage in high cutting speed. If the wire tension is high enough the wire stays straight otherwise wire drags behind. Within certain range, an increase in wire tension significantly increases the cutting speed and accuracy. The higher tension decreases the wire vibration amplitude and hence decreases the cut width so that the speed is higher for the same discharge energy. However, if the applied tension exceeds the tensile strength of the wire, it leads to wire breakage. This chapter focuses on investigations of different researchers while machining different materials on WEDM and also optimization of various responses involved in the process.

2.2. Optimization of MRR and SR

The first WEDM machine was produced by the Swiss firm Agie in 1969. These early machines are extremely slow but today, machines are equipped with automatic wire threading and can cut over 20 times faster (Carl and Steev, 2005). Tosun and Cogun (2003) carried experimental investigations to study the effect of cutting parameters such as pulse duration, open circuit voltage, wire speed and dielectric fluid pressure on wire wear of AISI 4140 steel in WEDM process. It is found experimentally that the increasing pulse duration and open circuit voltage increase the WWR, however the increase in wire speed and dielectric fluid pressure decrease the WWR. The level of importance of the machining parameters on the wire wear was

estimated by using ANOVA. By using regression analysis technique, mathematical models are developed for WWR with machining parameters.

Scott et al., (1991) presented a methodology to determine the optimal combination of control parameters such as discharge current, pulse duration, pulse frequency, wire speed, wire tension and dielectric flow rate in WEDM of D2 tool steel. The performance measures were MRR and surface roughness. As no single combination can be optimal for both MRR and surface roughness, this led to the notion of non-dominated points and the complementary optimization problems. Two different methods were used to obtain a set of non-dominated combinationations, one is explicit enumeration method and the other is dynamic programming. From the experimental results and ANOVA they found that discharge current, pulse duration and pulse frequency were significant control factors for both MRR and surface finish where as wire speed, wire tension and dielectric flow rate were relatively insignificant.

Liao et al., (1997) carried out an experimental investigation to determine the parameters setting during the machining of SKD11 alloy steel. Based on the Taguchi quality design method and the analysis of variance, the significant factors affecting the machining performance such as MRR, gap width, SR, sparking frequency, average gap voltage and normal ratio (ratio of normal sparks to total sparks) are determined. By means of regression analysis, mathematical models relating the machining performance and various machining parameters such as pulse-on time, pulse-off time, table feed rate, flushing pressure, wire tension, wire velocity are established. Based on the mathematical models developed, an objective function under the multi-constraint conditions is formulated. The optimization problem is solved by the feasible direction method, and the optimal machining parameters are obtained. Experimental results demonstrate that the machining models are appropriate and the derived machining parameters satisfy the real requirements in practice.

Kuriakose et al., (2003) applied data mining technique to model the WEDM process. The process parameters such as applied machining voltage, ignition pulse current, pulse duration, idle (delay) time (time between two pulses), servo speed variation, servo-control reference voltage, wire speed, wire tension, and injection pressure for dielectric were considered to model the responses. A data mining technique C4.5 was used to study the effect of various input parameters on the outputs, namely the cutting speed and surface finish.

Konda et al., (1999) carried out experiments to optimize the WEDM process performances such as machining speed and surface roughness. Pulse duration, charge frequency, charge current and capacitance were taken as process parameters. Design of experiments strategy was used for experimental plan. Complimentary optimization technique (identifying the non-dominated points) was used to solve the multi-objective optimization problem.

Tarng et al., (1995) used feed forward neural network to construct the WEDM process model to associate the cutting parameters such as pulse-on time, pulse-off time, peak current setting, no-load voltage, servo reference voltage, capacitor setting, and servo speed setting and the responses include machined surface roughness and machining speed. Simulated annealing algorithm is then applied to the neural network for solving the optimal cutting parameters based on a performance index within the allowable working conditions.

Spedding and Wang (1997) applied artificial neural networks (ANN) to optimize the process parameters such as time between two pulses, pulse width, wire mechanical tension, and wire feed space by modeling the process. Cutting speed, workpiece surface roughness and waviness were selected as the performance measures. A multi layered feed-forward neural network is used to model the WEDM process, and the developed model is used for process performance prediction and parameter optimization.

Tosun and Pihtili (2003) conducted experimental investigation to study the effects of pulse duration, open circuit voltage, wire speed and dielectric flushing pressure on the dimension of craters in the wire in WEDM process. From the experimental results it was found that increasing the pulse duration, open circuit voltage, and wire speed increases the crater diameter and crater depth, whereas increasing the dielectric fluid pressure decreases these factors. This study is limited to one response only. Using the conducted experiments, the researchers could have studied metal removal rate, roughness of machined surface and dimensional deviation also.

Sarkar et. al. (2006) made an attempt to develop an appropriate machining strategy for a maximum process yield criteria. A feed forward back-propagation neural network was developed to model the machining process. Cutting speed, surface roughness and wire offset have been considered as measures of the process performance. The model is capable of predicting the response parameters as a function of six different control parameters such as pulse on time, pulse off time, peak current, wire tension, dielectric flow rate and servo reference voltage.

Experimental results demonstrate that the machining model is suitable and the optimization strategy satisfies practical requirements.

Manna and Bhattacharyya (2006) carried out an experimental investigation to determine the parameters setting during the machining of aluminium-reinforced silicon carbide metal matrix composite (Al/SiC-MMC). The Taguchi method was used to optimize the CNC-wire cut-EDM parameters. From experimental results and through ANOVA and F-test values, the significant factors were determined for each response performance, such as the metal removal rate, surface roughness, gap current and spark gap (gap width). Mathematical models relating the machining performance are established using the Gauss elimination method for the effective machining. Mahapatra and Patnaik (2007) attempted to determine the important machining parameters for performance measures like MRR, surface finish and kerf in WEDM on D2 tool steel. Using Taguchi's parametric design significant machining parameters affecting the performance measures are identified as discharge current, pulse duration, pulse frequency, wire speed, wire tension and dielectric fluid flow rate. Mathematical models are developed by means of non linear regression analysis for MRR, SR, and Kerf. Genetic algorithm is employed to optimize the WEDM process with Multiple-objectives. The above two studies involved application of Taguchi method, however, this method fails to show the significance of interaction effects.

Aravind et. al., (2012) used Taguchi's experimental design to obtaining the optimum machining parameters for the maximization of MRR and minimization of surface roughness separately in WEDM of brass material. They considered input voltage, current density, speed (feed rate), pulse-on time and pulse-off time as input parameters. They found that, the significant factors are pulse time and feed rate in both MRR and SR. Higher values of feed rate and pulse duration increase the MRR and decrease the surface roughness.

Khan et. al., (2006) conducted experimental investigations to establish relationships for surface finish with current and voltage. Work materials tested were mild steel, aluminium, cemented carbide, copper and stainless steel. They concluded that the machined surface becomes rougher with increase in current and voltage. Microstructures of the specimens show that craters on the finished surface becomes larger as a result of using higher current and voltage. Wires of smaller diameters give smother surface than those cut with that of larger diameter.

Guiqin et al., (2007) established a WEDM model in which combined modeling function of fuzzy inference with the learning ability of artificial neural network was integrated with genetic optimization. In this work they considered the MRR and SR as output parameters and workpiece thickness, pulse-on time, peak current and mean current are input parameters.

Yu et al., (2011) investigated the effect of various parameters on cutting speed, machine groove width and surface roughness in machining polycrystalline silicon. Pulse-on time and open voltage have significant influence on cutting speed. Increase in flushing rate improved cutting speed and reduced surface roughness. Strengthening wire tension showed significant improvement in machining grove width. Tosun (2003) studied variations of cutting performance with pulse on time, open circuit voltage, wire speed and dielectric fluid pressure on AISI 4140 steel. It was found experimentally that increase in pulse duration, open circuit voltage, wire speed and dielectric fluid pressure increased the cutting speed. The surface quality of the workpiece increased with decrease in pulse duration, open circuit voltage and wire speed, and with increasing dielectric fluid pressure. Regression analysis was used to develop mathematical models. Lee and Liao (2003) developed a gain Self-tuning fuzzy control system to cope with the conditions that often occur with wire rupture in WEDM process, such as an improper setting of machining parameters and machining the workpiece with varying thickness.

Manna and Bhttacharyya (2005) experimented to determine the parameters setting during the machining of aluminium-reinforced silicon carbide metal matrix composite (Al/SiC-MMC). The Taguchi method is used to optimize the CNC-wire cut-EDM parameters. From the experimental results and through ANOVA and F-test values, the significant factors are determined for each machining performance criteria, such as the MRR, surface roughness, gapcurrent and spark gap (gap width). The important controllable process parameters such as pulse on-time (T_{on}), pulse off-time (T_{off}), peak current (IP), pulse peak voltage (V_p), wire feed rate (WF), wire tension (WT) and spark gap voltage (SV) are considered in this study. Open gap voltage and pulse on period are the most significant machining parameters for controlling the MRR. The open gap voltage affects the cutting speed significantly. Wire tension (WT) and wire feed rate (WF) are the most significant machining parameters for the surface roughness (SR). Wire tension and spark gap voltage setting are the significant parameters for controlling spark gap (i.e. gap width, *W)* Open gap voltage and gap current are the significant parameters for controlling gap current (I_g).

Han et. al., (2007) experimented to study the influence of the machining parameters such as pulse duration, discharge current, sustained pulse time, pulse interval time, polarity effect, material and dielectric on surface roughness in the finish cut of WEDM. It is concluded that the surface roughness can be improved by decreasing both pulse duration and discharge current. The removal rate when a short pulse duration is used is much higher than when the pulse duration is longer. A short pulse duration combined with a high peak value can generate better surface roughness, which cannot be achieved with long pulses. In the study, it was also found that reversed polarity machining with the appropriate pulse energy can improve the machined surface roughness as compared to normal polarity in finish machining, however some copper from the wire electrode is accreted on the machined surface.

Saha et al., (2008) developed a second order multi-variable regression model and a feed-forward back-propagation neural network (BPNN) model to correlate the input process parameters, such as pulse on-time, pulse off-time, peak current, and capacitance with the performance measures namely, cutting speed and surface roughness while wire machining tungsten carbide-cobalt (WC-Co) composite material. Scanning electron micrographs reveal that at higher energy level, the machined surface is characterized by several micro-cracks and loosely bound solidified WC grains.

Gauri and Chakraborty (2009) worked on optimization of process settings with respect to all these performance measures. Taguchi's robust design method can only be applied to optimize a single-response problem where as the principal component analysis (PCA)-based approach for multi response optimization can effectively overcome those weaknesses. In this study, some modifications in the PCA based approach are suggested and two sets of experimental data published by the past researchers are analyzed using this modified procedure. The aim of this study was to optimize the settings of six controllable factors, e.g., pulse on time, pulse off time, peak current, wire tension, servo reference voltage and dielectric flow rate with respect to three performance characteristics of a WEDM process. The performance characteristics considered were cutting speed, surface roughness and dimensional deviation. The results demonstrate that the PCA-based optimization can lead to better overall quality than the constrained optimization-based approach, and the anticipated overall quality under the PCA and MRSN-based approaches are observed to be almost equivalent. This method gives optimal values for multiple responses

from the conducted experiments only. However, global optimal solution could lie outside these experiments.

Gauri and Chakraborty (2010) used two sets of experimental data on WEDM processes and analysed using four promising multi-response optimization approaches, such as GRA, MRSN ratio, WSN ratio, and VIKOR methods. The resulting optimal solutions for these four methods and the expected overall quality at these optimal solutions are compared. It is found that WSN ratio method can give better overall quality than other methods. The aim of this study was to optimize the settings of six controllable factors, such as pulse on time, pulse off time, peak current, wire tension, servo reference voltage and dielectric flow rate with respect to three performance characteristics such as MRR, surface roughness and Kerf. The results demonstrate that the WSN ratio based multi response optimization can lead to better overall quality than the GRA, VIKOR and MRSN-based approaches. These techniques can identify optimal solution within the conducted experiments only.

Satishkumar et al.,(2011) investigated the effect of parameters such as pulse-on time, pulse-off time, gap voltage and wire feed on MRR and surface roughness in metal matrix composites (MMCs) consisting of aluminium alloy(Al6063) and silicon carbide(SiCp) in various volume fractions(5%,10% and 15% of SiC) prepared through stir casting process. The experiments are carried out as per design of experiments approach using L9 orthogonal array. It is observed that the MRR was found to decrease with increase in the percentage of SiC particles in the MMCs, where as the Ra increases with increase in the percentage volume fractions of SiC. It is also found that the influence of gap voltage was more significant parameter than others.

Yang et al.,(2012) attempted to analyze variations in metal removal rate MRR, surface roughness Ra, and corner deviation in relation with WEDM process parameters such as pulse on time , the pulse off time, arc off time, the servo voltage, the wire feed rate, the wire tension, and the water pressure in cutting pure tungsten. This research proposes an effective process parameter optimization approach that integrates Taguchi's parameter design method, response surface methodology (RSM), back propagation neural network (BPNN), and simulated annealing algorithm (SAA) on WEDM processes. Simultaneously, RSM and SAA approaches were individually applied to search for an optimal setting. In addition, ANOVA was implemented to identify significant factors for the processing parameters. Furthermore, the field-emission SEM images show that a lot of built-edge layers were presented on the finished surface after the

WEDM process. Finally, the optimized result of BPNN with integrated SAA was compared with that obtained by an RSM approach. Comparisons of the results of the algorithms and confirmation experiments show that both RSM and BPNN/SAA methods are effective tools for the optimization of parameters in WEDM process. The results showed that, with the higher pulse on time, which leads to the discharge energy becoming more intense, the MRR was increased and the brass wire of cutting tool accelerates depletion, generates a larger built-up layer, and therefore produces rougher surfaces. Simultaneously, increasing the wire tension results in the decrease of corner deviation.

Kumar and Agarwal (2012) applied multi-objective genetic algorithm NSGA-II to optimize the multiple objectives of MRR and surface roughness with respect to process parameters such as pulse peak current, pulse-on time, pulse-off time, wire feed, wire tension and flushing pressure on machining high speed steel (M2,SKH9). Experiments, based on Taguchi's parameter design, were carried out to study the effect of various parameters and mathematical models were developed between machining parameters and responses like metal removal rate and surface finish by using nonlinear regression analysis. These mathematical models were then optimized by using multi-objective optimization technique based on NSGA-II to obtain a Pareto-optimal solution set. The results of optimization indicate that the MRR and surface finish are influenced more by pulse peak current, pulse duration, pulse-off period and wire feed than by flushing pressure and wire tension. Results also indicate that the surface quality decreases as the MRR increases and they vary almost linearly.

Sharma et. al., (2012) conducted experiments to investigate the effect of process parameters on cutting speed and dimensional deviations in cutting high-strength low-alloy steel (HSLA). The different process parameters considered in their study are Pulse on time, Pulse off time, Spark gap voltage, Peak current and Wire tension. To optimize the process parameters for cutting speed and dimensional deviation, Response Surface Methodology was used. From the experimental results it is found that pulse-on time was the most prominent factor for cutting speed and dimensional deviation.

Prasad and Krishna (2009) proposed a methodology to determine the optimal machining parameters to achieve high production rate and good surface finish of WEDM machined components. The process parameters considered are Pulse-on time, Pulse-off time, Wire tension, Dielectric flow rate, and Wire feed. Response surface methodology was used to develop the

mathematical models for MRR and surface roughness. Since the influence of process parameters on MRR and Ra are opposite, the problem is formulated as a multi-objective optimization problem. NSGA was used to obtain the Pareto optimal set of solutions.

Shah et al., (2011) investigated the effect of various wire electrical discharge machining parameters such as the material thickness, open voltage, pulse-on time, pulse-off time, servo voltage, wire feed velocity, wire tension, and dielectric pressure on the machining responses such as MRR, kerf, and surface roughness of tungsten carbide. Taguchi orthogonal design was used for experiments and ANOVA is used to identify the significant factors. Mathematical models are developed to optimize the responses such as MRR, Ra, and Kerf separately. From the experimental results it was observed that metal thickness has little effect on the material removal rate and kerf but is a more significant factor in terms of surface roughness.

Ramakrishnan and Karunamoorthy (2006),described a multi response optimization method (MRSN) using Taguchi's robust design for machining heat treated tool steel. Pulse on time, Wire tension, Delay time, Wire feed rate and ignition current intensity are taken as input process parameters and MRR, surface roughness and wire wear ratio are considered as responses. It was identified that the pulse on time and ignition current intensity have influenced more than the other parameters considered in their study.

Gauri and Chakraborty (2009) applied weighted principle component analysis method (WPC) to optimize the multiple responses of WEDM. In this approach, the set of multiple responses is first transformed into a set of a small number of uncorrelated principal components. Then, the weighted sum of all the principal components is taken as the multi-response performance index (MPI) and the optimal parametric settings that maximize the MPI are determined in an objective manner.

Datta and Mahapatra (2010) applied response surface methodology to developed quadratic mathematical models to represent the behavior of WEDM process parameters such as discharge current, pulse duration, pulse frequency, wire speed, wire tension and dielectric flow rate for the process responses such as MRR, surface roughness and kerf. Experiments are planned and conducted based on the Taguchi's orthogonal array principles. Grey relational analysis has been adopted to convert this multi-objective criterion into an equivalent single objective function; overall grey relational grade, which has been optimized (maximized) by using Taguchi technique. Experiments were conducted on D2 tool steel.

Muthu et. al., (2010) demonstrated the optimization of WEDM process parameters of Incoloy800 super alloy with multiple performance characteristics such as MRR, surface roughness and Kerf based on the Grey–Taguchi method by considering the process parameters such as gap voltage, pulse on-time, pulse off-time and wire feed. The variation of output responses with process parameters were mathematically modeled using non-linear regression analysis method. Optimal levels of process parameters were identified using GRA and the relatively significant parameters were determined using ANOVA.

Vundavalli et. al., (2012) applied multi-objective optimization techniques such as NSGA and particle swarm optimization (PSO) techniques to WEDM process as this process involves multiple-objectives like cutting velocity and surface finish. The various process parameters considered include applied voltage, ignition pulse current, pulse-off time, pulse duration, servo controlled reference mean voltage, servo-speed variation, wire speed, wire tension and injection pressure. Both the approaches are found to show similar trend on the Pareto- optimal fronts. Moreover, GA has slightly outperformed the PSO in terms of the optimal solution obtained. It is also important to note that PSO has produced the optimal front in less time when compared with the GA. It may be due to the simple structure associated with minimal parameter tuning of PSO.

Shandilya et al.,(2012) attempted to optimize the process parameters of WEDM during machining of SiC/6061 Al MMC using response surface methodology (RSM).Four input process parameters of WEDM namely servo voltage , pulse-on time, pulse-off time and wire feed rate were chosen to study the process performance in terms of cutting width (kerf). The ANOVA was carried out to study the effect of process parameters on process performance. Mathematical models have also been developed for response parameter and properties of the machined surface have been examined by using SEM.

Singh and Khanna, (2011) attempted to optimize the cutting rate of cryogenic-treated D-3 material with respect to their input process parameters such as pulse width, time between two pulses, maximum feed rate, servo reference mean voltage, short pulse time, and wire mechanical tension. Experimental results showed that cutting rate decreases with increase in pulse width, time between two pulses, and servo reference mean voltage also cutting rate first decreases and then increases with increase in wire mechanical tension.

Antar et. al., (2011) presented experimental data for workpiece productivity and integrity while machining Udimet 720 nickel based super alloy and Ti-6Al-2Sn4Zr-

6Motitaniumalloy,using Cu core coated wires (ZnCu50 and Zn rich brass). It was found that up to a 40 % for Udimet 720 and 70 % for Ti-6Al-2Sn4Zr-6Mo titanium alloy increase in productivity was possible compared to when using uncoated brass wires with the same operating parameters. The variation in surface roughness values, mainly during roughing, between the top, middle and bottom sections of the specimens could be related to 'imperfect' sparks generated due to erosion of the wire, leading to wider machining gaps. In terms of recast layer thickness, better results were achieved using the coated wire for both roughing and trim operations.

2.3. Evolutionary algorithms

Das et al. (2014) applied Artificial Bee Colony (ABC) algorithm to identify the optimal parameter values to yield minimum surface roughness. They conducted experiments for their investigation on EN 31 steel and also CCD of RSM was used for their experimental plan. Tharian et al. (2015) are also used ABC algorithm to estimate the optimal values for minimum surface roughness. They used AISI 202 stainless steel for experimentation and Taguchi L18 orthogonal array was used for experimental plan. For both their study results are verified with the experimental results and found they are in good agreement. Pasam et al. (2010) used Taguchi L27 for their experimental study to machine Titanium alloy on WEDM. Mathematical models are developed and these models are further optimized using GA. Shandilya et al (2012) and Sharma et al. (2014) studied the effect of WEDM process parameters in machining of metal matrix composites (MMC) and D-2 tool steel respectively. RSM was used to develop mathematical model for dimensional deviations and then GA was used for further optimization of process parameters.

Pawar (2011) applied a shuffled frog leaping (SFL) algorithm for simultaneous optimization of metal removal rate and wear ratio subjected to the constraints of surface roughness. Rao and Pawar (2010) and Rao and Venkaiah (2015) applied particle swarm optimization (PSO) technique to optimize WEDM process parameters to improve the machining speed for a desired value of surface finish. RSM was used for experimental plan and also to develop mathematical models. Whereas Muthukumar et al. (2015) applied a recently developed Accelerated PSO (APSO) to optimize the process parameters to maximize MRR and minimize SR and kerf. Mukherjee et al., (2012) carried out comparative study on different population based

non-traditional optimization techniques such as GA, PSO, ABC, sheep flock algorithm (SF), ant colony algorithm (ACO) and biogeography-based optimization (BBO) in selection of optimal WEDM parameters. They were taken two problems from the literature as case studies and applied the above algorithms for comparative study. They found that BBO out performance the others in terms of quick convergence, optimization performance and dispersion of the optimal solutions from their mean.

Cuckoo search algorithm, a meta-heuristic optimization algorithm, was developed by Yang and Deb (2009) based on the breeding behavior of cuckoos and the characteristics of Levy flights of some birds and fruit flies. Cuckoo search algorithm (CSA) was found to be efficient in yielding the global optimal value and this algorithm was found to outperform GA and PSO techniques in terms of speed, accuracy and simplicity of computations (Yang and Deb 2009, Yang and Deb 2010 and Gandomi et al. 2013). However, the accuracy of CS heavily depends upon the initial solution and its location from the target value and therefore it may involve many generations. This could lead to delay in convergence.

2.4. Geometrical errors

Circularity error is measured on components where the height of the component is less than the diameter. Whereas the cylindricity is measured on components where the height of the component is more than that of the diameter. There are two types of approaches to evaluate the circularity and cylindricity errors: one is using form data and the other one is CMM data. Though there are four methods available to assess the circularity error, least squares circle (LSC) method is used by most of the researchers due to easy and simple to apply and also it gives unique solution. It is proved by Shunmugam (1986), Thomas and Chan (1989), Kim and Kim (1996) and Qiu et al. (2000) that the error values estimated using LSC are generally higher. To evaluate roundness error, an optimization theory was formulated analytically by Kaiser and Morin (1994). This method involves conversion of circle into line and cylinder to plan by non-linear transformation. Chang and Lin (1993) employed a Monte Carlo simulation method for circularity error evaluation. To obtain minimum error value simplex linear programming has been applied by Carpinetti and Chetwynd (1994) and min-max algorithm described by Lin and Varghese (1995). Lai and Chen (1996) proposed a strategy for minimum zone (MZ) evaluation of cylinders

and circles. A vision based inspection system was developed by Chen et al. (1999) based on the stochastic optimization approach for reference circles. Simulated annealing and Hook-Jeeve's pattern search for roundness measurement also proposed by them. Genetic algorithm is also applied (Liao and Yu (2001) and Wen et al. (2006)) to assess the circularity error. Devillers and Ramos (2002) proposed discrete local optimization method and it works only if the object is round feature. A characteristic point-based method proposed by Deng et al. (2003) to find a MZ solution. An optimization known as semi-definite programming is proposed by Ding et al. (2007) to evaluate circularity error. Kovvur et al. (2008) and Sun (2009) are used particle swarm optimization technique to evaluate the roundness error.

In addition to the above techniques proposed by different researchers, computational geometry (CG) techniques can provide solutions for many geometric problems which can not be solved by classical methods. Lai and Wang (1988) proposed the convex hull concepts, CG based algorithm to evaluate circularity error for the first time. Samuel and Shunmugam (2000) applied computational geometric techniques of convex hulls, to assess the circularity error at different conditions. Apart from that, an equi-angular diagram concept was also employed to find circularity error. Zhu et al. (2003) presented a steepest descent algorithm for circularity error evaluation. An attempt was made by the Li and Shi (2009) to establish the relationship among the reference circles.

Cylindricity is also measured with circularity measuring instruments such as form tester and CMM with an additional straight datum. Measurements are carried out at few transverse sections of the cylinder. To evaluate the cylindricity error least-squares method was proposed by shunmugam (1986) and Tsukada et al. (1998), whereas the normal least-squares method was proposed by Murthy (1982). A non-linear optimization model was proposed by Carr and Ferreira (1995) for MZ cylindricity solution. Radhakrishnan et al. (1998) proposed a linear iterative cyclic coordinate search technique to obtain the near optimal solution for evaluation of cylindricity. A hyperboloid method was proposed by Devillers and Preparata, (2000) to evaluate the cylindricity error. Initial solution based methods like simulated annealing (Chen, 2002; Shakarji and Clement 2004), genetic algorithms (Sharma et al. 2000, Lai et al. 2000) and particle swarm optimization algorithm (Zhang et al. 2011) etc. have been used by some researchers to find the optimal cylindricity error values by applying to any of the cylindricity error measuring methods.

Though different techniques are available in literature to evaluate the geometric errors, modeling and optimization of geometric errors for the parts made by WEDM process are yet to be explored.

2.5. Neural networks

Neural networks (NN) are a family of models inspired by biological neural networks (the central nervous systems of animals, in particular the brain) and are used to estimate or approximate functions that can depend on a large number of inputs and are generally unknown. Artificial neural networks are generally presented as systems of interconnected "neurons" which exchange messages between each other. The connections have numeric weights (Choudhury and Bartarya 2003) that can be tuned based on experience, making neural nets adaptive to inputs and capable of learning. Like other machine learning methods - systems that learn from data - neural networks have been used to solve a wide variety of tasks that are hard to solve using ordinary rule-based programming, including computer vision and speech recognition. The most popular learning algorithm for multilayer networks is the back-propagation algorithm and its variants (Ebrahimi et al., 2006). The ANN is trained by a learning algorithm that performs the adaptation of weights of the network iteratively until the error between target vectors and the output of the ANN is less than an error goal (Joghataie and Amiri 2005)

Esme et al., (2009) carried out experimental investigations for comparative studies in using factorial design and NN. Both the methods are used for modeling and predicting the surface roughness in machining of AISI 4340 steel on WEDM. The predicted values using both the models are compared with experimental values. They found that the predicted values of NN model are close to the experimental values. Tarng et al. (1995) developed a neural network system to determine settings of pulse duration, pulse interval, peak current, open circuit voltage, servo reference voltage, electric capacitance and wire speed for the estimation of cutting speed and surface finish. Spedding and Wang (1997) presented a parametric combination by using artificial neural networks and they also characterized the roughness and waviness of the workpiece surface and cutting speed. Liao et al. (1997) performed an experimental study to determine the variation of the machining parameters on the MRR, gap width and surface roughness. They have determined the level of importance of the machining parameters on the metal removal rate (MRR). Lok and Lee (1997) compared the machining performance in terms of

MRR and surface finish by the processing of two advanced ceramics under different cutting conditions using WEDM. Ramakrishnan and Karunamoorthy (2008) developed an artificial neural network with Taguchi parameter design. Tsai et al. (2008) found relationships between the heterogeneous second phase and the machinability evaluation of the ferritic SG cast irons in the WEDM process. Sarkar et al. (2008) studied the features of trim cutting operation of wire electrical discharge machining of γ-titanium aluminide. Caydas et al. (2009) developed an adaptive neuro-fuzzy inference system (ANFIS) for modeling the surface roughness in the WEDM process. NN modeling of EDM process is also employed by Liao et al. (2002), Çaydaş and Hasçalık (2008), Chen et al. (2010), Guven et al. (2010), Sarkeyli et al. (2015), Ming et al. (2015), Patowari et al (2010), Yang et al. (2012), Shandilya et al. (2013) and Zhang et al. (2013) etc.

It can be noted that the NN modeling is mainly focused on the effect of machining parameters, discharge energy, theoretical and experimental verification and crater formation on the wire electrode. However, the present study involves the development of prediction models for geometrical errors such as circularity and cylindricity errors in machining of super alloys on WEDM.

2.6. Recast-layer and Micro-hardness

A portion of the melted workpiece material is removed by a dielectric circulation system. The remaining molten material will rapidly re-solidify to form a layer known as the recast layer (Goswami and Kumar, 2014). This recast layer affects the mechanical properties like hardness of the materials. Newton et al., (2009) investigated on characteristics of recast layer formed in machining of Inconel 718. They found that the hardness is increasing with distance from the top layer of WEDMed surface. Li et al. (2013) and Kumar et al. (2016) also observed that there is a dramatic reduction in hardness as compared to that of bulk material.

Recast layer and heat affected zones of EDMed surfaces were studied by Rajurkar and Pandit (1984), and also developed thermal models to predict the damage layer thickness. Hasçalık and Çaydaş (2007) performed experiments on titanium alloy with different electrode materials in EDM and explored the influence of parameters on white layer thickness, roughness, and hardness. Soni and Chakraverti (1996) investigated experimentally the change in resolidified

layers and micro-hardness of EDMed surfaces of Die steel. Studies were carried out by Cusanelli et al. (2004) on the formation of white layer and hardness of EDMed surfaces of steel. They also studied the white layer in submicron scale for phases present in white layer, micro cracks, Carbon content in the white layer and nano-hardness of the white layer. They found that the hardness of the white layer is more than that of the base material. Iqbal and Khan (2010) carried out experimental investigation on the influence of EDM process parameters on the recast layer thickness, micro cracks, and material migration in machining of stainless steel. Along with MRR and TWR, recast layer and micro hardness are also studied by Jabbaripour et al. (2012) for Titanium alloy in EDM process. Experimental investigations on the effect of WEDM parameters on the surface roughness and micro-hardness of HSLA material were carried out by Khan et al. (2014). They also used gray relational analysis to optimize surface roughness and micro hardness simultaneously.

2.7. Problem Statements and Motivation

Nickel-based super alloys are a special class of materials with an exceptional combination of high temperature strength, toughness, and resistance to degradation in corrosive or oxidizing environments. These materials are primarily used in the hot sections of jet turbine engines, such as the blades, vanes, and combustion chambers, constituting over 50 % of the engine weight. Inconel-690 is a high-chromium nickel alloy and is widely used for steam generator tubes, baffles, tube sheets, and hardware in nuclear power generation. Nimonic-263 is a nickel-chromium-cobalt-molybdenum alloy specially meant for use in high temperature and high strength applications. These super alloys are extremely hard to shape using traditional machining methods due to rapid work hardening. After the first machining pass, work hardening tends to plastically deform either the workpiece or the tool on subsequent passes. Therefore, modern machining methods such as sinker EDM and abrasive water jet machining (AWJM) are generally employed to machine these materials. The drawback with sinker EDM is that it can produce simple geometries like holes and AWJM consumes higher energy. However, WEDM can be used to machine complex shapes with lesser energy requirements. Further, adequate WEDM studies are not reported on these materials. Therefore, generation of machining data using WEDM on these materials assumes a great importance from the industry viewpoint.

Surface roughness affects several functional attributes of parts, such as friction, wear and tear, light reflection, heat transmission, ability of distributing and holding a lubricant and coating. Hence, assessment of surface roughness of the parts is important from the quality viewpoint. Further, in order to meet the customer requirement in terms of due date, the manufacturer always tries to maximize the MRR. Increasing the MRR is also important from the viewpoint of machining economics. Depending upon the requirements of the industry, these responses are to be optimized either individually or simultaneously. Although there are many optimization techniques, there is a possibility of improving them further to report the accurate results in much lesser time. Among various optimization techniques, cuckoo search (CS) algorithm was found to be efficient in yielding the global optimal value and this algorithm was found to outperform GA and PSO techniques in terms of speed, accuracy and simplicity of computations. However, the accuracy of CS heavily depends upon the initial solution and its location from the target value and therefore it may involve large number of generations. Furthermore, in this algorithm, the evolutionary operators are applied in each generation. This could lead to delay in convergence. Therefore, there is a scope for improving this algorithm.

In order to meet the desired functional and assembly requirements, engineering components need to have tighter dimensional and geometrical tolerances. Majority of the engineering components have circular and cylindrical features in them. These components are used for different applications such as rotating devices, transmission systems, injection moulds, bearings and engine cylinders. Producing straight cuts is easier as compared to machining of axi-symmetric components. The difficulties are further amplified while machining such features on super alloys with the stochastic nature of WEDM process. Although most of the WEDM literature is focused on responses such as MRR, SR, Kerf and WWR. Studies on geometrical errors of axi-symmetric components are not yet reported. Therefore it is required to model the geometrical errors in order to accurately predict these errors to reduce the rejection rate of the components during inspection.

Mechanical properties of any material after machining will vary due to the machining phenomena of sudden heating and cooling. It is difficult to retain the base material properties after machining. In WEDM process, a huge amount of heat is generated is used to melt the workpiece. A portion of the melted workpiece material is removed by a dielectric circulation

system. The remaining molten material will rapidly re-solidify to form a layer known as the recast layer. This recast layer thickness affects the surface integrity aspects such as hardness and other surface properties of the materials. Lack of adequate studies on surface integrity on Inconel-690 and Nimonic-263 materials is another motivation for the present work.

2.8. Objectives of the work

Following objectives are formulated for the present work.

1. To generate WEDM data on material removal rate, surface roughness, form errors, recast layer thickness and micro-hardness for Inconel-690 and Nimonic-263 materials.
2. To analyze the existing cuckoo search algorithm for its effectiveness and formulate an effective algorithm to yield optimal material removal rate and surface roughness.
3. To formulate non-dominated sorting modified cuckoo search algorithm to yield simultaneous optimal solutions for MRR and SR.
4. To develop predictive models for form errors such as circularity and cylindricity using ANN approach and minimize them for WEDMed components.
5. To investigate and model recast layer thickness and micro-hardness of WEDMed surfaces.

CHAPTER 3

EXPERIMENTAL SETUP AND MEASUREMENT OF RESPONSES

3.1. Introduction

Analysis of any response of a system heavily depends on how well the experiments are planned, conducted and measured. The measurement process may also include calculations. For example, material removal rate cannot be measured directly. It can be estimated by measuring the dimensions of work material and observed time. Therefore conducting experiments and measuring the responses is crucial part in any investigation. Ranges of variables should be identified after trial experiments. In the present study RSM has been used for experimental plan and also for developing predictive models for various responses such as MRR, SR, RLT and MH. However, to develop robust predictive models, accurate measurement or estimation of response is essential. This chapter describes experimental setup and measurement of responses. Details of the machine (WEDM), experimental plan, and different instruments to measure the responses such as surface roughness, circularity, cylindricity, re-cast layer thickness, and micro-hardness are also presented.

3.2 Experimental setup

A WEDM of Eletronica make Eco-cut machine has been used to conduct the experiments (Figure 3.1). De-ionized water is used as di-electric fluid and zinc coated brass wire of 0.25 mm diameter is used as wire electrode. In order to identify the feasible ranges for each parameter for uninterrupted machining, trial experiments were conducted. For example, at T_{off} - 50, I_p - 12 and S_v - 40, the upper limit of T_{on} is fixed at 125. If T_{on} is increased beyond this value, wire breakage was observed. Further, at T_{off} - 60, I_p -10, and S_v - 60, the lower limit of T_{on} is fixed at 105. If T_{on} is set lesser than this value, there is no machining taking place due to wire shorting. Similar experimental trials were conducted to fix the ranges for other parameters also. After observing the results of trial experiments the ranges and levels are fixed as presented in the Table 3.1.

Table 3.1 Process parameters: Ranges and levels

Variables	Units	Level 1	Level 2	Level 3
Pulse on time- T_{on}, (A)	µs	105	115	125
Pulse off time- T_{off}, (B)	µs	50	55	60
Peak current- I_p, (C)	A	10	11	12
Servo voltage- S_v, (D)	V	40	50	60

In order to generate machining data, a face centered central composite design (CCD) of RSM is used for the experimental plan in the present study. The detailed experimental plan involving number of experiments has been given in respective chapters. Design Expert 9 software has been used in the present work for RSM analysis. RSM consists of mathematical and statistical techniques utilized in the development of adequate functional relationships among responses and process parameters.

Figure 3.1. WEDM machine

Trchnical specifications of WEDM machine

Make : ELECTRONICA (INDIA)
Software : ELCAM
Specification : X: 250 mm, Y: 350 mm, Z: 200 mm
Control system : CNC
Axis control : 4 Axis
Taper : +/- 5 deg/100mm
Resolution : 0.001 mm
Dielectric tank capacity : 140 liters
Least I/P increment : 0.001mm
Wire Material : Zinc coated Brass wire
Wire Diameter : 0.25 mm
Input Parameters available: Pulse-on time, pulse-off time, peak current, flushing pressure, wire feed rate and servo voltage.

In the present work, an attempt has been made to investigate the effect of process parameters such as pulse on time (T_{on}), pulse off time (T_{off}), peak current (I_p) and servo voltage (S_v), on the response parameters such as MRR, SR, circularity and cylindricity errors, re-cast layer thickness and micro-hardness. Inconel-690 and Nimonic-263, nickel based super alloys being extensively used in aerospace, automotive and nuclear power applications were chosen as work materials. In this study, holes of 10 mm diameter (Figure 3.2) were machined on the Inconel-690 plate of 6.35 mm thickness and Nimonic-263 plate of 18.5 mm respectively.

3.3. Calculation of material removal rate

Material removal rate is the amount of material removed per unit time. Machining is done to produce circular holes as shown in Figure 3.2. MRR for the circular holes can be calculated using the equation (3.1).

$$MRR = \frac{® \ W_t(D^2 - d^2)}{4T} \text{ mm}^3/\text{ min} \qquad (3.1)$$

where, W_t = thickness of work piece (mm), D = diameter of the hole (mm), d = diameter of the boss (mm) and T = Time taken for machining (min).

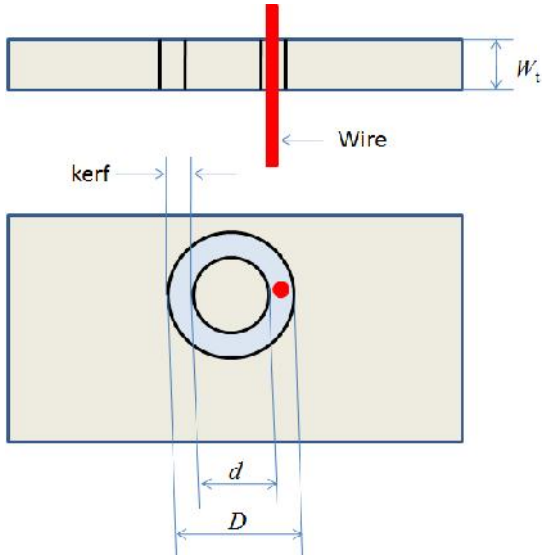

Figure 3.2. Circular hole machined by WEDM

Here the diameters of hole and the removed blanks are measured using co-ordinate measuring machine (CMM), and time taken to cut these holes at different sets of input levels are measured using a stop watch.

3.4. Measurement of Surface roughness

The German make Marsurf M-400 (Figure 3.3) surface roughness tester with a profile resolution of 8 nm has been used to measure the SR value of the machined parts directly.

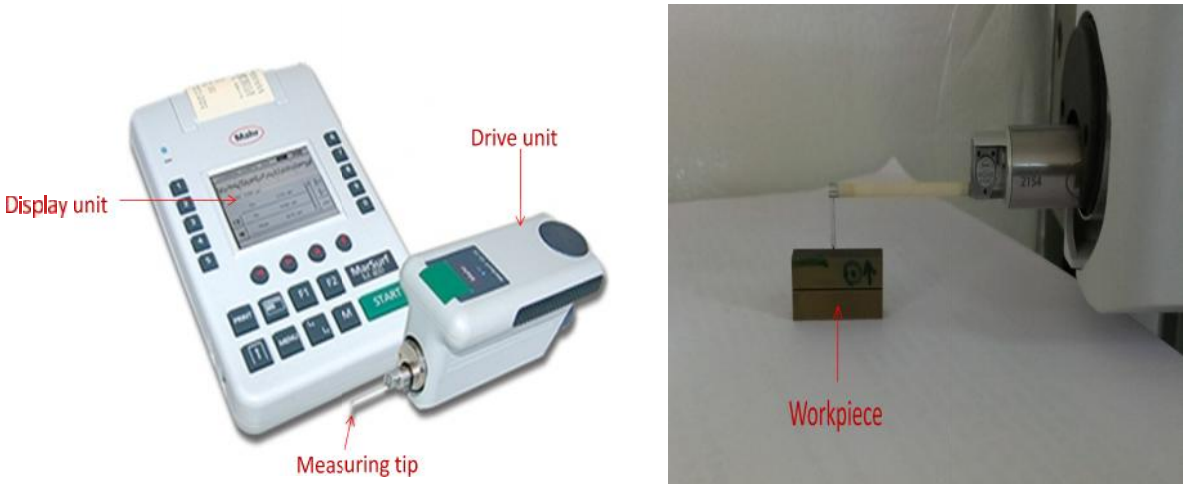

Figure 3.3. Marsurf M - 400

For use as a small measuring station as well as a mobile unit, the MarSurf M 400 fulfills the needs on the shop floor and in production and the measuring room. The skidless probe BFW 250 and the drive unit SD 26 enable the measurement and evaluation of not only the roughness depth but also waviness and profile criteria. The magnetic probe arm holder allows different probe arms to be changed quickly and easily within seconds without the use of tools. The motorized height adjustment enables automatic zero positioning and probe lifting. The Bluetooth function enables cable-free operation with this unit as well. Up to 250 measurements can be conducted with main-free operation due to the built-in battery. Traversing length of 5.6 mm, evaluation length of 4 mm have been set while measuring the samples. The number of readings taken in the present study is 5 for each sample and the average value has been calculated. The workpiece is oriented such that tracing is done across the predominant lay direction in order to capture the roughness details. Utmost care has been taken to isolate the measuring instrument from the external disturbances.

Technical specifications of MarSurf M400:

Type: Portable

Standard Parameters: As per DIN/ISO/JIS/ASME/MOTIF

Number of sampling lengths (n) (as per ISO/JIS): selectable 1 to 5

Measuring range: Min 350 micron

Traversing length (as per ISO/JIS): 1.75 mm, 5.6 mm, 17.5 mm, automatic, free entry.

Evaluation length (as per ISO/JIS): 1.25 mm, 4.0 mm, 12.5 mm.

Cut-off length (as per ISO/JIS): 0.25 mm, 0.8 mm, 2.5 mm, automatic

Profile resolution : Measuring range : ±250 µm = 8 nm.

Drive Unit SD26: Traversing length : 26 mm, measuring speed : 0.2 mm/s, 1 mm/s, Inclination adjustment: ±1.5^{o}, Height adjustment : 7.5 mm motorized.

Column & Stand: Granite base with support stand attachment.

Calibrated on: August, 2013.

3.5. Measurement of circularity and cylindricity

Circularity and cylindricity errors of the machined components are measured directly using a CMM of Mitutoyo make, CRT-Apex C-544 model, and the in-built algorithm software is based on least squares principle. It is a bridge type CNC controlled CMM consisting of a contact probe of touch and trigger type, and a means of positioning the probe in three dimensional space relative to the surface of a work part in order to obtain the data concerning the part size and geometry. The generated data is further converted into the required form using the inbuilt software. The resolution of this machine is 0.0001 mm and the software used in the CMM is MCOSMOS. The data generated from the measurements represent the position of the probe with respect to machine. This coordinate data is transferred to the computer system where the software converts it into the required form. The samples are oriented in vertical direction. To estimate the circularity error the data is collected at one section, on the periphery of the components. However, for cylindricity estimation, data is generated from three sections on the periphery of cylindrical components. Procedures for assessing the geometric errors are detailed in chapter 5.

Figure 3.4. Co-ordinate measuring machine

Technical specification of CMM:

Name: 544 Crysta

Made: Mitutoyo Corporation, Japan

Probe: Touch trigger type

Measuring range: X Axis – 505 mm, Y axis – 405 mm, Z Axis – 405 mm

Accuracy: MPEE (1.7+3L/1000) µm

Resolution: 0.0001 mm

Drive Speed: Moving speed – 0 - 80 mm/sec

Measuring speed - 3 mm/sec

Specification of Probe: Make: Renishaw

Type: Touch trigger

Probe diameter: 3 mm

Calibrated date: 2013

3.6. Measurement of re-cast layer thickness

The re-cast layer of the machined surfaces are observed and measured using scanning electron microscopy (SEM) of Tescan make VEGA 3 LMU model as shown in Figure 3.5. It is a fully PC controlled unit with conventional tungsten heated cathode intended both for high vacuum as well as low vacuum operations. Outstanding optical properties, flicker-free digital image with good clarity, sophisticated user-friendly software for microscope control and image capturing using Windows platform, standard formats of stored images, easy image management, processing and measurements, automatic setup of the microscope and many other automated operations are among the characteristic features of the equipment. An inbuilt mechanism to draw the lines and to measure the distance between lines is available in the existing PC software. By using this phenomenon the re-cast layer thickness has been measured. As the recast layer thickness is not constant throughout the periphery of the component, it is measured at different locations and the average value has been considered.

Figure 3.5. Scanning electron microscope

Technical specifications of SEM:

Electron Gun: Tungsten heated cathode

Resolution: High Vaccum Mode (SE): 3 nm at 30 kv / 2 nm at 30 kb

Low Vaccum Mode (BSE, LVSTD): 3.5 nm at 30 kv / 2.5 nm at 30 kv

Magnification: 2x – 1,000,000x (for 5" image width in Continual Wide field/Resolution

Maximum field of view: 24 mm at WD 30 mm

Accelerating Voltage: 200 V to 30 kV

Probe current: 1 pA to 2 µA

Scanning Speed: From 20 ns to 10 ms per pixel adjustable or continuously

Number of ports: 11

Chamber suspension: pneumatic

Specimen Stage: Type: Compucentric, fully motorized

Stage Movements: X=80 mm (-40 mm to + 40 mm)

Y=60 mm (-30 mm to + 30 mm)

Z= 47 mm

Rotation: 360º continuous

Tilt: -80º to + 80º (WD and sample size dependent)

3.7. Measurement of micro-hardness

The term hardness is the ability of a material to resist permanent deformation. The larger the resistance to deformation, the harder the body appears. There are four common methods available to measure the hardness of any material such as Brinell, Knoop, Rockwell, and Vicker's hardness tests. Vickers hardness testing method is simple as compared to others and is suited well for all metals (Herrmann, 2011). In this method an indenter of a straight diamond pyramid with an angle between opposite faces of 136^0, is applied under a specific load on to the surface of the material to be tested for a set time interval. According to the law of proportional resistance, the indentation surface is proportional to the force applied. For micro hardness studies usually the range of load is taken to be 5 g to 1000 g and the dwell time is considered in the range 10 to 15 sec. In the present study a load of 500 g is applied for 10 sec as dwell time.

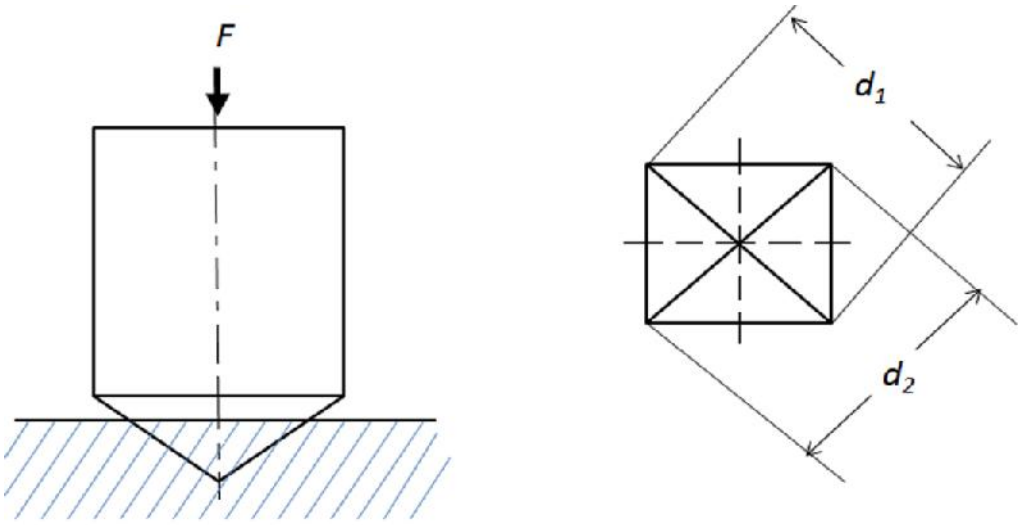

(a) Indentation (b) Measurement of indent

Figure 3.6. Hardness measurement using Vicker's hardness tester

After the test, an indentation is formed as shown in Figure 3.6. From the indentation, diagonals are measured. Micro hardness of the machined sample for Vickers method is estimated as

$$HV = \frac{0.1891F}{d^2} \tag{3.2}$$

where d is the arithmetic mean of diagonals and F is the load applied on the work material. Micro-hardness of the machined surfaces is measured using Chennai Metco make Economet VH 1 MD model as shown in figure 3.7.

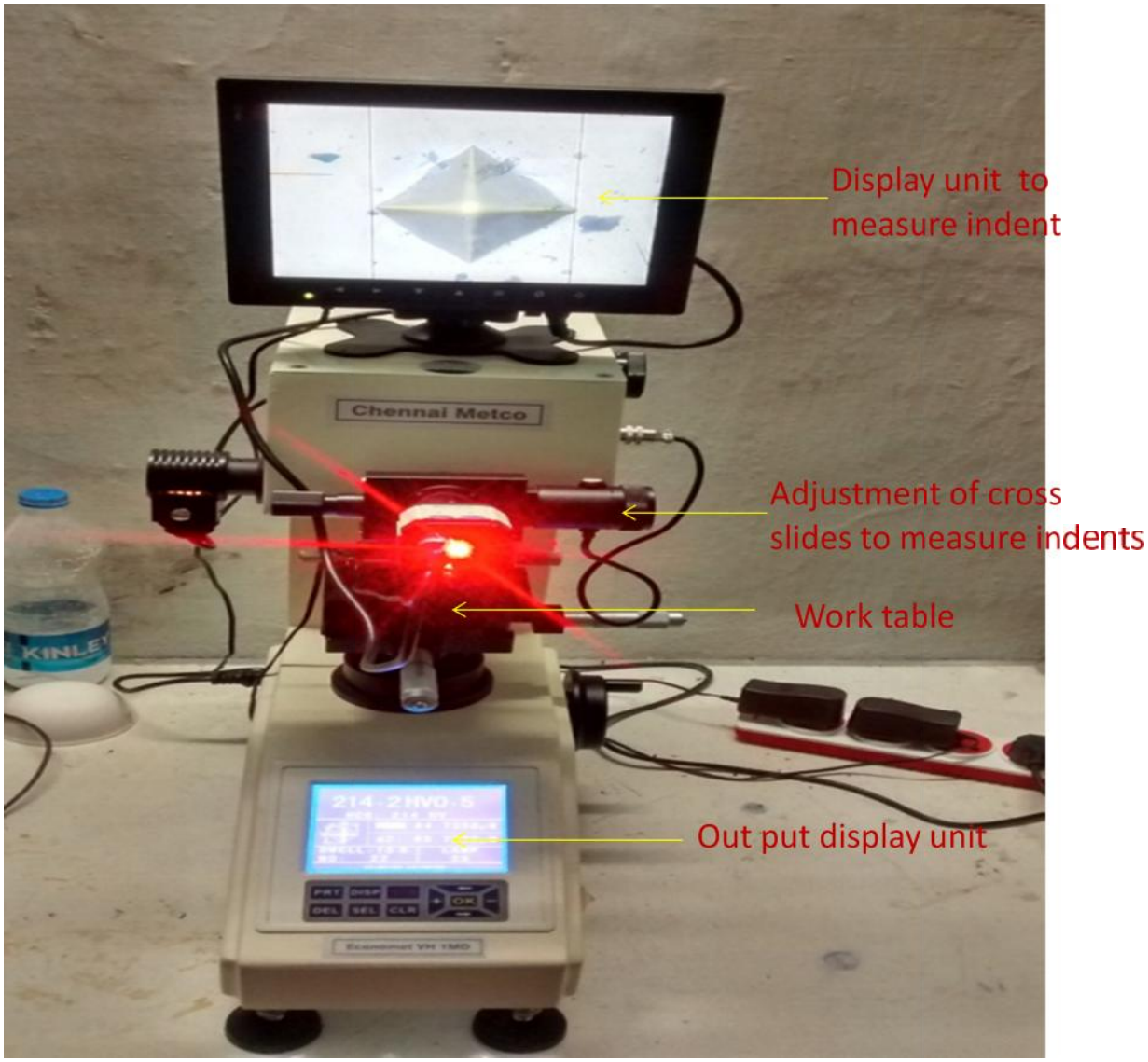

Figure 3.7. Vickers hardness tester

Technical specifications of Vicker's hardness tester:

Model : Econonet VH-1 MD Digital Automatic Turret Micro Vickers Hardness Tester with digital display

Usage Range: Heat treatment, carbide, quench hardened layer, the surface coating layer, steel, non-ferrous metal and small and thin shape parts, etc

Test Load: 10gf (0.098N)、25gf (0.245N)、50gf (0.49N)、100gf (0.98N)、 200gf (1.96N)、300gf (2.94N)、500gf(4.9N)、1kgf (9.8N)

Method of testing force applied: Automatic (Loading, Dwell, Unloading）

Test microscope magnification: 400X(Measuring)，100X（observation）

Duration time: 0 to 60 s

Min measuring unit: 0.031 μm

Hardness measuring range: 8 to 2900 HV

Conversion Scale: HRA, HRB, HRC, HRD, HRF, HV, HK, HBW, HR15N, HR30N, HR45N, HR15T, HR30T, HR45T

Data output: LCD screen display, Inside Printer, RS-232 Max Height of Specimen: 80mm

Distance of Indenter to outer wall: 95mm X-Y Testing table:

Dimension: 100*100mm Max mobile：25*25mm Power supply: AC220V+5%，50-60Hz

Overall Dimension: 405*290*480mm Net weight: About 25Kg

3.8. Energy Dispersive Spectroscopy (EDS)

Energy-dispersive X-ray spectroscopy (EDS or EDX), sometimes called energy dispersive X-ray analysis (EDXA) is an analytical technique used for the elemental analysis or chemical characterization of a sample. A beam of electrons is focused on the sample being studied. At rest, an atom within the sample contains ground state (or unexcited) electrons in discrete energy levels or electron shells bound to a nucleus. The electron beam may excite an electron in an inner shell, ejecting it from the shell while creating an electron hole where the electron was. An electron from an outer, higher energy shell then fills the hole and the difference in energy between the higher energy shell and the lower energy shell may be released in the form of an x-ray.

The number of x-rays emitted from a specimen can be measured by an EDS spectrometer. As the energy of the x-rays are characteristic of the difference in energy between the two shells and of the atomic structure of the element, from which they were emitted, this method allows the elemental composition of the specimen to be measured. An EDS coupled with SEM as shown in Figure 3.8 was used in the present study.

Figure 3.8. EDS coupled with SEM

CHAPTER 4

A MODIFIED CUCKOO SEARCH ALGORITHM FOR OPTIMIZATION OF MRR AND SR

4.1. Introduction

The performance of WEDM process is assessed in terms of material removal rate (MRR), surface roughness (SR), wire wear rate (WWR), kerf and cutting speed etc. However, MRR and SR are very important response parameters for any machining process. Surface roughness affects several functional attributes of parts, such as friction, wear and tear, light reflection, heat transmission, ability of distributing and holding a lubricant and coating. The desired surface finish is usually specified for the components and appropriate processes are required to maintain the quality. Hence, the inspection of surface roughness of the work piece is important to assess the quality of a component. MRR is the rate at which the material is removed. In order to meet the customer requirement in terms of due date, the manufacturer always tries to maximize the MRR. Optimization of these response parameters is essential for any machinist to meet their functional and economical aspects. From the literature it can be observed that, several attempts have been made to investigate the influence of WEDM process parameters on the response parameters and also to optimize them. Researchers in the past used grey relational analysis (Chiang and Chang 2006; Balasubramanian and Ganapathy 2011) and Taguchi (Sarkar et al. 2006, aravind et al. 2010) techniques to optimize the responses. Although, in reality, a process parameter varies continuously, experiments are conducted, based on these designs, at discrete levels. Therefore, these techniques can only yield sub-optimal solutions. Global optimal solution may lie outside the conducted experiments. In order to determine the global optimal solution, researchers in the past applied other optimizing techniques such as GA, PSO, and ABC (Mahapatra and Patnaik 2007, Rao and Pawer 2009, Rao and Pawar 2010) etc.

Among different optimization techniques, Cuckoo search (CS) algorithm was found to be efficient in yielding the global optimal value and this algorithm was found to outperform GA and PSO techniques in terms of speed, accuracy and simplicity of computations (Yang and Deb 2009, Yang and Deb 2010 and Gandomi et al. 2013). However, the accuracy of CS heavily depends

upon the initial solution and its location from the target value and therefore it may involve many generations. Furthermore, the evolutionary operators are applied in each generation. This could lead to delay in convergence. In order to improve the performance of cuckoo search further, an attempt has been made in the present work to propose a modified cuckoo search involving two-stage initialization. Benchmark functions have been used to test the performance of the proposed method. Furthermore, the proposed method has been applied to WEDM process. Inconel-690 and Nimonic-263, nickel based super alloys, have extensive applications in aerospace, automobile and nuclear power sectors. The proposed algorithm was found to be accurate and fast as compared to the existing cuckoo search. The machining data generated in this work on these super alloys will also be useful to the industry.

This chapter describes cuckoo search algorithm and its steps, modified cuckoo search algorithm and application of this proposed method to optimize MRR and SR of Inconel-690 and Nimonic-263. This chapter also gives the Pareto optimal solutions of MRR and SR for Inconel-690 and Nimonic-263 work materials.

4.2. Cuckoo search algorithm

Cuckoo search algorithm, a meta-heuristic optimization algorithm, was developed by Yang and Deb based on the breeding behavior of cuckoos and the characteristics of Levy flights of some birds and fruit flies. Some cuckoo species lay their eggs in the host nests. The basis for this optimization algorithm lies in the laying of eggs and breeding of cuckoos. Some cuckoos imitate the colors and pattern of eggs of a few species, which they select as host nest. This will reduce the probability of eggs being abandoned by the host bird and also increases their re-productivity. The eggs, which are not similar to that of host bird nest, are detected and killed. The grown eggs reveal the suitability of the nests in that area. The cuckoo optimization algorithm searches the area in which more eggs will survive and re-productivity is higher (Rajabioun 2011). The major assumptions in the cuckoo search algorithm are:

- Each cuckoo lays one egg, in a randomly selected nest at a time.
- The nests of high quality eggs carry over to next generations.

- There is a chance of alien egg getting recognized due its quality by the host bird with a probability of $p_a \in [0, 1]$. The host bird will abandon the nest completely or destroy the alien egg if recognized, and build a new nest at new location.

The major steps involved in cuckoo search algorithm have been described (Valian et al. 2013) below.

Initialization

In any evolutionary algorithm, the initial population is generated for each control variable using the following equation (4.1) (El Ela et al. 2010). The value of j^{th} variable's i^{th} particle is given by:

$$x_{i,j} = x_j^{min} + \text{rand}(0, 1) \left(x_j^{max} - x_j^{min} \right) \quad (4.1)$$

Where, $i = 1, 2, \ldots, ps$; $j = 1, 2, \ldots, ncv$, ps = population size, and ncv = number of control variables. x_j^{min} and x_j^{max} are the lower and upper bounds of j^{th} control variable. In general, the initial population vector (pv) of size ($ps \times ncv$) is generated and is used for further evolutionary operations. The single stage initialization of any evolutionary algorithm is shown in equation (4.2).

$$pv = \begin{bmatrix} x_{11} & x_{12} & x_{13} \ldots\ldots\ldots x_{1ncv} \\ x_{21} & x_{22} & x_{23} \ldots\ldots\ldots x_{2ncv} \\ \ldots\ldots\ldots\ldots\ldots\ldots\ldots \\ x_{ps1} & x_{ps2} & x_{ps3} \ldots\ldots x_{ps\,ncv} \end{bmatrix} \quad (4.2)$$

Levy flights

The cuckoo randomly chooses the position of host nest to lay an egg using Levy flights random walk and is given in equations (4.3), (4.4) and (4.5) (Chandrasekaran and Simon 2012).

$$x_{pq}(t+1) = x_{pq}(t) + s_{pq} \sim Levy(\alpha) \quad (4.3)$$

$$s_{pq} = x_{pq}^t - x_{fq}^t \quad (4.4)$$

$p, f \in \{1,2,\ldots nhn\}$ and $q \in \{1,2,\ldots ncv\}$

$$Levy(\alpha) = \left| \frac{\Gamma(1+\alpha) \times \sin\left(\frac{\pi \times \alpha}{2}\right)}{\Gamma\left(\frac{1+\alpha}{2}\right) \times \alpha \times 2^{\left(\frac{\alpha-1}{2}\right)}} \right|^{1/\alpha} \quad (4.5)$$

where, $x_{pq}(t+1)$ is the value of q^{th} variable in p^{th} host nest at next generation, s_{pq} is the step size, λ is a constant and is generated randomly in between1 and 3, t is the current generation number, α is a constant generated randomly between -1 and 1, *nhn* is the number of host nests and *ncv* is the number of control variables.

Recombination or survival rate of eggs

There is a chance for the host bird to identify the alien egg, with a probability value associated with the quality of an egg, Pro_p as estimated using equation (4.6).

$$Pro_p = \frac{0.9Fit_p}{\max(Fit)} + 0.1 \quad (4.6)$$

Where, Fit_p is the fitness value of an individual p and is proportional to the quality of that egg in that corresponding nest. If the calculated Pro_p is greater than that of randomly generated $p_a \in [0,1]$, the egg will be survived and carried to the next generation, otherwise egg will be recognized by the host bird and it will be destroyed or abandon the existing nest and build a new nest at new location. Then the cuckoo will find a new nest to lay an egg. These newly generated nests are combined with the earlier survived ones to form a new population vector for further operations.

Selection

In the present work, sorting and ranking selection process has been used. With this method, at each generation, the fitness value and its associated strings are ranked. Then, the optimal value and its corresponding string are selected based on the objective function for the next generation until the stopping criterion is reached.

Stopping criteria

The following are the criteria commonly used to stop an iterative process:

1) Maximum number of generations: When the number of generations equals the maximum number of generations specified by the user, the process comes to end.
2) Specified tolerance: If the accuracy obtained during iterative process is less than specified tolerance, the execution will be terminated.

Based on the observed results on several data sets, first criterion is used in the current work.

4.3. Modified cuckoo search algorithm

In any evolutionary algorithm, the optimization process will start with initialization step. Once the initialization is done, all the operators of the algorithm are applied in a sequence to find feasible solutions in each generation. In order to guide the search to global optimal solution, the optimization process will be repeated until a stopping criterion is met. This procedure is followed in the existing cuckoo search also. However, the accuracy and the convergence rate will heavily depend upon the initial population and its location from the target value. Furthermore, this method applies all the operators of the algorithm in every iteration and this could delay the convergence. However, the modified cuckoo search (MCS) proposed in this work involves two-stage initialization process. This process enhances the probability of finding optimal solution. The methodology is presented in Figure 4.1. In the first stage, a sub population vector of size (*sspv*×*ncv*) is formed. The value of objective function for each string is evaluated in the sub population vector. The best string from the sub population vector based on its fitness is selected. This procedure is repeated for all the sub-population vectors. In the second stage, all the best strings from the sub population vectors are combined to form a new population vector of size (*nspv*×*ncv*) and the evolutionary operators are applied on this newly formed population vector.

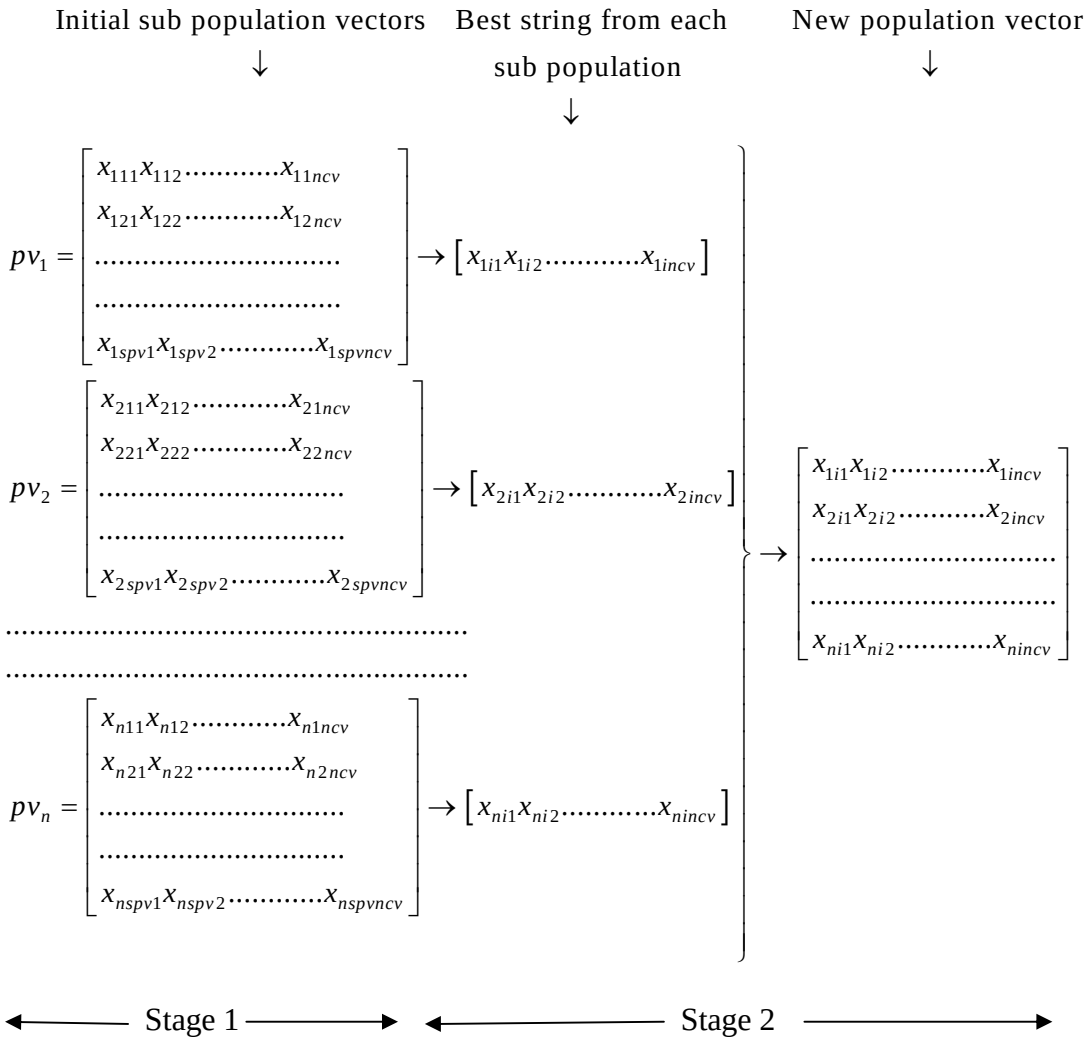

Figure 4.1 Two stage initialization of proposed MCS algorithm

It should be noted that application of evolutionary operators will consume some computational time. Therefore, in the proposed method, evolutionary operators were not applied on the earlier sub-population vectors. Only fitness of the strings was evaluated. Operators were applied only after the new population vector is formed. Therefore accuracy and fast convergence resulted from the proposed method can be attributed to the following reasons:

(1) The newly formed population vector will be closer to the global optimal solution and therefore, overall number of generations required to reach the target value will be reduced significantly.

(2) Evolutionary operators are applied from the second stage of the process instead of initial sub-populations.

Furthermore, the proposed method requires less memory for storing the populations. The steps in the proposed two-stage cuckoo search algorithm have been shown in Figure 4.2.

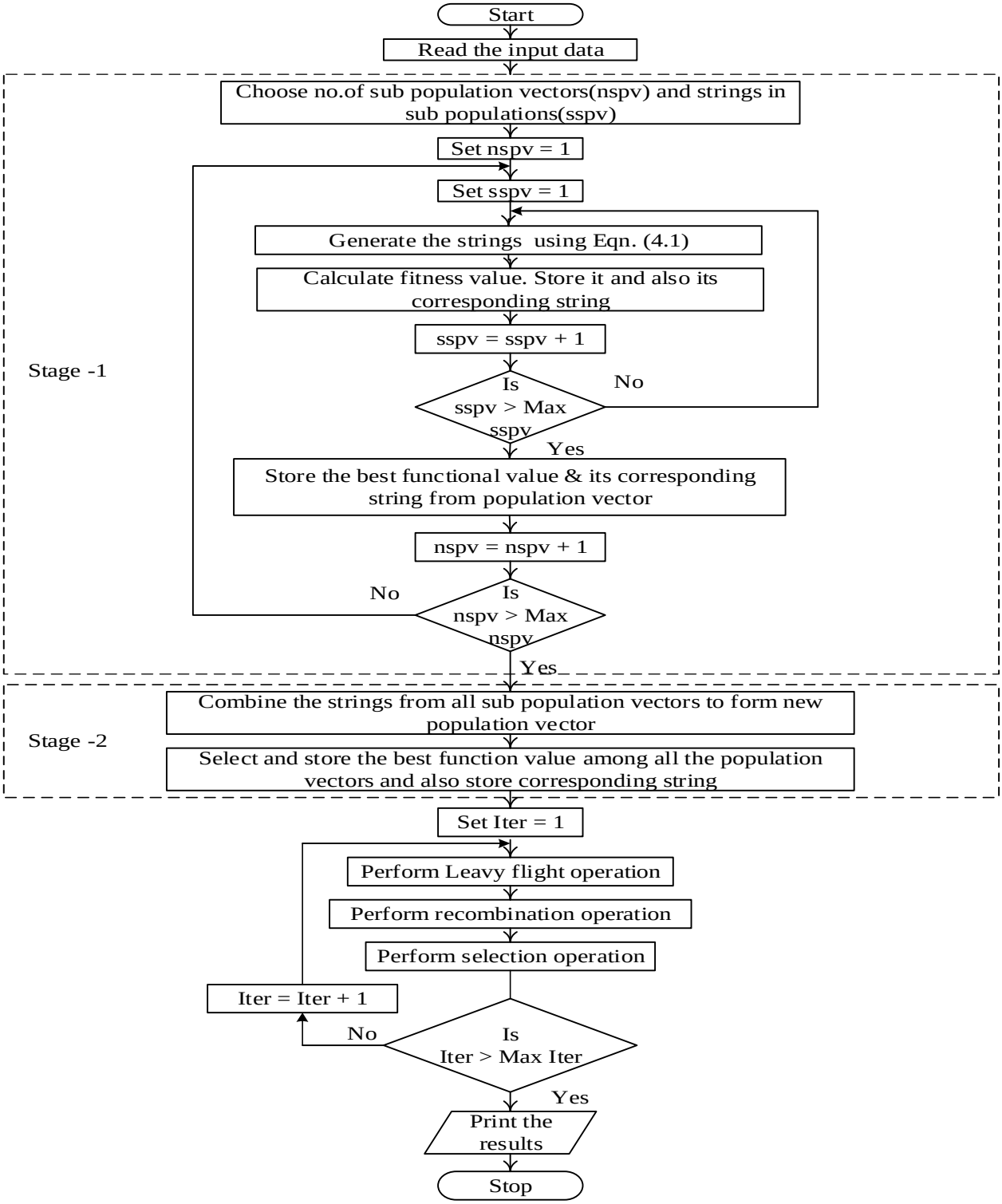

Figure 4.2. Steps in proposed MCS algorithm

4.4. Testing of proposed method

In order to test the robustness of the existing cuckoo search and the proposed algorithms, they are tested against benchmark functions such as Himmelblau function, Booth's function, Freudenstein Roth function, Goldstein Price function, and Leon function. The test results for Himmelblau function and Booth's function are presented in this section.

Himmelblau function

The objective of Himmelblau function is to minimize and is given as in equation (4.7).

$$f(x_1, x_2) = \left(x_1^2 + x_2 - 11\right)^2 + \left(x_1 + x_2^2 - 7\right)^2 \quad (4.7)$$

Where, the variables are in the interval $(0 \leq x_1, x_2 \leq 6)$.

The function value is 0 at $x_1 = 3$ and $x_2 = 2$.

The function was solved using GA (Deb, 2013), existing cuckoo search and proposed methods. Comparisons are presented in Table 4.1.

Table 4.1 Comparison of results using standard functions for 100 generations

Standard Test Function	Parameter	Existing GA method	Existing Cuckoo search	Proposed MCS method
Himmelblau function	$x_1$value	3.003	3.001	3.0004
	x_2 value	1.994	1.9887	1.9988
	Min functional value	0.001	0.000123	0.0001
	Number of generations	---	72	19
Booth's function	$x_1$value		0.9994	0.9998
	x_2 value		2.9625	3.0002
	Min functional value		0.0018174	0.00029
	Number of generations		61	27

The Himmelblau function values with GA, existing cuckoo search method and proposed method are 0.001, 0.000123 and 0.0001 respectively. The proposed method, thus, is performing better. Furthermore, the existing cuckoo search and the proposed methods are tested for different number of generations such as 25, 50, 75 and 100 for the Himmelblau function. Plots for 25 and 100 generations are shown in Figure 4.3 and 4.4. It can be observed that the convergence rate of proposed method is faster than that of the existing cuckoo search. For 25 numbers of generations, convergence rate is almost same with both the methods. It can be observed from the figure that the initial solution with existing method is about 1.2. There was no improvement in the solution up to 5^{th} generation. However, there is a drastic improvement from 5^{th} to 6^{th} iteration and the value is about 0.4. Further, there were gradual improvements in the solution and the global optimal solution was obtained in the 14^{th} iteration with function value of about 0.05. However, the initial solution with the proposed MCS method is found to be 0.2, which is much better than the initial value of existing method. This initial solution is much closer to the target value and it was possible due to the mechanism of the proposed two-stage initialization concept as detailed in section 4.3. It can be observed from the Figure 4.3 that the there is no improvement in the functional value up to 7^{th} generation. Marginal improvements were observed from 7^{th} to 10^{th} iterations. The global optimal value of zero has been obtained at 14^{th} iteration. Hence, the proposed MCS method is performing better than the existing cuckoo search method in terms of accuracy and convergence rate. For 100 numbers of generations, the number of generations required to yield optimal functional value with proposed method and the existing method are respectively 19 and 72. Optimal values obtained are closely matching with both methods.

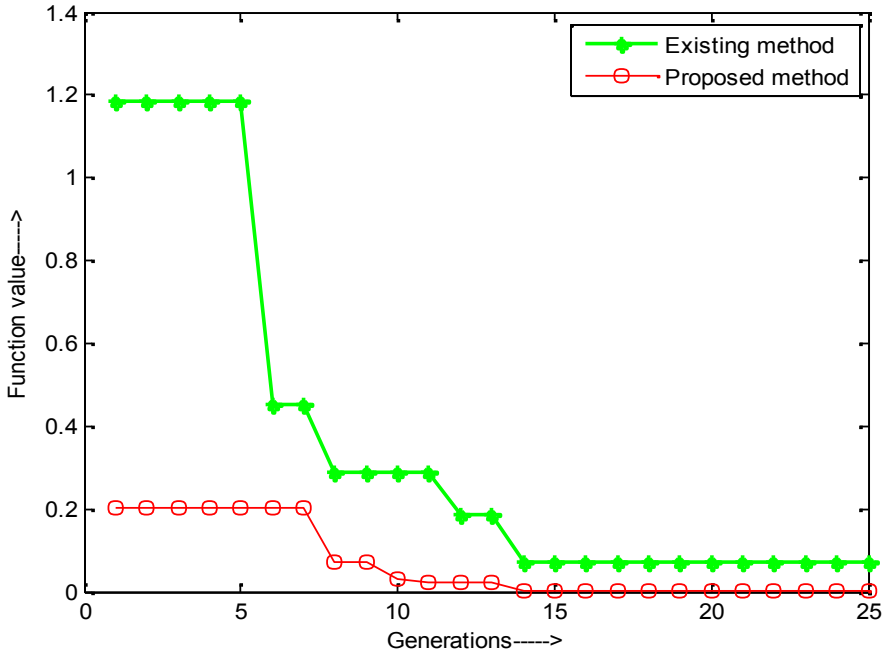

Figure 4.3. Performance of existing cuckoo and proposed methods against Himmelblau function for 25 generations

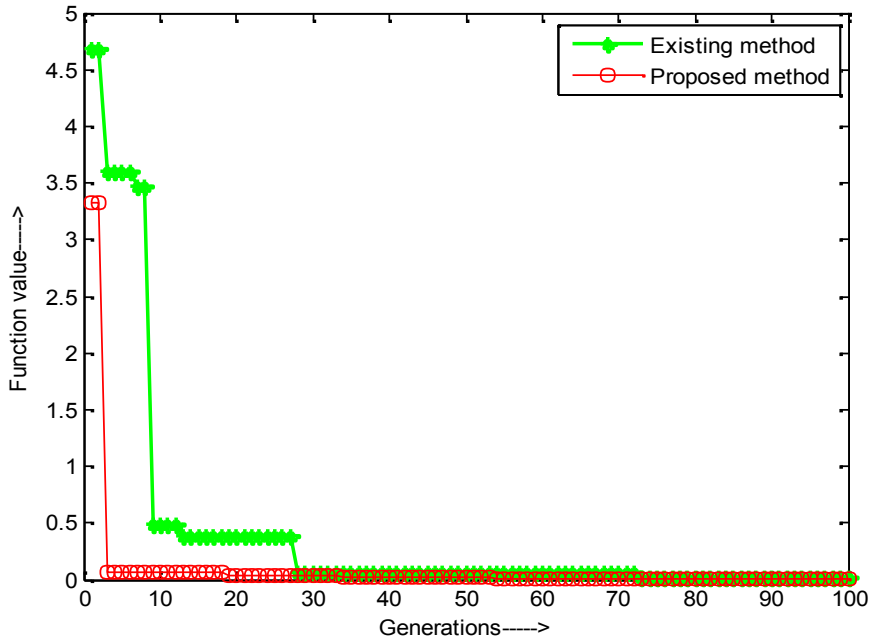

Figure 4.4. Performance of existing cuckoo and proposed methods against Himmelblau function for 100 generations

Booth's function

The objective of Booth's function is to minimize and is given by equation (4.8).

$$f(x_1, x_2) = (x_1 + 2x_1x_2 - 7)^2 + (2x_1 + x_2 - 5)^2 \quad (4.8)$$

Where $(-10 \le x_1, x_2 \le 10)$

The function value is 0 at x_1=1 and x_2=3.

The existing cuckoo search and proposed methods have been applied against the Booth's function and the results are presented in Table 4.1. The Booth's function values obtained by existing cuckoo search method and proposed method are 0.0018174 and 0.00029 respectively. Thus the proposed method is performing better. Furthermore, plots for 25 and 100 generations are shown in Figures 4.5 and 4.6. For 25 generations, the number of generations required to yield optimal functional value with proposed and existing methods are 11 and 23 respectively and proposed method yields better optimal value than that of existing method. For 100 generations, the number of generations required to yield optimal functional value with proposed and existing methods are 40 and 61 respectively and the proposed method yields better optimal value than that of existing method. These results show that the proposed method outperforms the existing method.

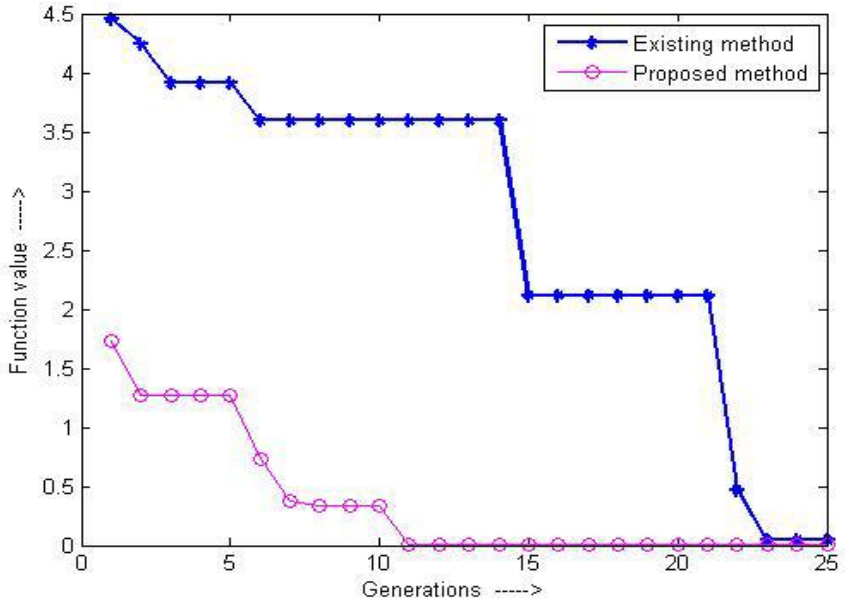

Figure 4.5. Performance of existing cuckoo and proposed methods against Booth's function for 25 generations

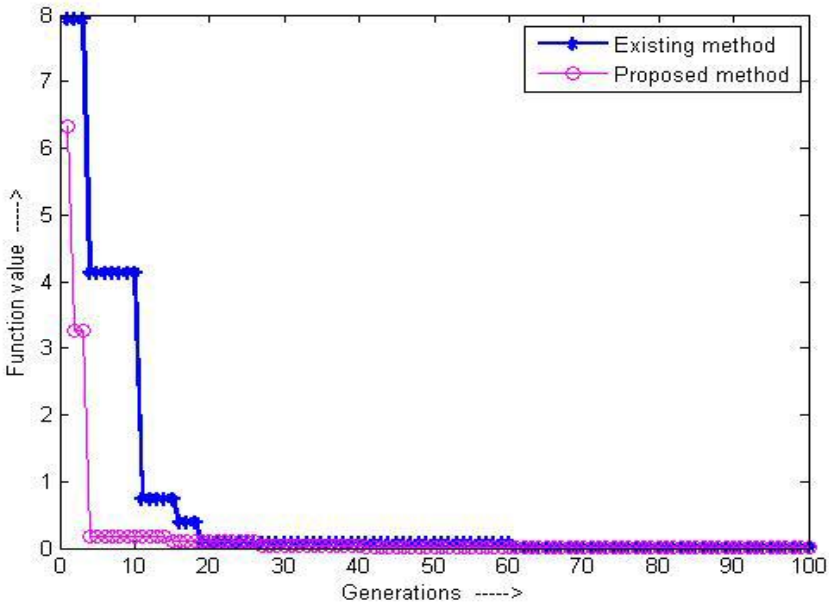

Figure 4.6. Performance of existing cuckoo and proposed methods against Booth's function for 100 generations

4.5. Application of MCS to optimize MRR and SR of Inconel-690

The modified cuckoo search approach has been applied to optimize MRR and SR while machining Inconel-690 using WEDM. In this study, holes of 10 mm diameter were machined on the Inconel-690 plate of 6.35 mm thickness as shown in Figure 4.7. In the present work, an attempt has been made to investigate the effect of process parameter such as pulse on time (T_{on}), pulse off time (T_{off}), peak current (I_p) and servo voltage (S_v), on the response parameters such as MRR and SR. The ranges and levels of process parameters are given in Table 3.1.

Figure 4.7. Inconel-690 material after machining

In order to generate machining data, a face centered central composite design (CCD) of RSM is used for the experimental plan in the present study. A CCD for 3 factors has been shown in Figure 4.8 for illustration purpose. Experimental points are classified into three categories such as centre, axial and cube (factorial) points. However, the present study involves 4 factors and it is difficult to present the graphical representation for the CCD of 4 factors. Therefore, the experimental plan is presented using Table 4.2 giving the details axial, cubical and center points information. A total of 30 experimental runs are conducted including 6 center points as presented in Table 4.2. After conducting trial experiments the ranges and levels are fixed Experiments are conducted as per the experimental plan and the results are presented in Table 4.3.

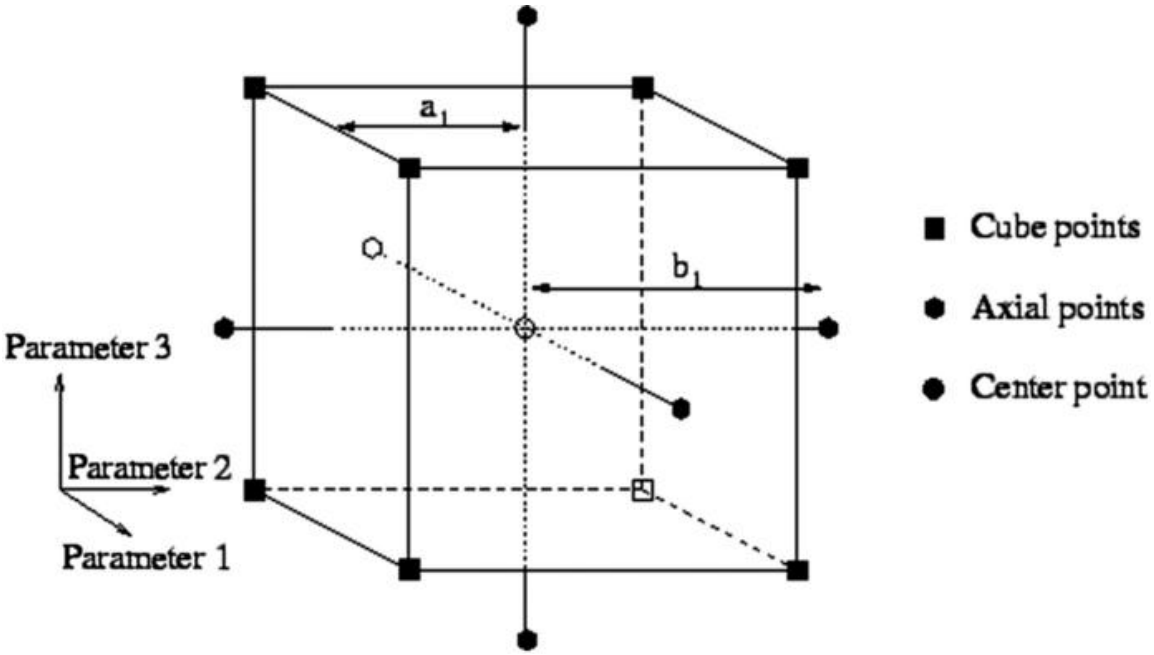

Figure. 4.8 CCD for 3 factors

Table 4.2 Experimental plan

Run order	Type of point	T_{on} (µs)	T_{off} (µs)	I_p (A)	S_v (V)
1	Center	0	0	0	0
2	Axial	0	1	0	0
3	Fact	1	-1	1	1
4	Axial	0	0	-1	0

5	Fact	-1	1	1	1
6	Axial	0	0	0	1
7	Fact	1	1	-1	-1
8	Center	0	0	0	0
9	Center	0	0	0	0
10	Fact	-1	-1	-1	-1
11	Axial	0	0	1	0
12	Fact	1	1	-1	1
13	Fact	1	-1	-1	-1
14	Fact	-1	1	1	-1
15	Center	0	0	0	0
16	Fact	-1	-1	-1	1
17	Axial	0	-1	0	0
18	Fact	-1	-1	1	1
19	Fact	-1	1	-1	-1
20	Fact	-1	1	-1	1
21	Axial	1	0	0	0
22	Axial	-1	0	0	0
23	Center	0	0	0	0
24	Fact	-1	-1	1	-1
25	Fact	1	-1	1	-1
26	Fact	1	1	1	1
27	Center	0	0	0	0
28	Fact	1	1	1	-1
29	Axial	0	0	0	-1
30	Fact	1	-1	-1	1

Table 4.3 Experimental results for Inconel-690

Run order	T_{on} (µs)	T_{off} (µs)	I_p (A)	S_v (V)	MRR (mm^3/min)	SR (µm)
1	115	55	11	50	0.3722	0.354
2	115	60	11	50	0.34049	0.357
3	125	50	12	60	4.06502	2.585
4	115	55	10	50	0.3648	0.336
5	105	60	12	60	0.499	0.559
6	115	55	11	60	0.345	0.373
7	125	60	10	40	0.4113	0.571
8	115	55	11	50	0.35309	0.371
9	115	55	11	50	0.3753	0.348
10	105	50	10	40	0.33727	0.378
11	115	55	12	50	1.71822	1.842
12	125	60	10	60	0.39578	0.377
13	125	50	10	40	0.58931	0.595
14	105	60	12	40	0.54517	0.669
15	115	55	11	50	0.36988	0.322
16	105	50	10	60	0.36228	0.371
17	115	50	11	50	0.37504	0.407
18	105	50	12	60	0.53466	0.447
19	105	60	10	40	0.27822	0.332
20	105	60	10	60	0.28444	0.276
21	125	55	11	50	0.43536	0.431
22	105	55	11	50	0.31819	0.317
23	115	55	11	50	0.3457	0.392
24	105	50	12	40	0.8808	0.761
25	125	50	12	40	5.843	3.253
26	125	60	12	60	2.1615	2.786
27	115	55	11	50	0.32263	0.422

28	125	60	12	40	3.44124	3.012
29	115	55	11	40	0.35897	0.533
30	125	50	10	60	0.38071	0.436

4.5.1. Results and analysis

(a) *ANOVA analysis for MRR*

ANOVA has been applied for each response to investigate the significance of process parameters and their contributions for the Inconel-690 work material. ANOVA is also used to model the response parameters in relation to their influencing parameters. The results of ANOVA for MRR are presented in Table 4.4.

Table 4.4 ANOVA results of MRR for Inconel-690

Source	SS	DOF	MS	F value	p-value	Percentage contribution
Model	5.160	6	0.860	138.80	< 0.0001	97.358
A- T_{on}	1.080	1	1.080	174.64	< 0.0001	20.377
B- T_{off}	0.100	1	0.100	16.11	0.0005	1.887
C- I_p	2.560	1	2.560	413.00	< 0.0001	48.302
D- S_v	0.044	1	0.044	7.06	0.0141	0.83
AC	0.250	1	0.250	40.03	< 0.0001	4.717
C^2	1.130	1	1.130	181.95	< 0.0001	21.321
Residual	0.140	23	6.20E-03			2.641
Cor. Total	5.300	29				100.00

From the ANOVA results (Table 4.4 and Figure 4.9 (a) - (e)), it can be observed that T_{on}, T_{off}, I_p, S_v and interaction effect of T_{on} and I_p are influencing the MRR. When the T_{on} increases, the energy applied will also increase and more amount of heat energy will be generated during this period, thereby increasing the MRR. When the T_{off} decreases it allows more productive discharges per unit time thereby increasing the MRR. When I_p increases, it leads to more

discharge power thereby MRR increases. At smaller value of S_v, the mean gap will be narrowed which leads to an increase in number of electric sparks, to speed up the machining rate. These results are in agreement with that of Singh and Garg (2009). R-Squared, Adjusted R-Squared and Predicted R-Squared values were found to be 0.973124, 0.966113, and 0.950433 respectively.

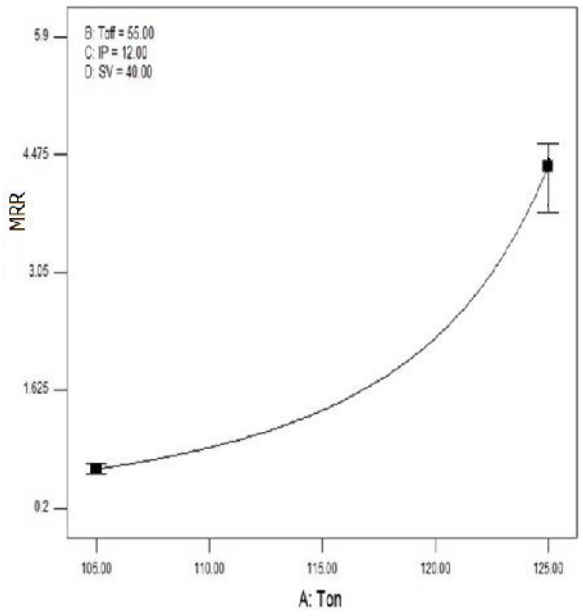

(a) Effect of T_{on} on MRR

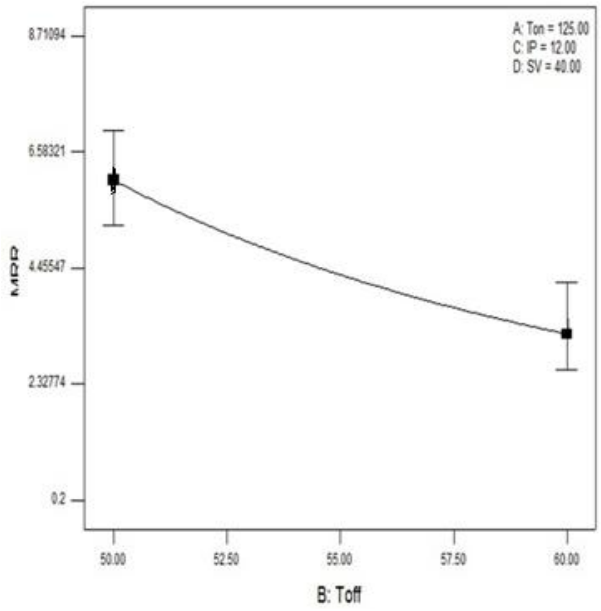

(b)Effect of T_{off} on MRR

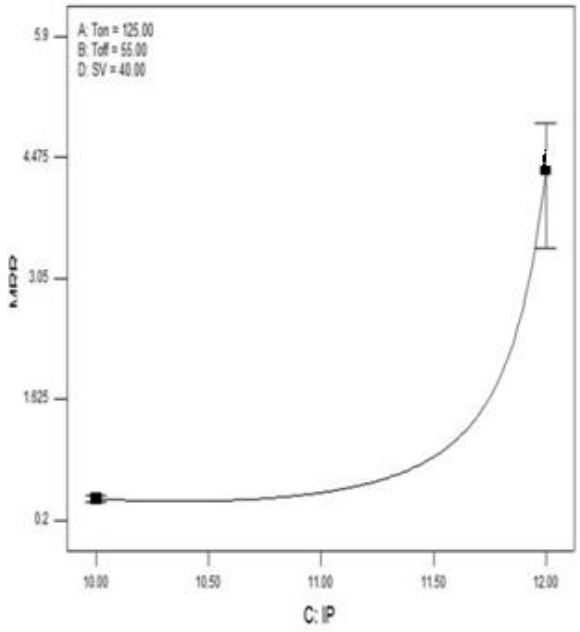

(c) Effect of I_p on MRR

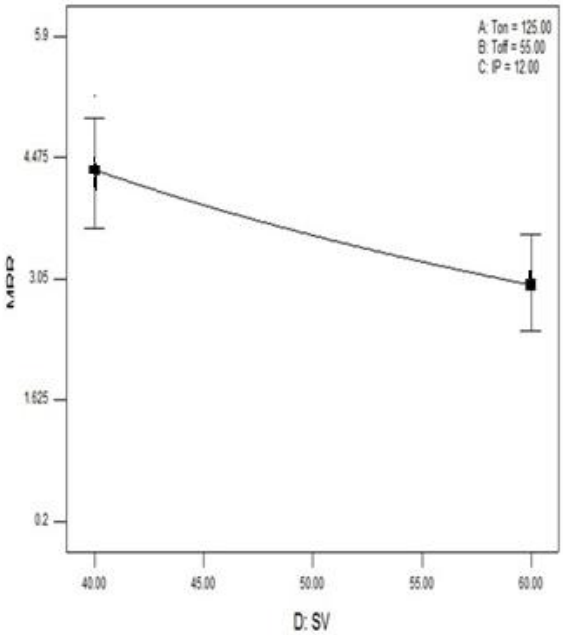

(d) Effect of S_v on MRR

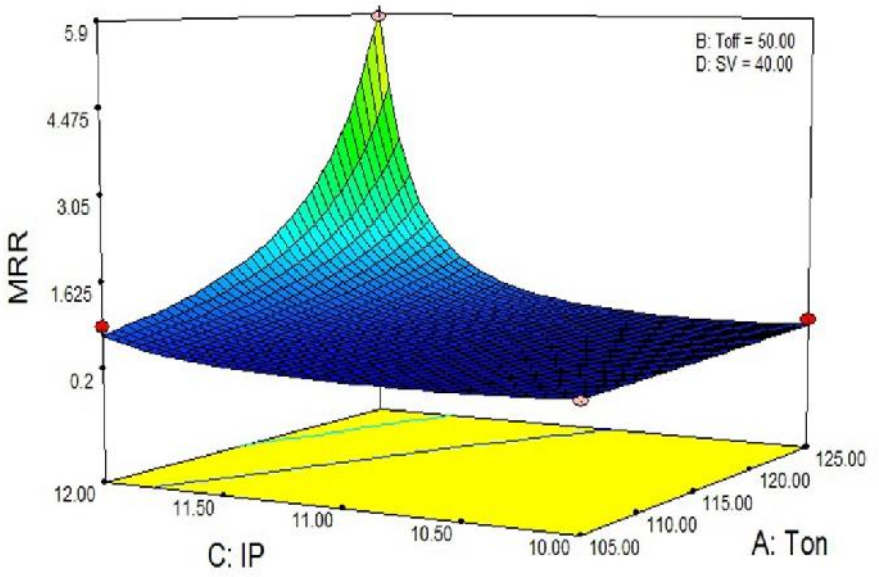

(e) Effect of interaction I_p and T_{on} on MRR

Figure 4.9. Effect of WEDM process parameters on MRR while machining Inconel-690

The mathematical model developed for MRR from ANOVA in coded form is given in equation (4.9).

$$MRR = \left(1.67 - 0.25A + 0.074B - 0.38C + 0.049D - 0.12AC - 0.40C^2\right)^{-1/2} \quad (4.9)$$

(b) ***ANOVA analysis for SR***

From the ANOVA results of SR as shown in Table 4.5 and Figure 4.10 (a) to (d), it is observed that T_{on}, I_p, S_v and interaction effect of T_{on} and I_p are influencing the SR. When the T_{on} increases, the energy applied will also increase and more amount of heat energy will be generated during this period which increases the machining speed and also increases the SR. When I_p decreases it leads to less discharge power thereby decrease the machining rate and SR. Kumar et al. (2012) confirmed that high pulse-on time and peak current will cause double sparking, which leads to increase in surface roughness. At higher values of S_v, the mean gap becomes wider which leads to decrease in number of electric sparks, thereby reducing the machining rate and increase

in surface finish. R-Squared, Adjusted R-Squared and Predicted R-Squared values were found to be 0.944074, 0.932422 and 0.91289 respectively.

Table 4.5 ANOVA results of SR for Inconel-690

Source	SS	DOF	MS	F value	p-value	Percentage contribution
Model	4.32633	5	0.86527	81.0273	< 0.0001	94.407
A- T_{on}	1.00238	1	1.00238	93.8671	< 0.0001	21.873
C- I_p	2.07037	1	2.07037	193.8790	< 0.0001	45.179
D- S_v	0.12986	1	0.12986	12.1609	0.0019	2.834
AC	0.18191	1	0.18191	17.0349	0.0004	3.969
C^2	0.94181	1	0.94181	88.1950	< 0.0001	20.552
Residual	0.25629	24	0.01068			5.593
Cor. Total	4.58262	29				100.000

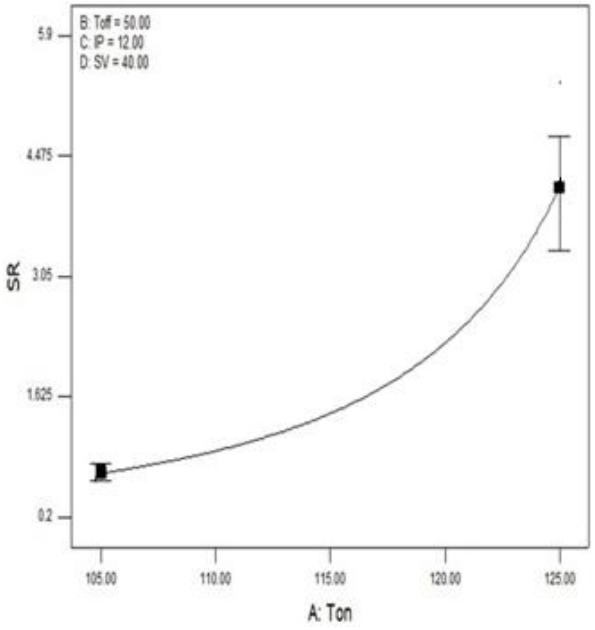

(a) Effect of T_{on} on SR

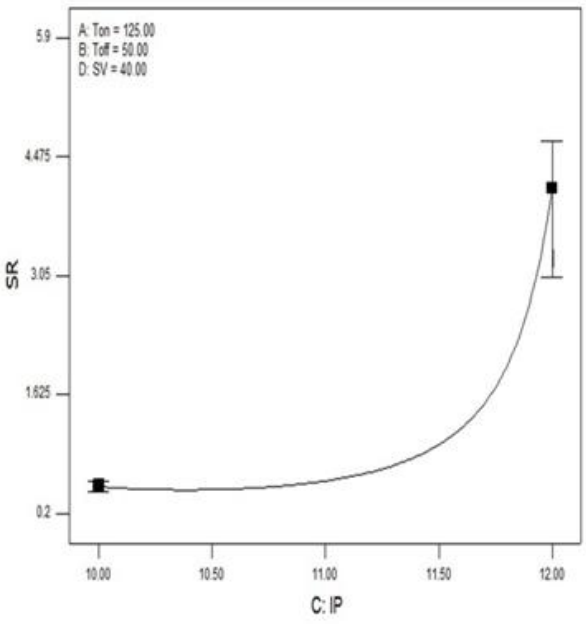

(b) Effect of I_p on SR

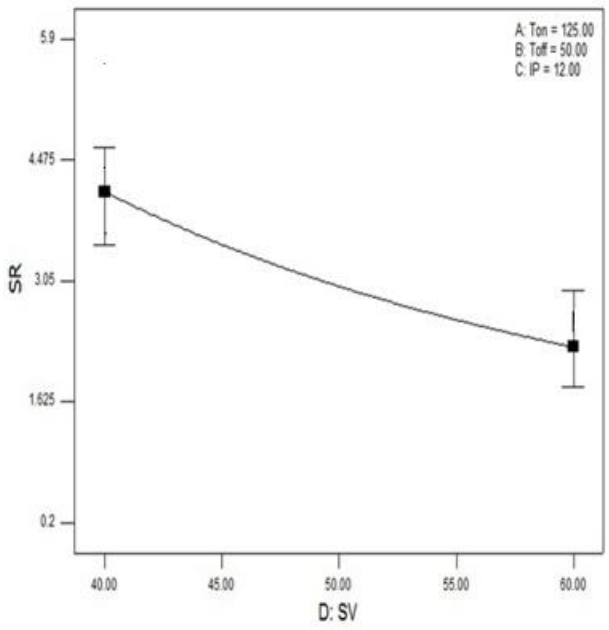

(c) Effect of S_v on SR

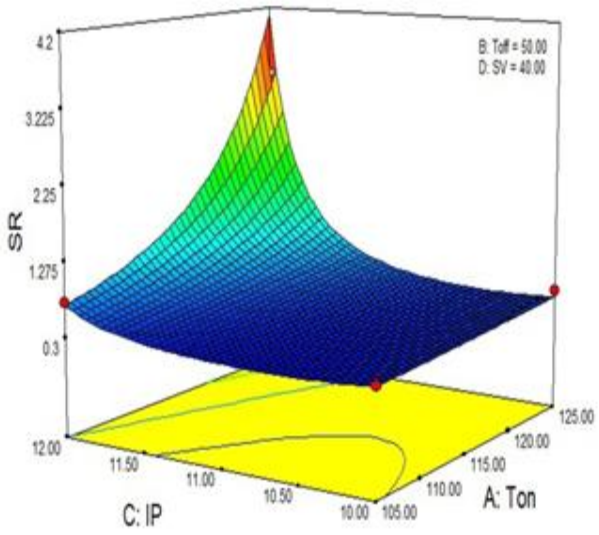

(d) Effect of interaction I_p and T_{on} on SR

Figure 4.10. Effect of WEDM process parameters on SR while machining Inconel-690

The mathematical model developed for SR from ANOVA in coded form is given in equation (4.10).

$$SR = \left(1.62 - 0.24A - 0.34C + 0.085D - 0.11AC - 0.36C^2\right)^{-1/2} \qquad (4.10)$$

Results obtained using RSM, existing cuckoo search and the proposed methods are presented in Table 4.6 along with machining conditions. From the results it is observed that, MRR values using RSM, existing cuckoo search and proposed method are 5.8912 mm^3/min, 5.9799 mm^3/min and 6.0537 mm^3/min respectively. It is also observed that the computational times to obtain the optimal values with existing cuckoo search and proposed method for MRR are 0.2511 s and 0.2049 s respectively. Correspondingly the number of generations is 60 and 32 as shown in Figure 4.11.

Table 4.6 Optimal results from different methods for Inconel-690

Method		RSM	Existing cuckoo	Proposed method
MRR (mm^3/min)	Optimal value	5.8912	5.9788	6.0537
	Optimal conditions	T_{on}: 125, T_{off}: 50.28, I_p: 12, S_v: 40	T_{on}: 125, T_{off}: 50.78, I_p: 12, S_v: 40.3269	T_{on}: 124.99, T_{off}: 50, I_p: 12, S_v: 40.023
	Computational time	---	0.2511	0.2049
SR (µm)	Optimal value	0.2713	0.2552	0.255
	Optimal conditions	T_{on}: 106, T_{off}: 50.41, I_p: 10.98, S_v: 59.82	T_{on}: 105, T_{off}: 51.47, I_p: 10.70, S_v: 59.9405	T_{on}: 105, T_{off}: 58.69, I_p: 10.68, S_v: 60
	Computational time	---	0.255	0.2166

SR values using RSM, existing cuckoo search and proposed method are 0.2713 µm, 0.2552 µm and 0.2550 µm respectively. It is also observed that the computational times to obtain these values with existing cuckoo search and proposed method are 0.2638 s and 0.2166 s respectively. Number of generations required to yield optimal SR using the existing cuckoo search and proposed methods are 37 and 13 respectively as shown in Figure 4.12.

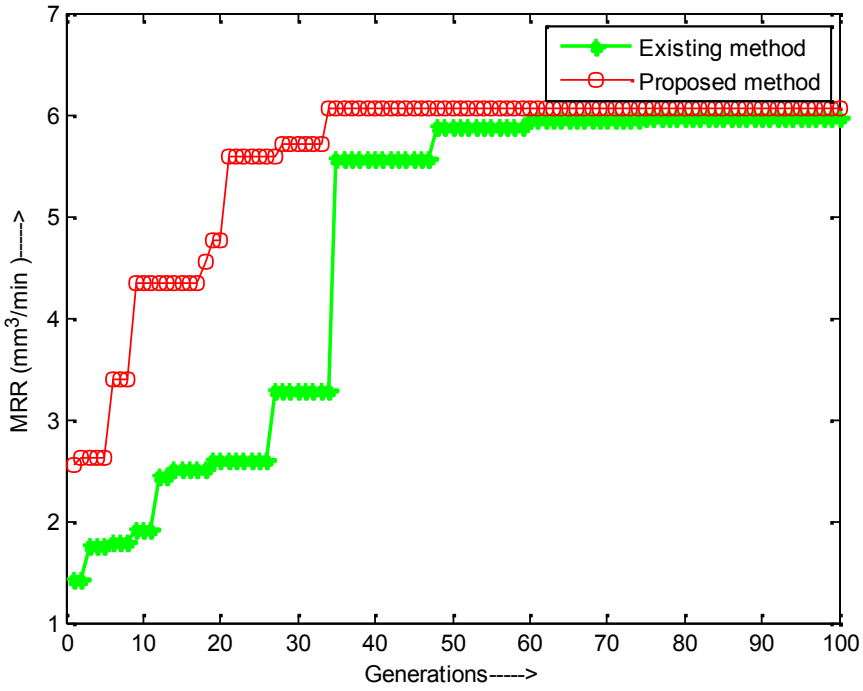

Figure 4.11. Performance of proposed method for MRR

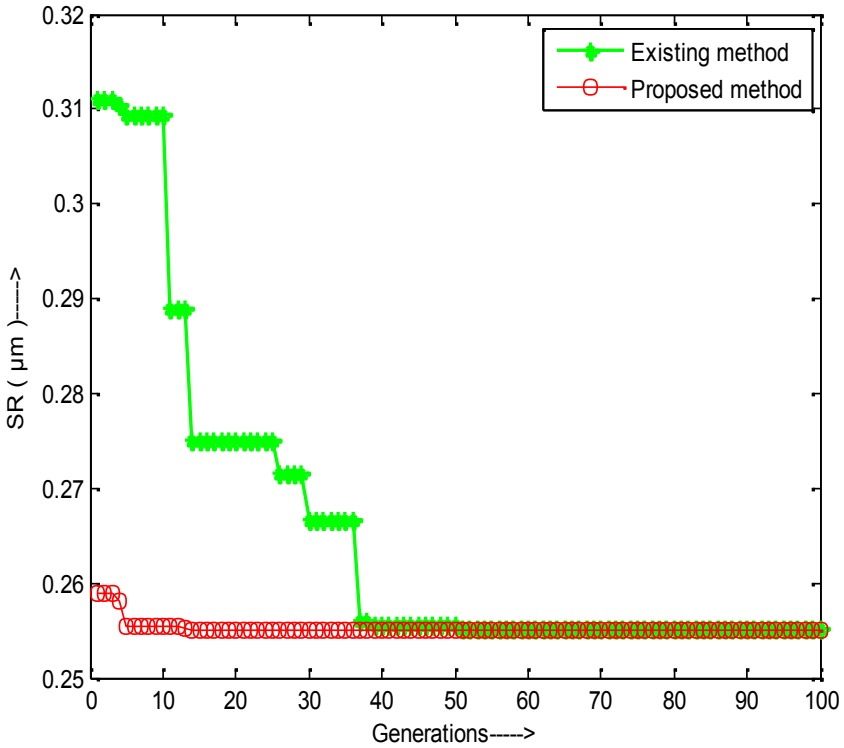

Figure 4.12. Performance of proposed method for SR

From the results, it is observed that the existing cuckoo search algorithm is giving better results than that of RSM. Furthermore, the results from the proposed algorithm are better than that of existing cuckoo search algorithm. The ranges of values for response parameters as obtained using the experimentation are observed to be too small. In general, if these ranges increase, the difference between the response values obtained by the RSM, existing cuckoo and the proposed methods may be significant and the importance of the proposed modified cuckoo search algorithm can be noticed. In order to minimize the manufacturing and measurement uncertainties, validation experiments were conducted three times and measurements were carried out for five times and then the average value has been reported for the comparison purpose. It can be observed that, the deviations between experimental results and the predicted values for MRR and SR are 3 % and 4 % respectively as presented in Table 4.7. Since the proposed algorithm does fine search around the global optimal solution, it is able to yield better results.

Table 4.7 Confirmation test results for Inconel-690

Response and Conditions	Predicted value from proposed method	Experimental Value	Deviation in percentage
MRR (mm^3/min)	6.0537	5.871	3
T_{on}: 125, T_{off}: 50, I_p: 12, S_v: 40			
SR (µm)	0.2550	0.265	4
T_{on}: 105, T_{off}: 59,I_p: 11, S_v: 60			

4.6. Application of MCS to optimize MRR and SR of Nimonic-263

The modified cuckoo search method has also been applied to optimize MRR and SR of Nimonic-263 while machining using WEDM. In this study, holes of 10 mm diameter were machined on the Nimonic-263 plate of 18.5 mm thickness as shown in Figure 4.13. Attempts are made to investigate the effect of process parameters such as pulse on time (T_{on}), pulse off time (T_{off}), peak current (I_p) and servo voltage (S_v), on the response parameters such as MRR and SR. In order to generate machining data, a Face centered Central Composite Design (CCD) of RSM is used for the experimental plan in the present study. After conducting trial experiments the ranges and levels are fixed. A total of 26 experimental runs are conducted including 2 center points as presented in Table 4.8.

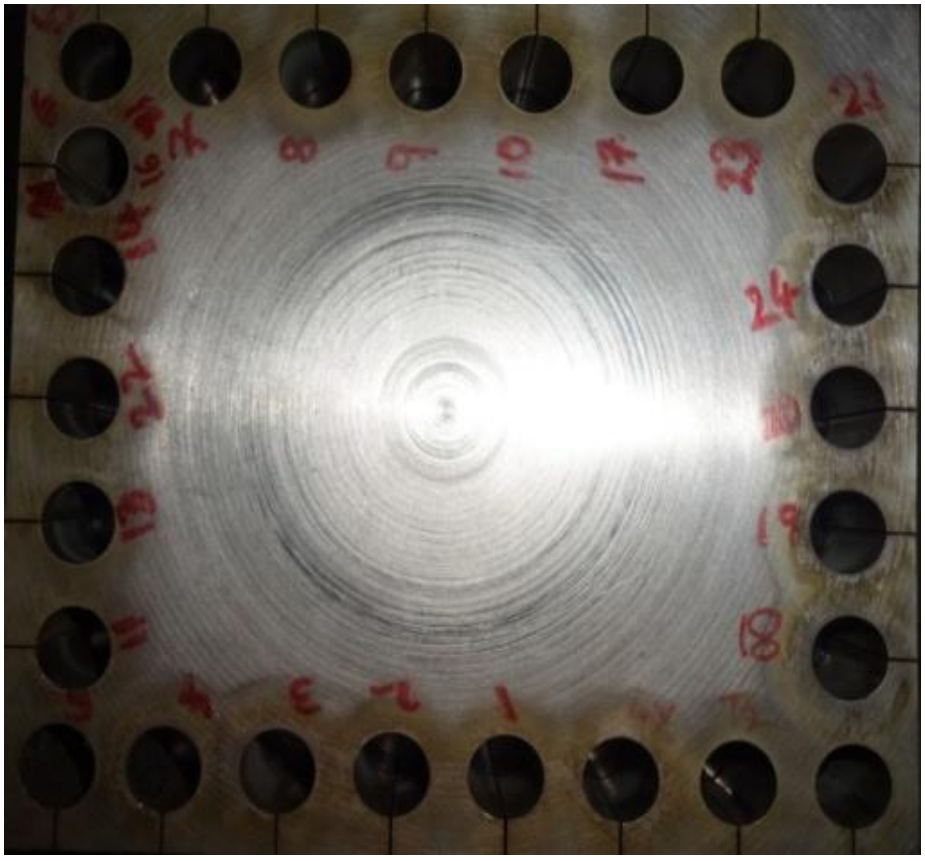

Figure 4.13. Nimonic-263 work material after machining

Tale 4.8 Experimental results for Nimonic-263

Run order	T_{on} (µs)	T_{off} (µs)	I_p (A)	S_v (V)	MRR (mm^3 / min)	SR (µm)
1	125	60	12	60	3.124	2.01
2	125	60	10	60	0.359	0.605
3	115	55	11	40	0.453	0.525
4	115	55	11	50	0.381	0.387
5	105	60	12	60	0.497	0.537
6	125	55	11	50	0.327	0.578
7	125	50	10	40	0.381	0.484
8	115	55	12	50	2.447	1.021
9	115	50	11	50	0.280	0.501
10	105	50	10	40	0.446	1.364
11	115	55	10	50	0.301	0.514
12	105	60	10	60	0.427	0.694
13	125	50	10	60	0.459	0.46
14	115	55	11	50	0.311	0.539
15	125	50	12	40	3.588	2.027
16	105	60	10	40	0.529	1.323
17	125	60	12	40	3.352	2.089
18	105	55	11	50	0.397	0.892
19	115	55	11	60	0.575	0.76
20	115	60	11	50	0.515	0.764
21	125	60	10	40	0.500	1.081
22	105	50	12	40	1.768	0.891
23	125	50	12	60	3.234	1.85
24	105	60	12	40	0.949	1.18
25	105	50	10	60	0.549	0.863
26	105	50	12	60	0.771	0.603

4.6.1. Results and Analysis

(a) *ANOVA analysis of MRR*

ANOVA has been applied for each response to investigate the significance of process parameters and their contributions for the Nimonic-263 work material. ANOVA is also used to model the response parameters in relation with their influencing parameters. The results of ANOVA for MRR and SR are explained in the following sections. The results of ANOVA for MRR are presented in Table 4.9.

Table 4.9 ANOVA results of MRR for Nimonic-263

Source	SS	DOF	MS	F value	P-value	Percentage Contribution
Model	29.3208	9	3.258	44.563	< 0.0001	96.164
A- T_{on}	4.492364	1	4.4928	61.449	< 0.0001	14.734
B- T_{off}	0.08323	1	0.0838	1.138	0.3018	0.2624
C- I_p	13.8341	1	13.834	189.232	< 0.0001	45.372
D- S_v	0.216133	1	0.216	2.956	0.1048	0.709
AC	5.718684	1	5.718	78.224	< 0.0001	18.756
BC	0.126007	1	0.126	1.724	0.2077	0.413
CD	0.24216	1	0.242	3.312	0.0875	0.794
A^2	0.012463	1	0.012	0.171	0.6852	0.041
C^2	2.960149	1	2.960	40.491	< 0.0001	9.708
Residual	1.169703	16	0.073			3.836
Cor. Total	30.49051	25				100

From the Anova Results of MRR, it can be observed that T_{on}, I_p, and interaction of T_{on} and I_p are significant model terms, and are shown in the Figurs 4.14 (a) to (c). Higher the pulse-on time, higher will be the energy applied there by generating more amount of heat energy during this period and it leads to higher MRR. Peak current is the amount of power used in discharge machining. Higher the peak current, higher will be the energy applied during machining and there by increasing the MRR. The mathematical model generated for MRR is given in equation (4.11), in the coded form. From the ANOVA, the R-Square, adjusted R-square and predicted R-square values were found to be 96.2 %, 94 % and 90 % respectively for the model.

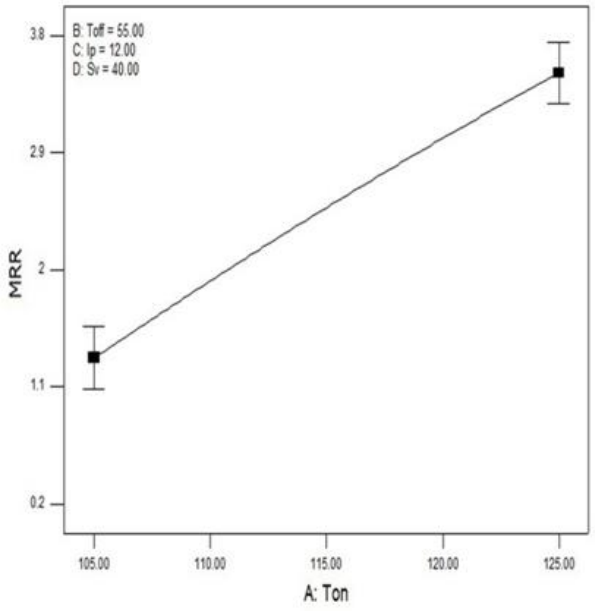

(a) Effect of T_{on} on MRR

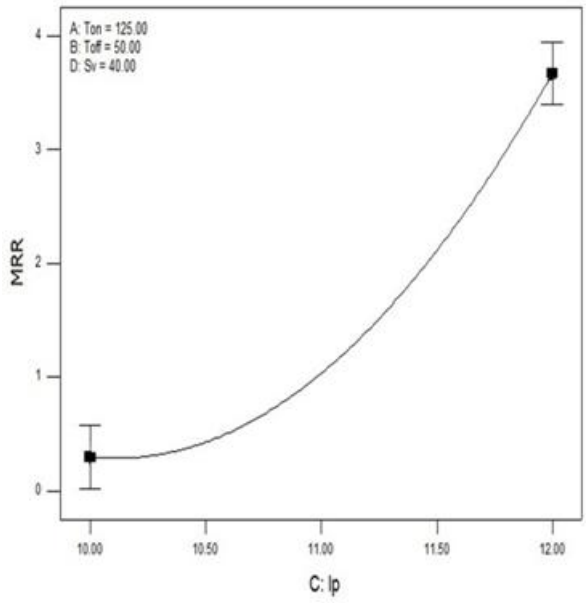

(b) Effect of I_p on MRR

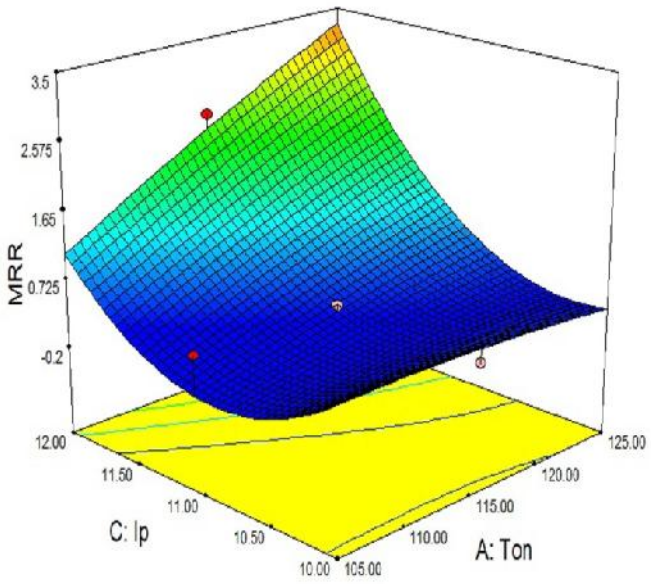

(c) Effect of T_{on} and I_p on MRR

Figure 4.14. Effect of WEDM process parameters on MRR while machining Nimonic-263

$$MRR = 0.42 + 0.50A - 0.068B + 0.88C - 0.11D + 0.60\,AC - 0.089\,BC - 0.12\,CD - 0.062\,A^2 + 0.95C^2 \quad (4.11)$$

(b) ***ANOVA analysis of SR***

From the ANOVA Results of SR (Table 4.10), it can be observed that T_{on}, I_p, S_v and interaction effects T_{on} and I_p are significant model terms, and are shown in the Figurs 4.15 (a) to (d). When the pulse-ontime increases, the number of discharges also increases. It leads to more heat energy there by increasing the machining rate and decresing the surface finish. Higher the peak current, higher will be the energy applied and it leads to higher maching rate and high surface roughness. At higher values of servo voltage, the gap between workpiece and wire becomes wider and it decreases the number of sparks, stabilizes electric discharge yielding better surface finish. The mathematical model generated for SR was given in equation (4.12) in the coded form.From the ANOVA, the R-Square, adjusted R-square and predicted R-square values were found to be 92 %, 84.22 % and 72 % respectively for the model.

Table 4.10 ANOVA results of SR for Nimonic-263

Source	SS	DOF	MS	F value	P-value	Percentage Contribution
Model	6.372	11	0.579	13.127	< 0.0001	91.161
A- T_{on}	0.447	1	0.447	10.132	0.0066	6.397
B- T_{off}	0.085	1	0.085	1.936	0.1859	1.222
C- I_p	1.291	1	1.291	29.247	< 0.0001	18.465
D- S_v	0.370	1	0.370	8.393	0.0117	5.298
AB	0.056	1	0.056	1.281	0.2767	0.808
AC	2.543	1	2.543	57.630	< 0.0001	36.384
AD	0.106	1	0.106	2.412	0.1427	1.523
BC	0.001	1	0.001	0.011	0.919	0.0067
CD	0.012	1	0.012	0.278	0.6063	0.175
A^2	0.234	1	0.234	5.303	0.0371	3.348
C^2	0.294	1	0.294	6.672	0.0217	4.212
Residual	0.618	14	0.044			8.838
Cor Total	6.990	25				100

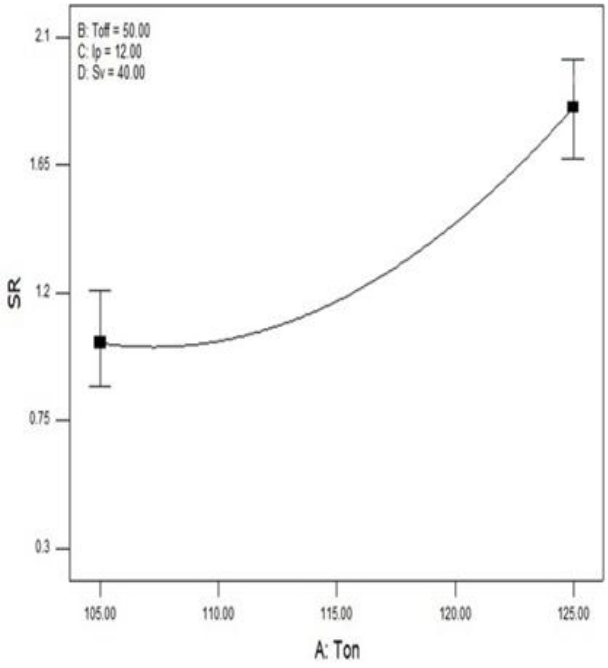

(a) Effect of T_{on} on SR

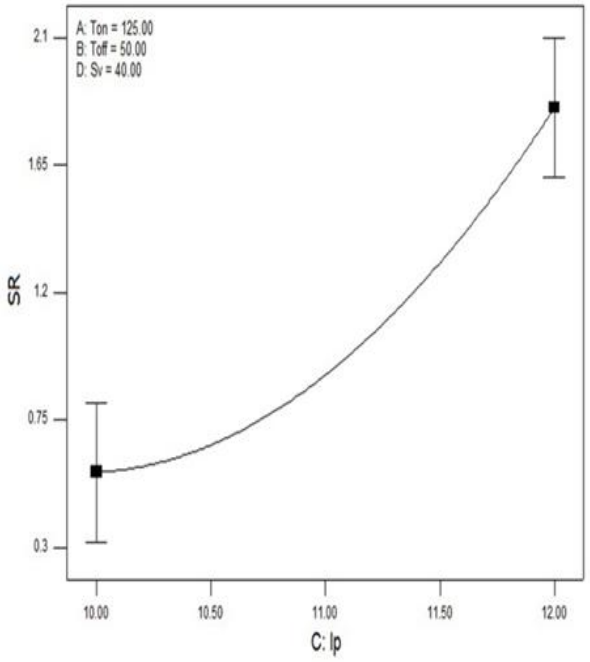

(b) Effect of I_p on SR

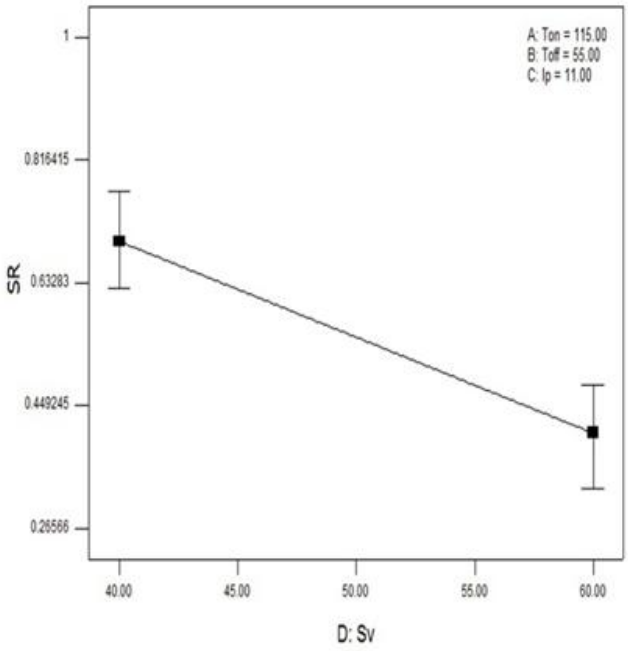

(c) Effect of S_v on SR

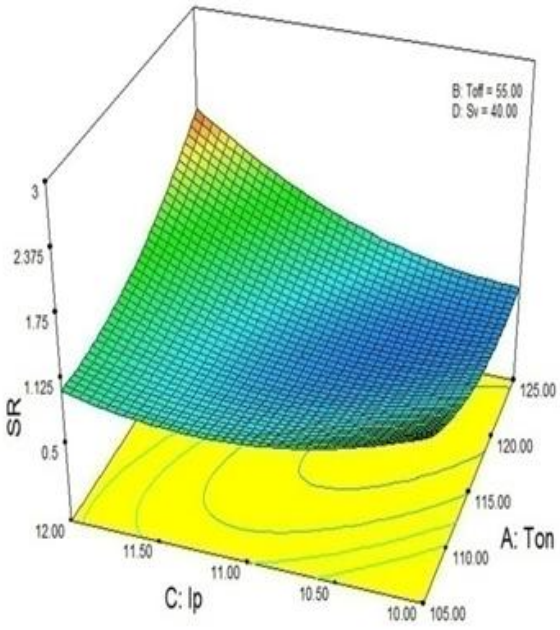

(d) Effect of T_{on} and I_p on SR

Figure 4.15. Effect of WEDM process parameters on SR while machining Nimonic-263

$$SR = 0.55 + 0.16A + 0.069B + 0.27C - 0.14D + 0.059AB + 0.40AC + 0.082AD - 0.005437BC + 0.028CD + 0.27A^2 + 0.30C^2 \quad (4.12)$$

The optimal values for MRR and SR were 3.59856 mm^3/min 0.363162 µm as found from RSM, respectively, along with their optimal parameters are given in Table 4.11. Similarly the optimal values found from existing cuckoo method for MRR and SR were 3.6681 mm^3/min and 0.26215 µm respectively. Whereas from modified two-stage cuckoo search algorithm the corresponding values are 3.6713 mm^3/min and 0.2619 µm. From these results it is observed that the proposed two stage cuckoo search method is yielding better results than the results of RSM and existing cuckoo search algorithm.

Table 4.11 Optimal results from different methods for Nimonic-263

Response		RSM	Existing method	Proposed method
MRR (mm^3/min)	Optimal value	3.59856	3.6681	3.6713
	Optimal parameters	T_{on}:125, T_{off}:52.14, I_p:12, S_v:42	T_{on}:125, T_{off}:51, I_p:12, S_v:42	T_{on}:125, T_{off}:50, I_p:12, S_v:42
SR (µm)	Optimal value	0.363162	0.26215	0.2619
	Optimal parameters	T_{on}:119, T_{off}:51, I_p:10, S_v:56	T_{on}:115.7, T_{off}:50, I_p:10.4, S_v:60	T_{on}:115.8, T_{off}:50, I_p:10.5, S_v:60

Confirmation tests have been conducted to check the effectiveness of proposed method for both MRR and SR, and the results are given in Table 4.12. It can be observed from the confirmation test results that the deviations between experimental values and the predicted values from the modified cuckoo search method are not exceeding 7 % for both MRR and SR. Hence the proposed method can be used for prediction of MRR and SR.

Table 4.12 Confirmation Test results for Nimonic-263

Response	Predicted value from Proposed method	Experimental Value	Deviation in percentage
MRR (mm^3/min) (T_{on}:125, T_{off}:50, I_p:12, S_v:40)	3.6713	3.614	2
SR (µm) (T_{on}:116, T_{off}:50, I_p:10, S_v:60)	0.2619	0.282	7

4.7. Non-dominated sorting modified cuckoo search algorithm

In order to generate simultaneous optimal solutions for MRR and SR, a well known non-dominated sorting principle has been applied to the proposed modified cuckoo search algorithm. The steps involved in the non dominated sorting modified cuckoo search algorithm (NSMCS) are given in Figure 4.16. This algorithm starts with two stage initialization. After initialization, each individual's objective functions are evaluated to rank and sort using non-dominated sorting principle before applying the other operators. Once the ranking is done, cuckoo search operators have been applied to generate new solutions for further generations. Then non-dominated sorting principle is applied to get a set of optimal solutions (Pareto front).

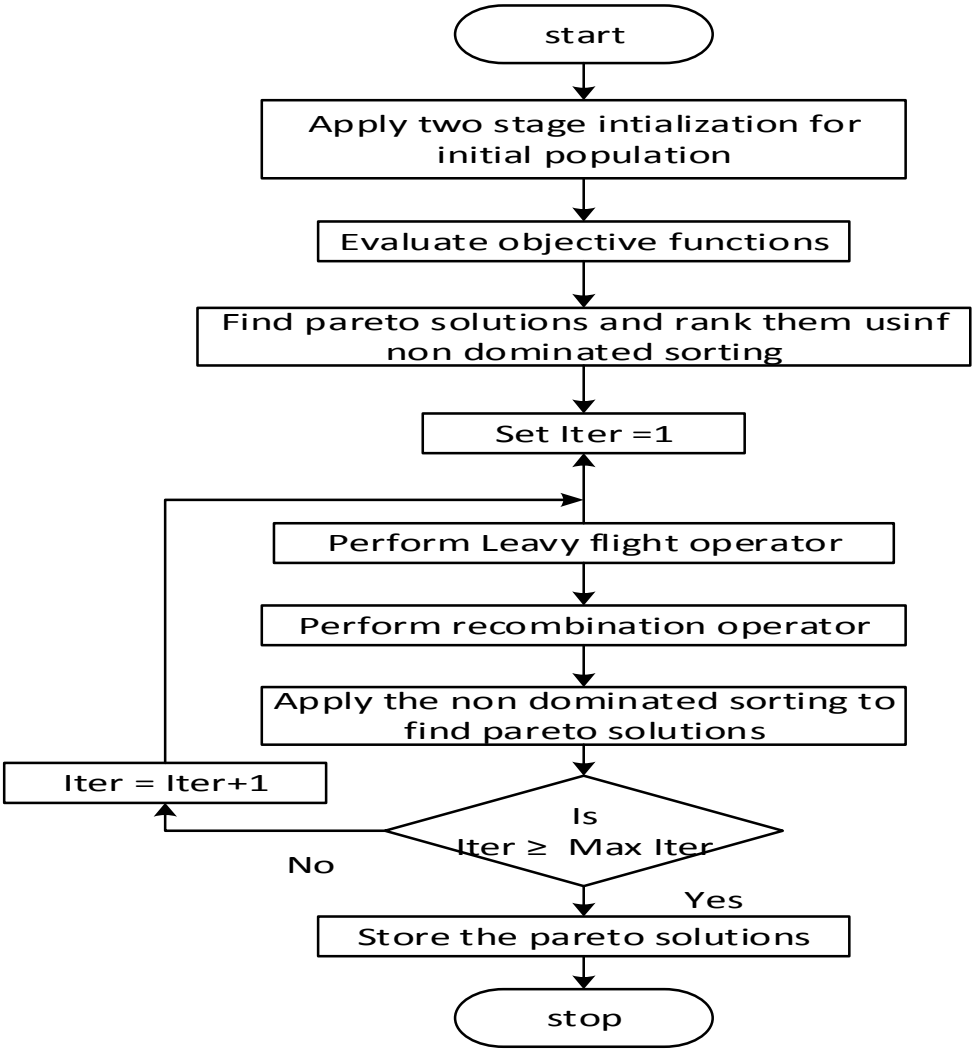

Figure 4.16. Flow chart of NSMCS

The Pareto front of optimal solutions have been generated for Inconel-690 and Nimonic-263 materials as shown in Figures 4.17 and 4.18 respectively. The MRR and SR values are also presented at different weights of the responses (Table 4.13 and 4.14) to enable the manufacturer to choose a solution and associated conditions as per the requirement for Inconel-690 and Nimonic-263 materials respectively.

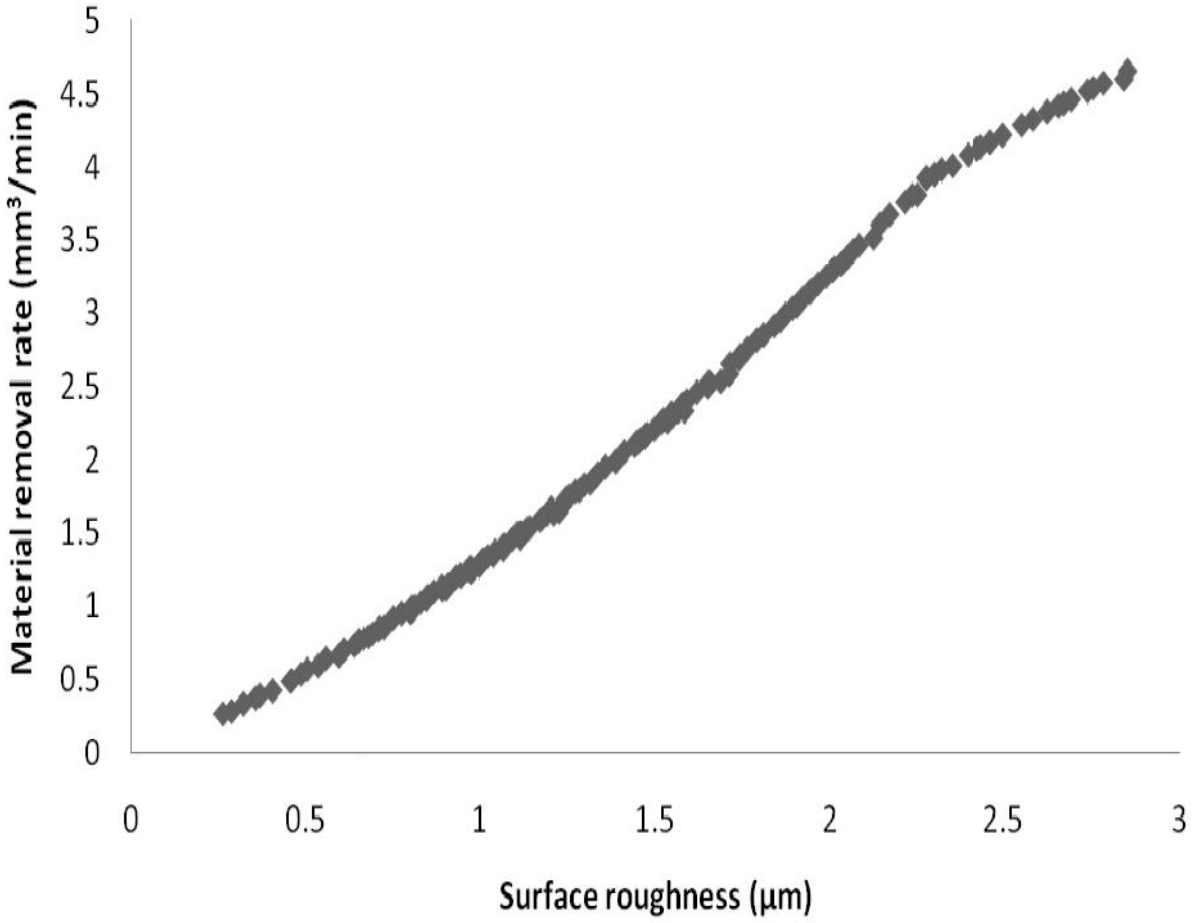

Figure 4.17. Pareto optimal solutions of MRR and SR for Inconel-690 alloy

Table 4.13 Optimal solutions of MRR and SR at different weights for Inconel-690

W_1 (SR)	W_2 (MRR)	SR (µm)	MRR (mm^3/min)	T_{on} (µs)	T_{off} (µs)	I_P (A)	S_v (V)
1	0	0.3309	0.347	105	54.56	10.68	60
0.9	0.1	0.3409	0.371	105	50	11.54	60
0.8	0.2	0.5038	0.5827	105	50	11.94	60
0.7	0.3	0.6484	0.7845	108.2	50	12	60
0.6	0.4	0.8003	1.0097	111.74	50	12	60
0.5	0.5	0.9696	1.2773	114.72	50	12	60
0.4	0.6	1.1733	1.6221	117.42	50	12	60
0.3	0.7	1.4418	2.1149	120.05	50	12	60
0.2	0.8	1.849	2.9469	122.89	50	12	60
0.1	0.9	2.2721	3.9234	125	50	12	60
0	1	3.248	5.843	125	50	12	40

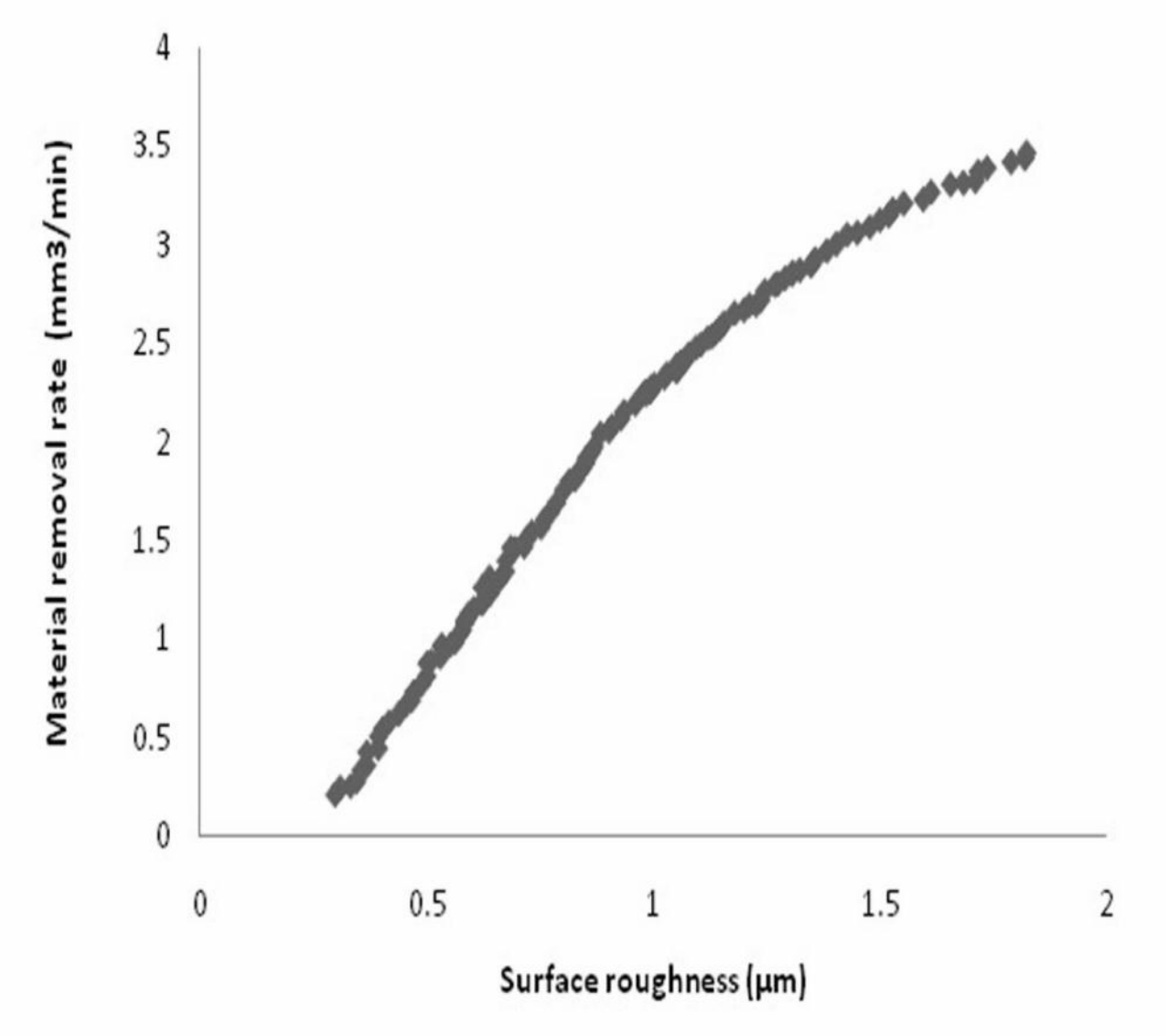

Figure 4.18 Pareto optimal solutions of MRR and SR for Nimonic-263 alloy

Table 4.14. Optimal solutions of MRR and SR at different weights for Nimonic-263

W_1 (SR)	W_2 (MRR)	SR (µm)	MRR (mm^3/min)	T_{on} (µs)	T_{off} (µs)	I_P (A)	S_v (V)
1	0	0.3618	0.2751	115.77	50	10.45	60
0.9	0.1	0.4084	0.5879	113.69	50	11.27	60
0.8	0.2	0.5074	0.9056	112.46	50	11.54	60
0.7	0.3	0.5961	1.2003	111.58	50	11.74	60
0.6	0.4	0.6872	1.5091	110.78	50	11.92	60
0.5	0.5	0.7576	1.7453	111.21	50	12	60
0.4	0.6	0.8218	1.9199	112.74	50	12	60
0.3	0.7	0.9236	2.1417	114.69	50	12	59.78
0.2	0.8	1.2667	2.8582	117.05	50	12	40
0.1	0.9	1.5991	3.3828	122.09	50	12	40
0	1	2.031	3.5713	125	50	12	40

4.8. Summary

Although WEDM is one of the advanced machining processes used to machine hard to cut materials, machining data for Inconel-690 and Nimonic-263 is not available in the literature. An attempt has been made in this work to study the machining behavior for Inconel-690 and Nimonic-263 using WEDM. By conducting the trial experiments, feasible ranges for process parameters have been identified for the material in order to avoid problems such as wire breakage and wire shorting. A face centered central composite design of RSM was used for the experimental design. Effects of process parameters and their interaction effects on performance measures such as MRR and SR have been investigated. Percentage contributions of each process parameter on various responses have been estimated using ANOVA. MRR and SR are significantly influenced by T_{on}, I_p and their interaction. In order to estimate the global optimal response values accurately, a modified cuckoo search algorithm has been proposed in this work. The proposed method has been successfully tested on standard bench-mark problems for its robustness in yielding the accurate results. The proposed algorithm was found to be accurate and fast as compared to existing cuckoo search and RSM methods. The proposed method is able to perform better than the existing cuckoo search technique in terms of accuracy and speed because of the novel two-stage initialization concept introduced in this work. Since the best strings, after the first generation, are grouped and further search is made around these solutions, the convergence rate is much faster. Though the proposed algorithm has been applied for optimizing the WEDM process, it can also be used for other applications. Confirmation tests were conducted to validate the proposed algorithm. The machining data generated for the first time for Inconel-690 and Nimonic-263 materials in this work helps the industry to understand the general behavior of WEDM. Based on this data, industry can carry out focused work to meet the specific needs. A non-dominated sorting principle is also applied to the modified two-stage cuckoo algorithm in order to generate Pareto front for both the materials. These Pareto fronts provide a set of optimal solutions. From this data, the manufacturer can select any solution based on the requirement.

CHAPTER 5

GEOMETRICAL ERRORS

5.1. Introduction

To meet the desired functional and assembly criteria, engineering components require tight dimensional and geometrical tolerances. Majority of the engineering components have circular and cylindrical features in them. These components are used for different applications such as rotating devices, transmission systems, injection moulds, bearings and engine cylinders etc. Circularity error is estimated for those components having size to height ratio less than unity, whereas cylindricity error is estimated for those components whose size to height ratio is greater than unity.

Researchers in the past made a number of attempts to assess the circularity error using coordinate data obtained from coordinate measuring machine (CMM) and also form data obtained from form testers. Murthy and Abdin (1990) applied Monte Carlo technique, normal least squares fit, simplex search and spiral search techniques. They found from their results, that Monte Carlo, spiral and simplex search were suitable for minimum zone evaluation. Chetwynd (1985) applied linear programming and developed a general approach for roundness evaluation. Shunmugam (1986) introduced a concept of median technique to minimize the error values. Sharma et al. (2000) used GA to optimize the solution for form tolerance evaluation. Samuel and Shunmugam (2000) applied computational geometric techniques involving convex hulls, to assess the circularity error at different conditions. They also employed an equi-angular diagram concept to find circularity error. Portman et al. (2002) applied statistical approach to measure roundness error. Venkaiah and Shunmugam (2007) introduced a control hull concept to evaluate circularity error. They compared their method against simplex search method and found that the proposed one gives accurate results and also takes lesser time. They also introduced a new procedure for updating the hull. Wen et al. (2006) implemented GA to search for the circularity error based on maximum inscribed circle (MIC), minimum circumscribed circle (MCC), minimum zone circles (MZC) and least squares circle (LSC). They found that GA gives better results than other existing methods. Sun (2009) applied Particle swarm optimization (PSO) algorithm to

compute the roundness error based on MIC, MCC and MZC methods. Results of PSO were compared against that of GA and found that PSO outperforms GA method.

Several researchers attempted to evaluate the cylindricity error using numerical techniques such as normal least squares (Murthy, 1982), least squares (Shunmugam 1986), non-linear optimization method (Carr and Ferreira, 1995) and hyperboloid method (Devillers and Preparata 2000) etc. Different optimization algorithms such as genetic algorithm (Sharma et al. 2000, Lai et al. 2000), geometry optimization search algorithm (Lei et al. 2011), PSO algorithm (Zhang et al. 2011) etc. have been used to find the minimum cylindricity error values.

Majority of engineering components consist of circular and cylindrical features somewhere in them. Errors on such features affect the functionality and assembly requirements of the components. Although various researchers made several attempts to assess the geometrical errors using different algorithms for the given data, comprehensive studies on geometrical features produced by WEDM process are not yet reported. For the first time, attempts are made in this work to investigate on the effect of process parameters on the circularity and cylindricity errors. ANN technique was used in the past to predict different responses such as MRR, SR, kerf and cutting speed etc. However, this technique has never been used for the prediction of the circularity and cylindricity errors. In the present work, prediction models are developed for these errors using a feed forward back-propagated neural network (BPNN) technique. A CMM, CRT-Apex C-544 model of Mitutoyo make has been used to generate the coordinate data from the circular and cylindrical parts. MCOSMOS software has been used to assess the errors directly from the measured data based on LSC principle.

5.2. Methodology

Flow chart (Figure 5.1) presents the sequence of steps in the proposed methodology. Trial experiments are conducted to fix the ranges for process parameters. Experiments are conducted at different levels of process parameters. Geometrical error is measured for the machined parts based on the LSC principle. Effects of process parameters such as pulse-on time, pulse-off time, peak current and servo voltage on circularity error are studied. An artificial neural network has been used to develop a modal to predict the geometrical error. Initially the developed model has

been trained using training data sets up to desired level of R-value. The performance of the neural network is expressed with its regression coefficient R. R value gives the correlation between target (experimental value) and network output (predicted value). If the R-value reaches 1, there is a strong correlation between experimental and predicted values. Once the model is trained, then the adequacy of the model will be validated with different data sets.

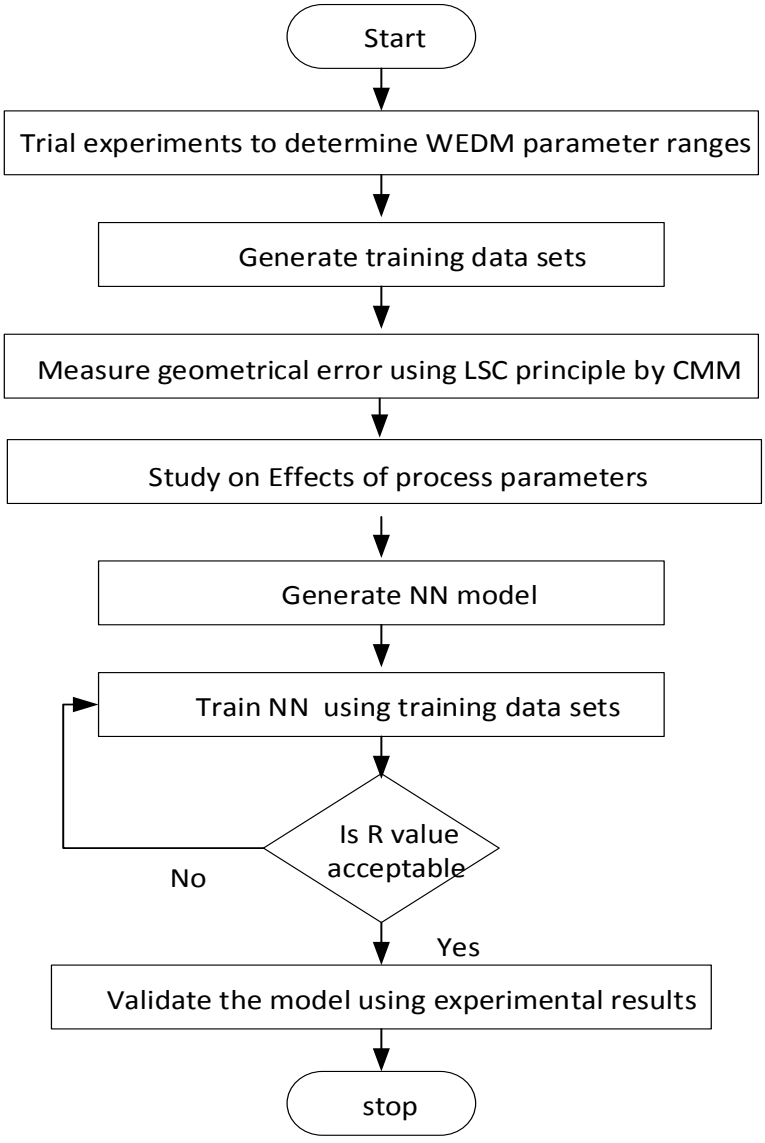

Figure 5.1. Steps in proposed methodology

5.3. Artificial Neural networks

"An artificial neural network system is an information-processing system that has certain performance characteristics in common with biological neural networks" (Fausette, 1994). Any neural network comprises of a large number of processing elements such as neurons, units and cells or nodes. A neural network is specified by

- its pattern of connections between the neurons - called its architecture
- its method of determining the weights on the connections - called its training or learning algorithm
- its activation function.

Each neuron is connected to other neurons by means of links with an associated weight. The weights represent information being used by the net to solve problem. Every neuron has an internal state called its activation level. Each neuron sends its activation or activity level as a signal to several other neurons. A feed forward back propagation neural network has been adopted in the present work to model the WEDM process to predict the geometric errors. This network comprises of large number of artificial neurons and these neurons are grouped into different layers such as input layer, hidden layers and output layer (Somashekhar et al. 2010, Benardos and Vosniakos, 2002) as depicted in Figure 5.2. The information contained in the input layer is transferred or mapped to the output layer through hidden layers (Tzeng et al. 2011).

The feed forward and back propagation network learning includes two phases. During feed forward (i.e. in the first stage), the input neurons receive input signal or information and transfer it to hidden neurons. Each hidden neuron computes its activation and convey its signal or information to output neurons. Each output neuron computes its activation to form the response of the net for the given input conditions. Each output unit compares its computed activation with target value to determine the associated error for that pattern with that unit. This error is back propagated from output layer to hidden layers in the second stage in order to minimize this error, modification of weights will be done. This process is repeated until the deviation reaches to the minimal or the user defined minimum value.

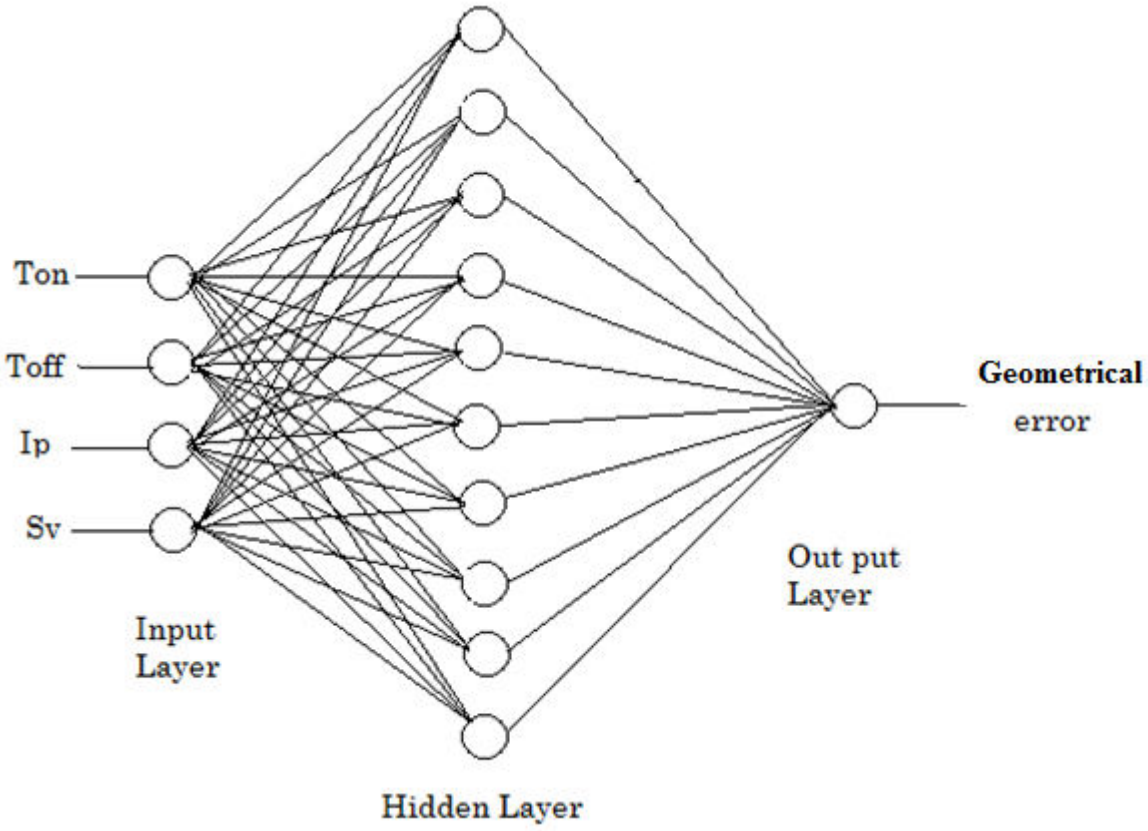

Figure 5.2. Network diagram

Artificial neural network models are widely used in prediction of outputs with respect to inputs of different machining processes where there is no linear relationship between input and output, complex machining processes and regular conventional methods fail to model the process. A 4-10-1 network has been selected in the present work to predict circularity and cylindricity errors as shown in Figure 5.2, in which 4 input neurons, 10 hidden neurons and one output neuron are considered. This network is trained for several times up to the desired value (more than 95 %) of regression coefficient (R). Once the prediction model is developed, goodness of the model must be verified using the confirmation tests.

5.4. Circularity error

Circularity or roundness is a tolerance of form that checks the periphery of any circular cross-section taken perpendicular to the axis of a cylinder or cone, or through the center of a sphere to ensure that all elements are within two concentric circle tolerance zones (ASME, 1994). Circularity error is estimated for those components having size to height ratio less than unity. The CMM gives coordinate data and the circularity profile drawn from this data is shown in Figure 5.3. Distance between the measured point on the circular profile and the center of the reference circle can be obtained as,

$$r_i = \sqrt{(x_i - x_0)^2 + (y_i - y_0)^2} \tag{5.1}$$

Where, (x_0, y_0) represents the center of the circle.

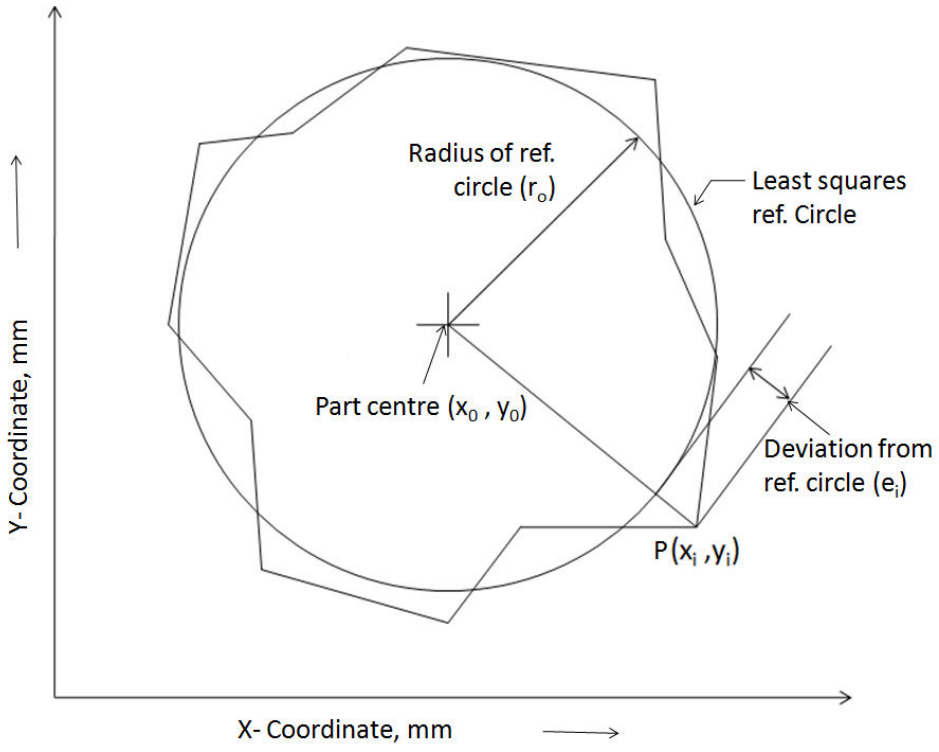

Figure 5.3.Circularity error evaluation

The deviation between the measured point and the reference circle is given by,

$$e_i = r_i - r_0 \tag{5.2}$$

Where, r_0 is radius of the reference circle and is calculated as the mean of the radial distances from the measured points to the center coordinates of the reference circle. The deviations above the reference circle are taken to be positive and that below the circle are treated negative.

Let

e_{max} = maximum (e_i), $\quad i = 1, 2\ldots., N.$

e_{min} = minimum (e_i), $\quad i = 1, 2\ldots., N.$

Where, N is the total number of measured points.

The circularity error is evaluated as the absolute sum of maximum and minimum deviations from the reference circle as given by Eq. 5.3

Circularity error, $\Delta = |e_{max}| + |e_{min}|$ (5.3)

It is to be noted that reference circle is established using various methods such as MIC, MCC, MZC and LSC as shown in Fig. 5.4.

MIC method: MIC is the largest circle that can be drawn inside the profile without cutting across the profile. The roundness error is specified as the distance of the largest peak above the circle. To illustrate the concept, following deviations from the MIC may be considered:

Deviations: + 2, +5, 0, + 3, +0, +6, 0, +1 units

Circularity error = largest peak = $|e_{max}| = |+6| = 6$ units

MCC method: MCC is the smallest circle that will completely enclose the profile without cutting it. Its center and radius can be found in the similar manner to that of the inscribed circle. The roundness error is the distance of the lowest valley from the circle.

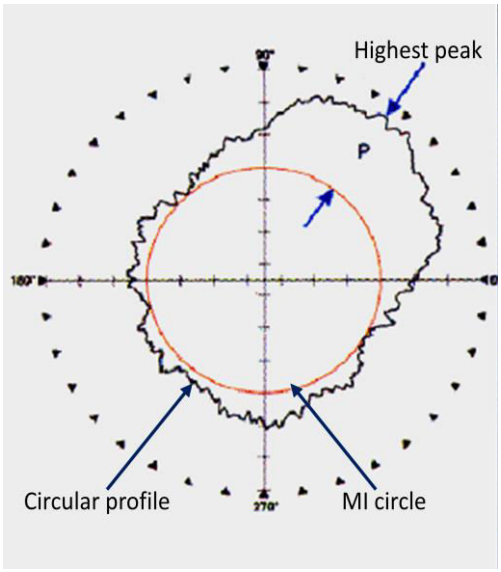

a) Maximum inscribed circle

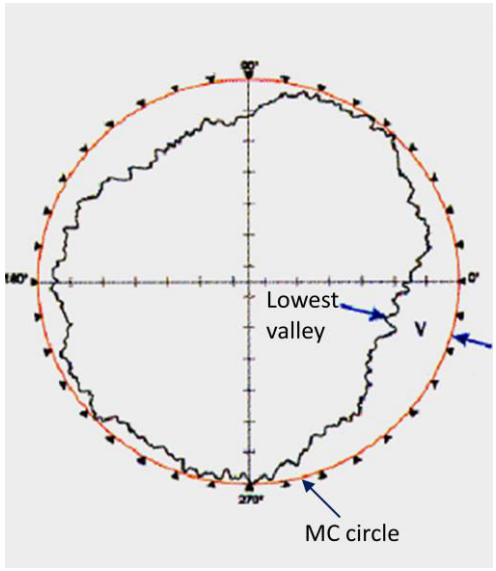

b) Minimum circumscribed circle

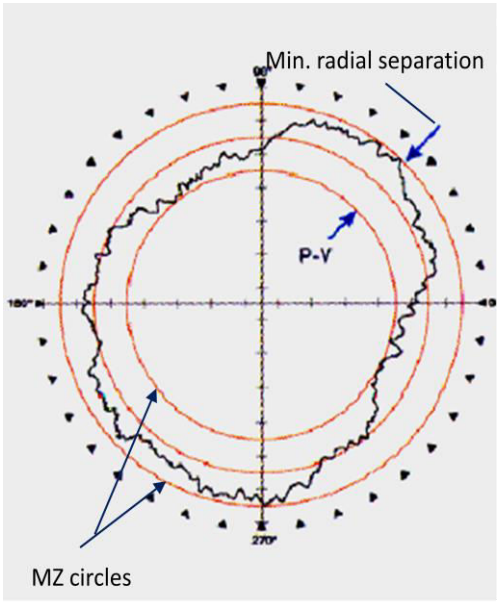

c) Minimum zone circles

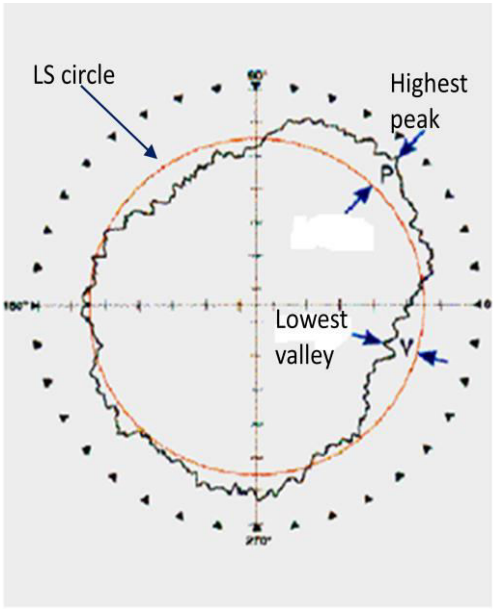

d) Least squares circle

Figure 5.4. Methods to assess circularity error

Let the deviations be - 1, 0, - 4, - 3, 0, - 5, 0, - 1 units

Circularity error = lowest valley = $|e_{min}| = |\ \ 5| = 5$ units

MZC method: In Minimum zone circles method there are two concentric circles that just enclose the profile and have minimum radial separation. The value of the roundness error is the radial distance between the two circles.

Let the deviations be + 1, 0, - 4, - 2, + 4, - 3, - 4, - 1, + 4 units

Circularity error = $|e_{min}| + |e_{max}| = |\ \ 4| + |+4| = 8$ units

5.4.1. Least-squares method for circularity error

Principle of LSC method involves fitting a circle to the profile data points of the part such that sum of the squares of the deviations of the actual profile from the fitted circle is minimum. Circularity error is defined as the radial distance of the maximum peak from this circle (P) plus the distance of the maximum valley from this circle (V) i.e. P + V. Unlike the other three methods, LSC method is the most straight forward in the sense that all the data of the profile is used to establish the circle. Other advantages of this method include sound mathematical basis, unique solution, ease of implementation and low computational time. Therefore, LSC method is popular even today in the industry. The only disadvantage is that this method slightly overestimates the error. In spite of this, LSC method is implemented in the present work, as the scope of the work is to investigate the influence of various process parameters on circularity error.

LSM is based on minimizing the sum of the squares of the deviations as given by,

$$\text{Minimize} \sum_{i=1}^{N} e_i^{\,2} \qquad (5.4)$$

The circularity error is evaluated as the absolute sum of maximum and minimum deviations from the reference circle as given by Eq. 5.3

Since the circularity error function is non-linear, a non-linear LSM, often called as Gauss-Newton method is employed to solve this problem. A complete derivation of the method (Nash and Sofer 1996, Wolf and Ghilani 1997) is not given here, however a functional description is provided. This method needs Jacobian matrix to be formed. The Jacobian matrix (J) is the matrix of partial differentials of the deviation Eq. 5.5 with respect to each parameter.

$$\mathrm{J} = \begin{bmatrix} \frac{\partial e_1}{x_o} & \frac{\partial e_1}{y_o} & \frac{\partial e_1}{r_o} \\ \frac{\partial e_2}{x_o} & \frac{\partial e_2}{y_o} & \frac{\partial e_2}{r_o} \\ \frac{\partial e_3}{x_o} & \frac{\partial e_3}{y_o} & \frac{\partial e_3}{r_o} \\ & \cdot & \\ & \cdot & \\ & \cdot & \end{bmatrix} \tag{5.5}$$

where

$$\frac{\partial e_i}{x_o} = \frac{x_o - x_i}{\sqrt{x_i^2 - 2x_o x_i + y_i^2 - 2y_o y_i + x_o^2 + y_o^2}}$$

$$\frac{\partial e_i}{y_o} = \frac{y_o - y_i}{\sqrt{x_i^2 - 2x_o x_i + y_i^2 - 2y_o y_i + x_o^2 + y_o^2}}$$

$$\frac{\partial e_i}{r_o} = -1$$

The solution requires multiple iterations and an initial solution for the unknowns (x_o, y_o, r_o) is needed. The initial solution may be obtained as follows:

$$\begin{aligned} x_o &= \frac{1}{N}\sum x_i \\ y_o &= \frac{1}{N}\sum y_i \\ r_o &= \sqrt{(x_1 - x_o)^2 + (y_1 - y_o)^2} \end{aligned} \tag{5.6}$$

The vector of residuals, K is given by

$$K = \begin{matrix} 0 \\ 0 \\ 0 \\ \\ \\ \end{matrix} \begin{matrix} \left(\sqrt{(x_1 \quad x_o)^2 + (y_1 \quad y_o)^2} \quad r_o\right) \\ \left(\sqrt{(x_2 \quad x_o)^2 + (y_2 \quad y_o)^2} \quad r_o\right) \\ \left(\sqrt{(x_3 \quad x_o)^2 + (y_3 \quad y_o)^2} \quad r_o\right) \\ . \\ . \\ . \end{matrix} \tag{5.7}$$

It is essential to solve for adjustment values, ΔV. The vector of adjustments for the parameters is given below.

$$V = \begin{bmatrix} x_o \\ y_o \\ r_o \end{bmatrix} \tag{5.8}$$

The adjustments of the parameters, Δx_o, Δy_o and Δr_o can be solved using the equation

$$\Delta V = (J'J)^{-1} J'K \tag{5.9}$$

On solving the adjustment values, the circle parameters are then adjusted as

$$\begin{aligned} x_o' &= x_o + \Delta x_o \\ y_o' &= y_o + \Delta y_o \\ r_o' &= r_o + \Delta r_o \end{aligned} \tag{5.10}$$

This new solution is now used to compute a new Jacobian matrix and a new residual vector, which are then used to get a new adjustment vector ΔV. This procedure is continued until the adjusted values are closer to zero. In fact, even today, most of the CMMs use the LSM to report the final solution due to its advantages such as sound mathematical formulation, unique solution and less computational effort.

5.4.2. Results and analysis

Since the studies on effects of process parameters on the circularity error are not reported in literature, attempts are made to carry out these studies in the present work. In order to establish the relationship between process parameters and circularity error, experiments were conducted and 60 data sets were generated as presented in Table 5.1 along with the associated circularity error. These data sets are used to develop predictive model for circularity error using ANN. Another set of 10 experiments was conducted to validate the model.Inconel-690 has been used as workpiece material and 10 mm circular holes were produced on 6.5 mm thick plate. The circularity error was measured directly using CMM, and the in-built algorithm involved in MCOSMOS software is LSC method. The ranges for the process parameters were fixed as pulse on time (T_{on}) 105-125 µs, pulse off time (T_{off}) 50-60 µs, peak current (I_p) 10-12 A and servo voltage (Sv) 40-60 V after conducting trial experiments.

Table 5.1 Training data set to train NN model for circularity error

S. No.	T_{on} (µs)	T_{off} (µs)	I_p (A)	S_v (V)	Circularity error (µm)
1	115	60	11	50	9
2	115	55	10	50	7
3	105	60	12	60	9
4	115	55	11	60	13
5	115	55	11	50	13
6	115	55	11	50	8
7	115	55	12	50	5
8	125	60	10	60	28
9	125	50	10	40	26

10	105	60	12	40	4
11	115	55	11	50	9
12	105	50	10	60	12
13	105	60	10	40	16
14	105	60	10	60	11
15	125	55	11	50	6
16	115	55	11	50	9
17	125	50	12	40	6
18	115	55	11	50	12
19	115	55	11	40	8.5
20	125	50	10	60	4
21	110	50	11	40	5
22	110	50	11	45	13.3
23	110	50	11	50	16
24	110	50	11	55	17
25	110	50	11	60	16.7
26	110	50	12	40	4
27	110	50	12	45	5
28	110	50	12	50	15

29	110	50	12	55	20
30	110	50	12	60	19
31	110	55	11	40	4
32	110	55	11	45	6.1
33	110	55	11	50	8
34	110	55	11	55	10
35	110	55	11	60	11
36	110	55	12	40	4
37	110	55	12	45	4
38	110	55	12	50	6
39	110	55	12	55	10.7
40	110	55	12	60	11.5
41	120	55	11	40	10.1
42	120	55	11	45	9
43	120	55	11	50	7
44	120	55	11	55	5.9
45	120	55	11	60	5
46	120	55	12	40	4
47	120	55	12	45	6.7

48	120	55	12	50	11.4
49	120	55	12	55	12
50	120	55	12	60	12
51	120	60	11	40	29.5
52	120	60	11	45	29
53	120	60	11	50	25.7
54	120	60	11	55	9
55	120	60	11	60	4
56	120	60	12	40	4.1
57	120	60	12	45	6.8
58	120	60	12	50	11.5
59	120	60	12	55	10
60	120	60	12	60	9.2

The influence of process parameters such as pulse-on time, pulse-off time, peak current and servo voltage on the circularity error are shown in Figure 5.5 (a), (b), (c) and (d) respectively while machining Inconel-690 using WEDM.

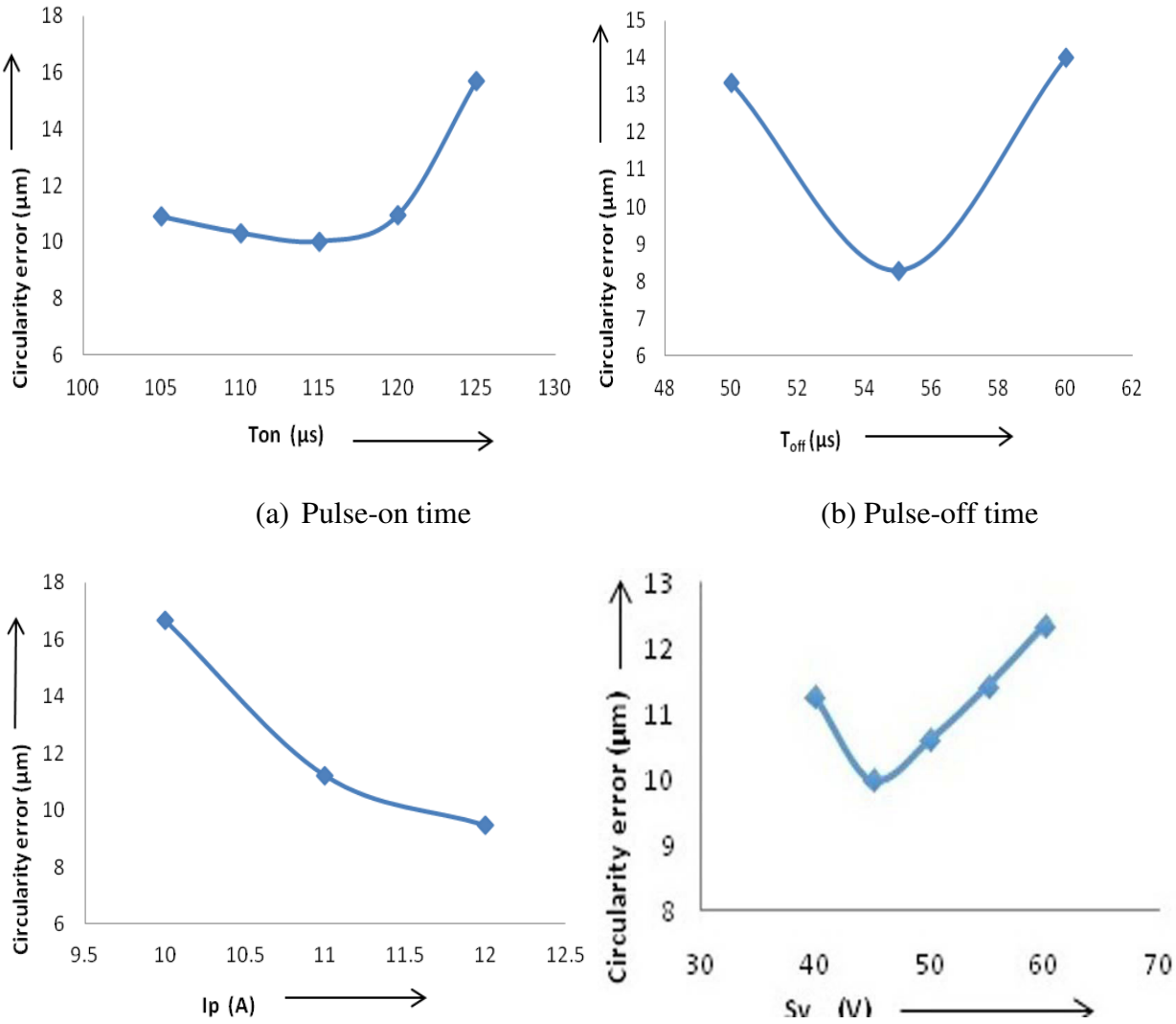

(a) Pulse-on time (b) Pulse-off time

(c) Peak current (d) Servo voltage

Figure 5.5. Effect of process parameters on circularity error

Figure 5.5 (a) shows the effect of pulse-on time on circularity error. During the pulse-on time, energy is discharged between electrode and work material. It is observed that up to 120 µs of pulse-on time, circularity error is low. This can be attributed to the fact that cutting speed is moderate and the sparks are generated uniformly between wire electrode and workpiece towards the cutting direction yielding uniform material removal. During this range of pulse-on time, the effect of pulse-on time on circularity error is also marginal. However, beyond 120 µs of pulse-on time, the energy is applied for a longer duration thereby generating more amount of heat and it leads to increase in material removal rate (Mahapatra and Patnaik, 2009). This increased cutting

speed leads to increased wire wear and formation of craters on machined surface which in turn results in higher circularity error. The increase in circularity error may also be attributed to the fact that the higher cutting speed at higher pulse-on time does not permit the effective flush out of the debris from the machined zone. The left over debris may weld to the machined surface causing higher circularity error.

Pulse-off time or pulse interval is the time interval between discharges. At lower pulse-off time, more amount of heat is generated resulting in higher material removal, overload of wire and instability in machining (Fuller, 1996). Further, lower pulse-off time causes incomplete flush out of the debris. Due to these reasons, circularity error increases at lower pulse-off time as shown in Figure 5.5(b). Increasing the pulse-off time up to 55 µs slows down the cutting speed allowing uniform material removal rate and stability in machining, which results in reduced circularity error. However, beyond this value of pulse-off time, cutting speed drops drastically. During this phase of machining, sparks are not continuous causing the wire vibration and inconsistent machining, which increases the circularity error.

Peak current is the amount of current supplied during machining. The discharge energy is directly proportional to the peak current (Singh and Garg, 2009). At low peak current, cutting speed is low and there is no continuous in spark generation causing inconsistent machining producing more undulations on the machined surface resulting in higher circularity error. As the peak current increases, sparks are generated uniformly yielding uniform material removal thereby decreasing the circularity error as shown in Figure 5.5(c).

Servo voltage is the reference voltage and is used to control the wire retracts and advances. At lower value of servo voltage, the gap between wire and workpiece becomes narrow, which allows more number of sparks per unit time and more amount of heat is generated (Ghodesiyeh et al., 2013) and cutting speed increases thereby increasing the circularity error. Furthermore, at low servo voltage, wire will be overloaded causing the frequent wire breaks and it results in discontinuities on the machined surface leading to higher circularity error. As the servo voltage increases, the cutting speed will be moderate and circularity error decreases up to 45 V as shown in Figure 5.5(d). Further increase in servo voltage leads to increase in circularity error due to low cutting speed and sparks are not generated continuously causing non-uniform material removal and wire vibration.

Artificial neural network toolbox has been used to develop predictive model for the circularity error. The NN tool internally divides the total data sets into 70 %, 15 % and 15 % for training, validation and testing respectively. While developing the model, the neurons are trained to the desired level using the 70 % of data sets. Once the model is developed, prediction accuracy will be verified with validation and testing data sets. Correlations between experimental and predicted values are expressed by regression coefficient R in NN modeling. If the regression coefficients for training, validation and testing data are acceptable, training may be stopped and the developed model can be used to predict the circularity error. The regression coefficients of the developed NN model are found to be 96 %, 97 %, 98 % and 96 % for training, validation, testing and overall model respectively as shown in Figure 5.6 (a) to (d).

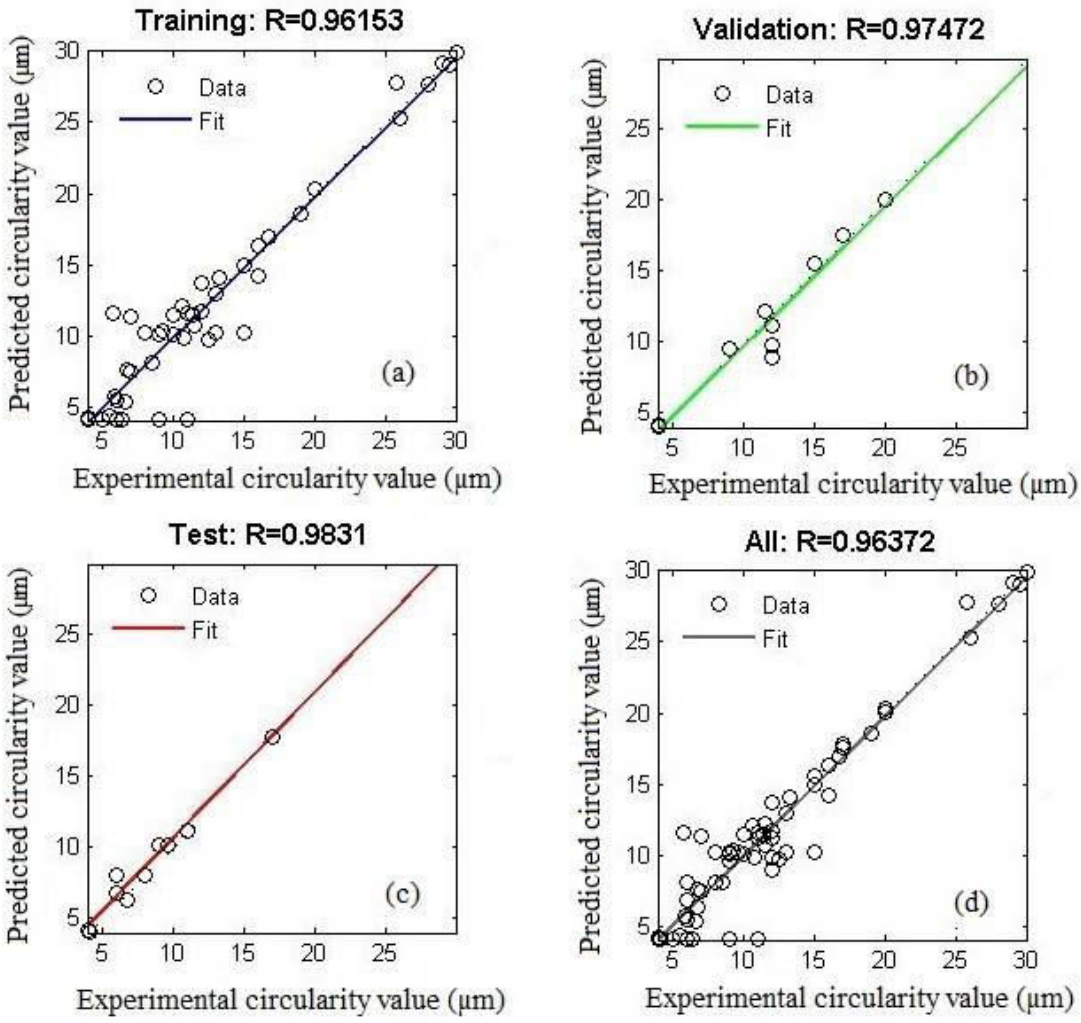

Figure 5.6. Correlation between experimental and predicted circularity errors with associated R values

Effectiveness of the model was validated against 10 experimental data sets. Table 5.2 presents the percentage of deviation between the experimental and predicted circularity errors for the validation data sets. Figure 5.7 shows the graphical representation of the confirmation test results. It can be observed that the deviations between experimental and predicted values are marginal. It was found from the results of confirmation test data sets that the average deviation of circularity error from experimental value to the predicted value is 5.08 %. Therefore, the developed model can be used to predict the circularity error.

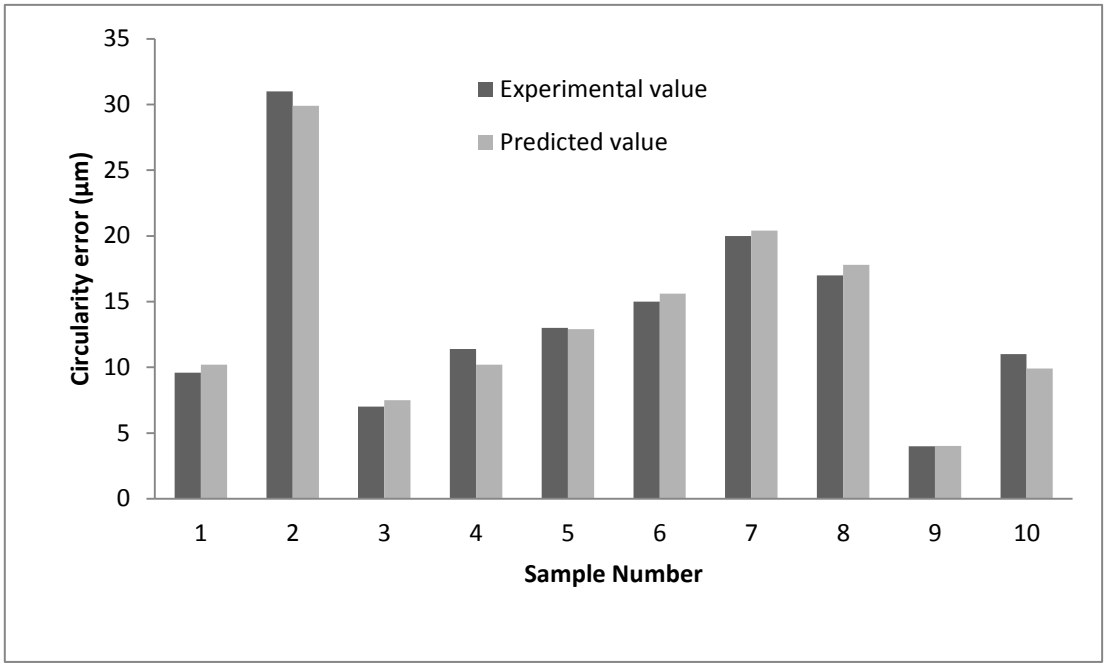

Figure 5.7. Experimental and predictive circularity errors in testing of NN model

Table 5.2 Experimental data to validate NN model for circularity error

S. No.	T_{on} (µs)	T_{off} (µs)	I_p (A)	S_v (V)	Experimental circularity error (µm)	Predicted circularity error using NN (µm)	Deviation in %
1	115	55	11	50	9.6	10.2	5.88
2	125	60	10	40	31	29.9	3.68

3	105	55	11	50	7	7.5	6.67
4	125	60	12	60	11.4	10.2	11.76
5	125	50	12	60	13	12.88	0.93
6	105	50	10	40	15	15.6	3.85
7	105	50	12	60	20	20.4	1.96
8	115	50	11	50	17	17.8	4.49
9	105	50	12	40	4	4.02	0.49
10	125	60	12	40	11	9.9	11.11

5.5. Cylindricity error

Cylindricity error is estimated for those components having size to height ratio greater than unity. Cylindricity is a condition where all points on the surface of a cylinder are equidistant from the axis. There are four standard methods available to assess the cylindricity namely least-squares (LS), minimum circumscribing (MC), maximum inscribing (MI) and minimum zone (MZ) method as depicted in Figure 5.8 (a) to (d). In LS method, the cylinder axis is generated by working out the LS centers of all the levels. The best-fit line is established from the centers and then the deviations at each level are found from the cylinder generated using this axis. The cylindricity is usually given by the farthest peak deviation added to the lowest valley deviation from the LS radius of all the data. MC cylinder is the smallest cylinder around the data. Once this cylinder is found using the points, the cylindricity error can be estimated as the deepest valley distance from the MC cylinder. MI cylinder is the biggest cylinder inscribing the data. The cylindricity error is estimated as the maximum peak distance from the MI cylinder. MZ cylinders are the coaxial cylinders with least radial separation containing the data points in the annular zone. ISO guidelines suggest the MZ cylinders as the preferred method but do not specify the method to establish them.

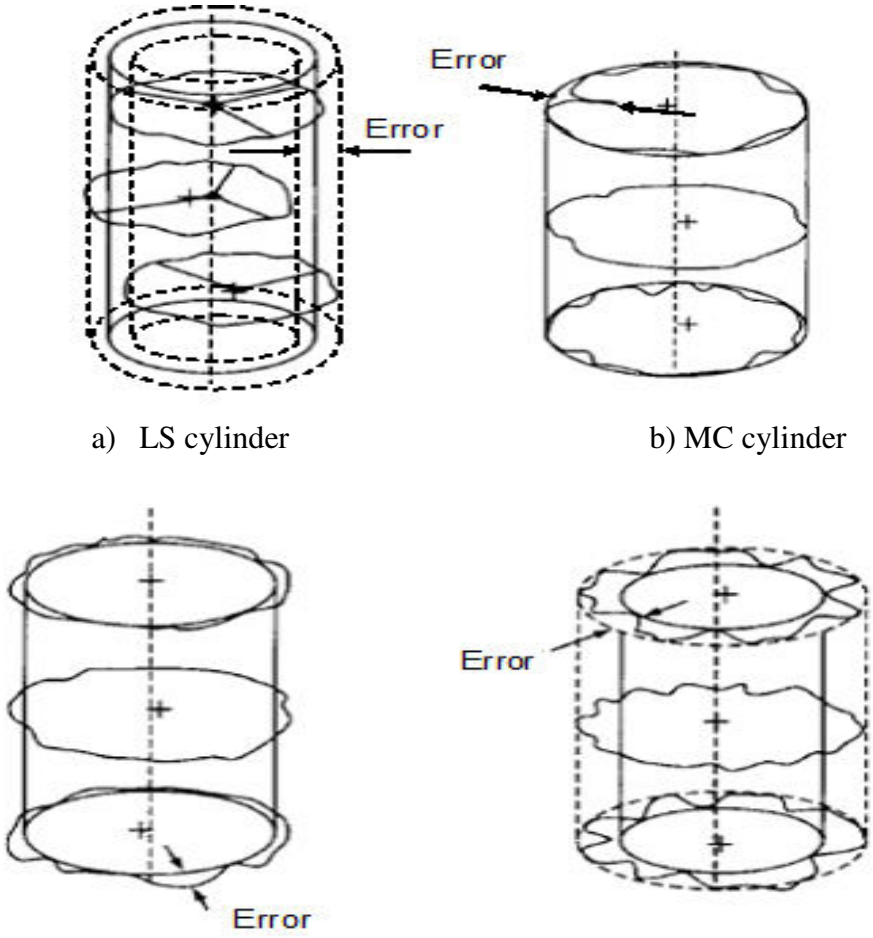

a) LS cylinder b) MC cylinder

c) MI cylinder d) MZ cylinder

Figure 5.8. Various reference features for cylindricity assessment (Whitehouse, 2002)

5.5.1. Least-squares method for cylindricity error

Figure 5.9 shows measured profiles at different sections of a cylindrical feature and a point on the measured profile is indicated by P_1 (x_i,y_i,z_i). The figure also shows the reference circular-cylinder used for the assessment of the cylindricity error. By convention, deviation of a measured point lying outside the reference cylinder is taken to be positive and a point inside is considered to have negative deviation. The cylindricity error (Δ) is, therefore, obtained as an absolute sum of the maximum and minimum deviations.

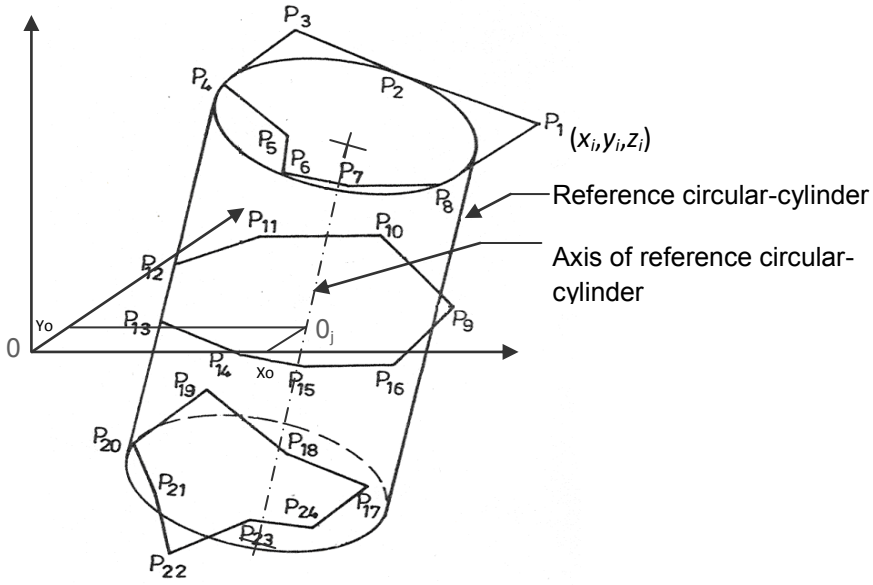

Figure 5.9. Cylindricity data and circular-cylinder

Cylindricity measurements are denoted by (x_i,y_i,z_i). If the assessment cylinder, whose radius is r_o, is represented by the axis $x_0 + l_0 z_i$ and $y_0 + m_0 z_i$, the normal deviation e_i from the i^{th} measured point to the cylinder is given by

$$e_i = \left\{ \left[(x_i - x_0) - l_0 z_i \right]^2 + \left[(y_i - y_0) - m_0 z_i \right]^2 + \left[m_0 (x_i x_0) - l_0 (y_i - y_0) \right]^2 \right\}^{1/2} \left\{ 1/(1 + l_0^2 + m_0^2) \right\}^{1/2} - r_0 \quad (5.11)$$

Where (x_0, y_0) is a point on the axis of the assessment cylinder and (l_0, m_0) are the slope values with respect to x and y-axis

5.5.2. Results and analysis

Though researchers in the past made several attempts to assess the cylindrical features using different algorithms, studies on influence of process parameters on cylindricity error are not reported yet. Also, it is to be noted that cylindricity is basically a complex geometry and producing such a feature on a super alloy with acceptable deviation from the nominal size and

shape makes it much more complex. Therefore, for the first time, attempts are made in this work to investigate the effect of process parameters on the cylindricity error. A predictive model for cylindricity error is also developed using a feed forward back-propagated neural network (BPNN) technique. For this study, Nimonic-263 has been used as workpiece material and 10 mm holes of 18.5 mm length were produced on 120 mm × 110 mm × 18.5 mm. Experiments were conducted and 60 data sets were generated as presented in Table 5.3 along with the associated cylindricity error. CMM data generated from the circular-cylindrical components was used to assess the cylindricity error. The influence of process parameters such as pulse-on time, pulse-off time, peak current and servo voltage on the cylindricity error are shown in Figure 5.10 (a) to (d) respectively in machining of Inconel-690 using WEDM.

Table 5.3 Training data set to train NN model for cylindricity error

S. No.	T_{on} (µs)	T_{off} (µs)	I_p (A)	S_v (V)	Cylindricity error (µm)
1	125	60	12	60	38.84
2	125	60	10	60	15.86
3	115	55	11	50	41.24
4	125	55	11	50	29.07
5	125	50	10	40	29.06
6	115	55	12	50	22.24
7	115	50	11	50	27.49
8	115	55	10	50	38.98
9	115	55	11	50	39.64
10	105	60	10	40	40.74

11	125	60	12	40	31.21
12	105	55	11	50	27.56
13	115	55	11	60	37.07
14	115	55	11	50	40.89
15	125	60	10	40	28.44
16	105	50	12	40	18.96
17	105	60	12	40	21.89
18	105	50	10	60	40.50
19	105	50	12	60	24.22
20	115	55	11	50	39.24
21	110	50	11	40	29.52
22	110	50	11	45	25.32
23	110	50	11	50	24.02
24	110	50	11	55	27.53
25	110	50	11	60	35.75
26	110	50	12	40	17.89
27	110	50	12	45	17.95
28	110	50	12	50	19.93
29	110	50	12	55	27.57

30	110	50	12	60	43.39
31	110	55	11	40	39.71
32	110	55	11	45	45.22
33	110	55	11	50	45.36
34	110	55	11	55	43.25
35	110	55	11	60	42.95
36	110	55	12	40	21.51
37	110	55	12	45	19.13
38	110	55	12	50	18.86
39	110	55	12	55	21.47
40	110	55	12	60	29.62
41	120	55	11	40	44.42
42	120	55	11	45	43.67
43	120	55	11	50	37.16
44	120	55	11	55	24.57
45	120	55	11	60	19.82
46	120	55	12	40	28.09
47	120	55	12	45	21.91
48	120	55	12	50	18.74

49	120	55	12	55	22.07
50	120	55	12	60	39.09
51	120	60	11	40	38.94
52	120	60	11	45	35.98
53	120	60	11	50	38.57
54	120	60	11	55	43.46
55	120	60	11	60	44.58
56	120	60	12	40	37.22
57	120	60	12	45	45.95
58	120	60	12	50	49.27
59	120	60	12	55	48.66
60	120	60	12	60	48.42

Pulse-on time is the time during which the energy is discharged between wire and workpiece. At low pulse-on time the energy discharged is low, load on the wire is low and machining will be stable. As a result, the cylindricity error is low. When the pulse-on time increases, the energy supplied increases, load on the wire increases. Inconsistent machining produces more undulations on the machined surface, thereby increasing the cylindricity error as shown in Fig. 5.10 (a). Further increase in pulse-on time from 115 to 125 μs, the machining speed was found to be high and uniform and therefore wire vibrations were diminishing thereby decreasing the cylindricity error.

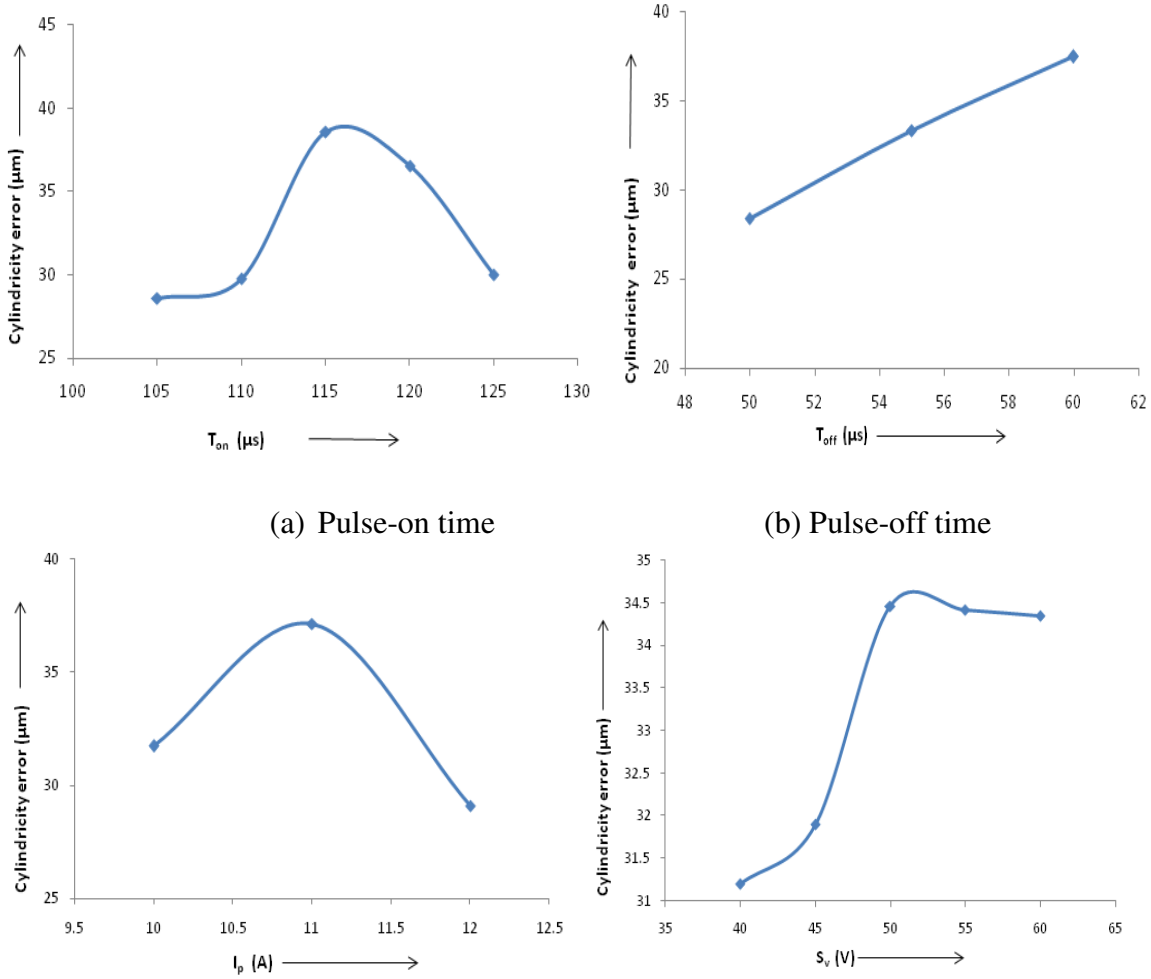

(a) Pulse-on time (b) Pulse-off time

(c) Peak current (d) Servo voltage

Figure 5.10. Effect of process parameters on cylindricity error

Pulse-off time is the interval between discharges. At lower pulse off time there is a uniform material removal and stability in machining leads to low cylindricity error. Whereas with increase in the pulse-off time the gap between discharges increases, there by sparks are not continuous and inconsistent machining, causes to increase in circularity as shown in Figure 5.10 (b).

Peak current is the amount of current supplied at the time of machining. Machining speed is directly proportional to the amount of current supplied during the process. Fig. 5.10 (c) shows the effect of peak current on cylindricity error. At low peak current the machining speed is very

low and uniform and therefore cylindricity error is less. When the peak current increases, inconsistent machining takes place and it produces more undulations thereby increasing the cylindricity error up to certain level. Further increase in peak current causes the sparks to produce continuously and the machining becomes uniform and stable thereby reducing the cylindricity error.

Servo voltage, also called as the reference voltage, controls the wire advance and retracts. At low servo voltage, the gap between the wire and workpiece becomes narrow and more number of sparks are generated continuously, which results in uniform material removal thereby decreasing the cylindricity error. When servo voltage increases, the gap between wire and workpiece increases thereby generating the sparks inconsistently causing vibrations of wire. These vibrations produce more undulations causing higher cylindricity error as depicted in Fig 5.10 (d). However, beyond 50 V the effect of change in servo voltage on the cylindricity error was found to be negligible.

To develop prediction model for the cylindricity error, neural network toolbox has been used in the present study. The total data sets are internally divided into 70 %, 15 % and 15 % for training, validation and testing respectively. The neurons are trained using the 70 % of data in developing the model. Once the model is developed, prediction accuracy was verified with validation and testing data sets. The regression coefficient, R is used to express the correlations between experimental and predicted values in NN modeling. The training may be stopped when the regression coefficients for training, validation and testing data are acceptable, and the developed model can be used to predict the cylindricity error. The regression coefficients of the developed NN model are found to be 98 %, 99 %, 97 % and 98 % for training, validation, testing and overall model respectively as shown in Fig. 5.11 (a) to (d)

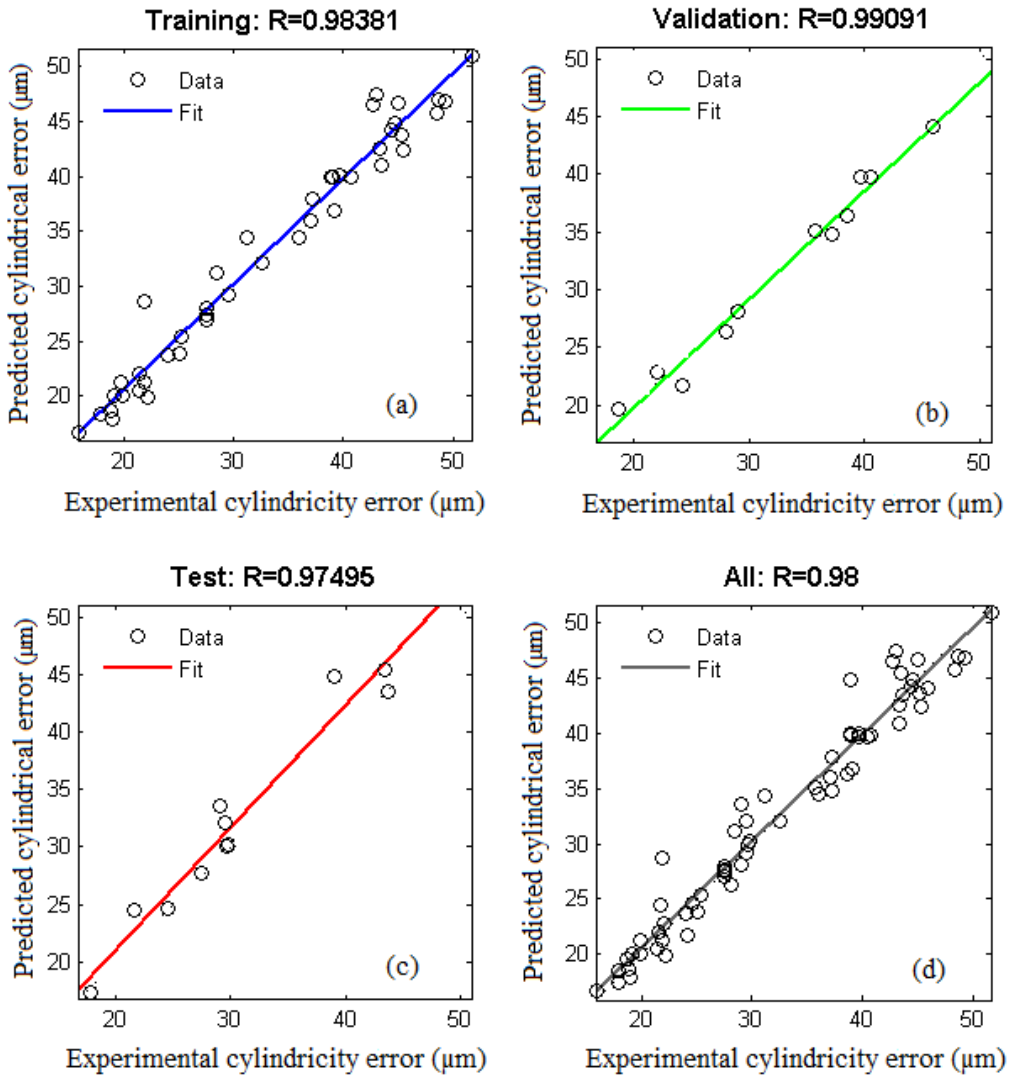

Figure 5.11. Correlation between experimental and predicted cylindricity errors with associated R values

Effectiveness of the model was validated against 10 experimental data sets. Table 5.4 presents the percentage of deviation between the experimental and predicted cylindricity errors for the validation data sets. Figure 5.12 shows the graphical representation of the confirmation test results. It can be observed that the deviations between experimental and predicted values are marginal. It was found from the results of confirmation test data sets that the average deviation of cylindricity error from experimental value to the predicted value is 4.87 %. Therefore, the developed model can be used to predict the cylindricity error.

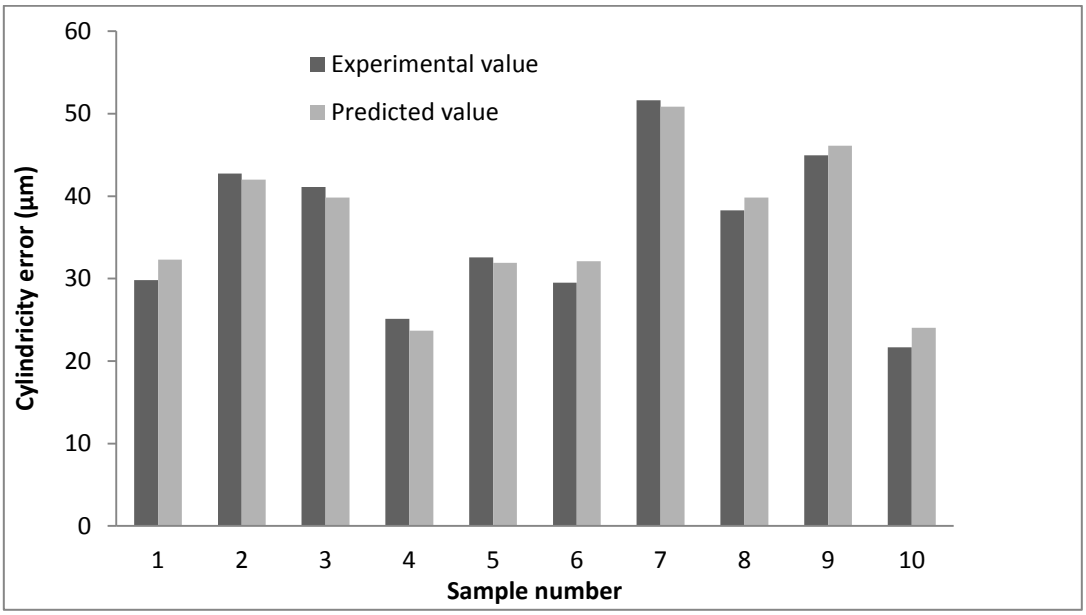

Figure 5.12. Experimental and predictive cylindricity errors in validation of NN model

Table 5.4 Experimental data to validate NN model for cylindricity error

S. No.	T_{on} (µs)	T_{off} (µs)	I_p (A)	S_v (V)	Experimental cylindricity error (µm)	Predicted cylindricity error using NN (µm)	Deviation in %
1	125	50	10	60	29.81	32.294	8.33
2	125	50	12	60	42.75	42.003	1.75
3	115	55	11	50	41.11	39.847	3.075
4	125	50	12	40	25.12	23.686	5.715
5	105	50	10	40	32.56	31.931	1.95
6	105	60	10	60	29.50	32.116	8.86
7	115	60	11	50	51.61	50.874	1.44
8	115	55	11	50	38.28	39.847	4.10
9	115	55	11	40	44.96	46.127	2.59
10	105	60	12	60	21.65	24.025	10.95

5.6. Summary

Inconel-690 and Nimonic-263, nickel based super alloys, are very hard to cut using the conventional machining processes. WEDM, being an advanced machining process, can be used to machine electrically conductive materials of any hardness. Majority of engineering components have axi-symmetrical features in them. In order to minimize the rejection rate during inspection, these features are to be manufactured with strict control with regard to their tolerances. Machining of circular and cylindrical components with minimum circularity or cylindricity errors to meet their functional and assembly criteria is always a challenging task especially with a stochastic machining process like WEDM. Since the studies on influence of process parameters on the circularity error and cylindricity errors in WEDM are not yet reported, attempts are made in this work to carry out these investigations.

Summary of the findings on circularity error:

- It is observed that, up to 120 µs of pulse-on time circularity error is low and further increase in pulse-on time increases the circularity error.
- The circularity error decreases with increase in pulse-off time up to 55 µs and further increase in pulse-off time increases circularity error.
- Circularity error decreases with increase in peak current.
- It is also observed that the circularity error decreases with increase in servo voltage up to 45 V and further increase in servo voltage increases the circularity error.

Summary of the findings on cylindricity error:

- It is observed that, up to a pulse-on time of 115 µs cylindricity error is increased and further increase in pulse-on time decreases the cylindricity error.
- The cylindricity error steadily increases with increase in pulse-off time.
- Cylindricity error was found to increase with increase in peak current up to 11 A and further increase in peak current decreases the cylindricity error.
- It is also observed that the cylindricity error sharply increases with increase in servo voltage up to 50 V and remains constant beyond 50 V.

Robust prediction models for the circularity error and cylindrical errors can reduce the rejection rate and yield parts of better quality. For the first time, attempts are made to develop

predictive models for the circularity error and cylindrical errors in WEDM process. Neural network technique is used and the models are trained, validated and tested with different data sets. Deviations between experimental and predicted values are estimated for all the data sets. Since the regression coefficient values are above 96 % for all the data sets, correlations between experimental and predicted values are strong. Furthermore, all the deviations of the circularity error and cylindricity errors are in acceptable range and therefore, the models developed in this work can be applied for accurate prediction of the circularity and cylindricity errors. The machining data generated in the present work for the Inconel-690 and also Nimonic-263 using WEDM process will be useful to the industry.

CHAPTER 6

EXPERIMENTAL INVESTIGATION ON RE-CAST LAYER THICKNESS AND MICRO-HARDNESS OF WEDMed SURFACES OF INCONEL-690 AND NIMONIC-263

6.1. Introduction

The mechanical properties of any material after machining will vary due to the machining phenomena of sudden heating and cooling. The base material properties cannot be maintained by the machined components. Therefore, the mechanical properties of the machined components such as micro-hardness (MH), recast layer thickness (RLT) are very essential to know whether they are meeting the functional requirements or not. In WEDM process, when the workpiece approaches the electrode, the gap between workpiece and wire reaches a certain threshold value, the insulating liquid breaks down and discharging channel forms thereby sparks are generated resulting in high temperature instantaneously up to about 10000º C. A huge amount of heat is generated due to these sparks and this heat is used to melt workpiece. A portion of the melted workpiece material is removed by a dielectric circulation system. The remaining molten material will rapidly re-solidify to form a layer known as the recast layer (Goswami and Kumar, 2014). This recast layer affects the mechanical properties like hardness of the materials. The hardness of the WEDMed surfaces will depend on the recast layer thickness. Newton et al. (2009) investigated on characteristics of recast layer formed in machining of Inconel-718. They found that the hardness is increasing with distance from the top layer of WEDMed surface. Li et al. (2013) and Kumar et al. (2016) also observed that there is a dramatic reduction of hardness as compared to bulk material.

As the nickel based super alloys are using in various applications such as nuclear, automobiles and aerospace etc., it is required to investigate the recast layer thickness and

hardness of the machined surfaces along with MRR, SR and kerf etc. Most of the researchers concentrated in modeling of WEDM responses like MRR, SR and kerf etc. using regression (Mahapatra and Patnaik, 2007; Sadeghi et al. 2011), neural networks (Spedding and Wang 1997; Sarkar and Mitra 2006; Saha et al. 2008) and RSM (Datta and Mahapatra, 2010; Shandilya et al., 2012) etc. No importance is given for modelling and prediction of recast layer thickness and hardness of WEDMed surfaces. In the present study RSM is used to generate mathematical models and optimization of recast layer thickness and hardness for first time. The data generated may be useful to the industry.

This chapter describes the modeling of RLT and hardness of the machined components for both Inconel-690 and Nimonic-263. It is also describe the influence of various process parameters like pulse-on time, pulse-off time, peak current and servo voltage and their interactional effects on RLT and MH.

6.2. Modeling of RLT and MH for Inconel-690

In this study the face cantered central composite design with six centre points has been used. The workpiece material of Inconel-690, a nickel based super alloy, of size 100 mm × 50 mm × 6.5 mm is used. Holes of 10 mm size are produced on the material with zinc coated brass wire as electrode and deionized water as di-electric fluid. The re-cast layer has been observed using Scanning Electron Microscope (SEM) of Tescan make VEGA 3 LMU model and micro-hardness of the machined surfaces is measured using Econamet VH 1 MD, Chennai Metco, India and are shown in Figure 3.5 and Figure 3.7 respectively. A load of 500 gm for a dwell time of 10 min was applied to measure the micro-harness. Prediction models are generated for RLT and MH using RSM and the adequacies of these models are expressed in terms of R-square values.

6.2.1. Results and analysis

Experimental results of RLT and MH are given in Table 6.1 in the coded form along with the measured responses of hardness and recast layer thickness. ANOVA has been conducted for both RLT and MH to study the significance of parameters and their interaction effects.

Table 6.1 Experimental plan and results for Inconel-690

S. No.	T_{on}	T_{off}	I_p	S_v	RLT (µm)	MH (HV)
1	2	2	2	2	31.07	139.7
2	2	3	2	2	27.86	143
3	3	1	3	3	38.4	133
4	2	2	1	1	19.14	155.3
5	1	3	3	3	27.24	144.5
6	2	2	2	3	27.66	143.4
7	3	3	1	1	23.13	159.67
8	2	2	2	2	30.25	139.9
9	2	2	2	1	29.37	141
10	1	1	1	1	16.48	157.1
11	2	2	3	1	41.98	133
12	3	3	1	3	14.55	161
13	3	1	1	1	26.66	145
14	1	3	3	1	33.14	138.2
15	2	2	2	2	28.68	142.7
16	1	1	1	3	11.4	167.4
17	2	1	2	2	31.83	139.7
18	1	1	3	3	32.14	139
19	1	3	1	1	12.84	161
20	1	3	1	3	10.06	171
21	3	2	2	2	28	141.2
22	1	2	2	2	26.24	147.1
23	2	2	2	2	29.29	142
24	1	1	3	1	36.16	134
25	3	1	3	1	49.34	122.5

26	3	3	3	3	37.91	134
27	2	2	2	2	29.22	142.1
28	3	3	3	1	47.42	128.6
29	2	2	2	1	35.5	137.9
30	3	1	1	3	16.37	158

(a) ***ANOVA analysis of recast layer thickness***

It is observed from the ANOVA results of RLT (Table 6.2) that the factors influencing the RLT are pulse-on time, peak current and servo voltage and are shown in Figure 6.1 (a) to (c). The factors for which the P value is less than 0.05 will influence the model. A mathematical predictive model has been developed using ANOVA.

Table 6.2 ANOVA results of RLT for Inconel-690

Source	SS	DF	MS	F	P
Model	2777.04	12	231.42	99.94484	< 0.0001
A-T_{on}	321.565	1	321.565	138.8762	< 0.0001
B- T_{off}	33.7021	1	33.7021	14.55512	0.0014
C-I_p	2071.53	1	2071.53	894.6466	< 0.0001
D-S_v	234.289	1	234.289	101.1839	< 0.0001
AB	1.65122	1	1.65122	0.713125	0.4101
AC	13.0682	1	13.0682	5.643858	0.0295
AD	28.9982	1	28.9982	12.52365	0.0025
CD	0.8281	1	0.8281	0.357637	0.5577

A^2	29.8336	1	29.8336	12.88441	0.0023
B^2	1.15728	1	1.15728	0.499802	0.4892
C^2	0.00564	1	0.00564	0.002437	0.9612
D^2	2.94788	1	2.94788	1.273119	0.2749
Residual	39.3631	17	2.31548		
Lack of Fit	35.653	12	2.97108	4.004009	0.0681
Pure Error	3.71013	5	0.74203		
Cor. Total	2816.4	29			

The predictive model in coded form is given in Equation (6.1). For this model R-square, adjusted R-square and predicted R-square values are 98.6 %, 97.62 % and 94.91 % respectively.

$$RLT = 30.08 + 4.23A - 1.37B + 10.73C - 3.61D + 0.32AB + 0.9AC - 1.35AD - 0.23CD - 3.39A^2 - 0.67B^2 + 0.047C^2 + 1.07D^2 \quad (6.1)$$

Influence of process parameters on recast layer thickness is shown in Figure 6.1 (a) to (f). It can be observed from the Figure 6.1 (a) that RLT increases as pulse-on time increases. Since pulse-on time corresponds to amount of time allowed to discharge energy in machining process, amount of energy increases with pulse-on time. Higher the energy discharged, higher will be the MRR and cutting speed. As the material removal increases, it causes more oxides to form and the dielectric fluid will not be able to flush away the debris effectively at higher cutting speed. Therefore, at high pulse-on time, chances of increasing the recast layer thickness on the machined surface will be high. Pulse-off time is the time interval between discharges. Behavior with this factor is opposite to that of pulse-on time as shown in Figure 6.1 (b). Peak current is the amount of current applied during machining. The discharge energy is directly proportional to the current. At high peak current, more energy is discharged resulting in more MRR and there is continuous spark generation and therefore, the cutting speed increases. Under these conditions, more amount of material is removed from workpiece as well as electrode and also more oxides will form on the

surface therefore chances of forming the RLT will be high as shown in Figure 6.1 (c). Servo voltage is the reference voltage and is used to control the wire retracts and advances. At lower value of servo voltage, the gap between wire and workpiece becomes narrow allowing more number of sparks per unit time. More amount of heat is generated causing cutting speed to increase thereby increasing the RLT. In other words, as the servo voltage increases, the cutting speed decreases which causes RLT to decrease as shown in Figure 6.1 (d). The interaction effects on RLT are also shown in Figure 6.1 (e) and (f).

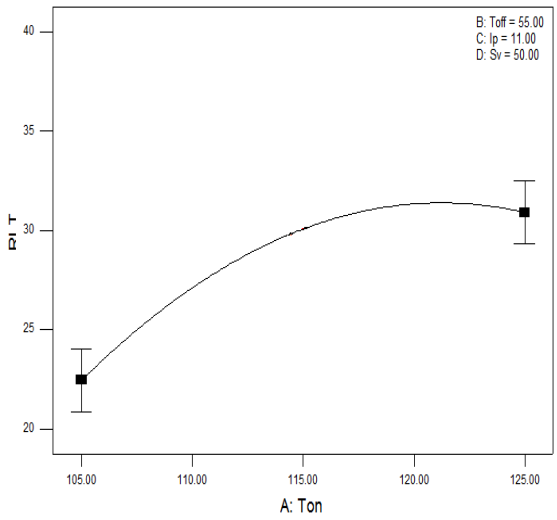

(a) T_{on} (µs)

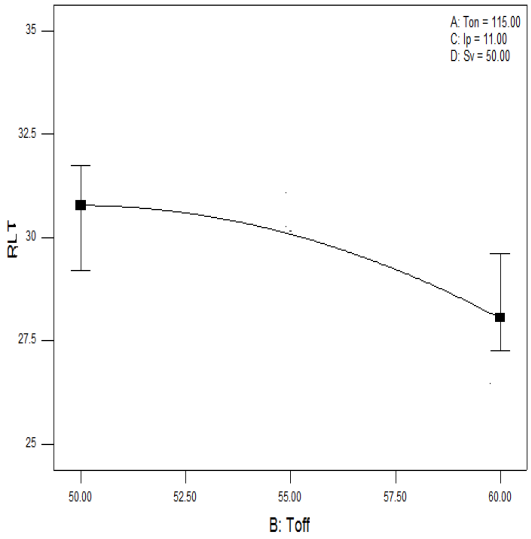

(b) T_{off} (µs)

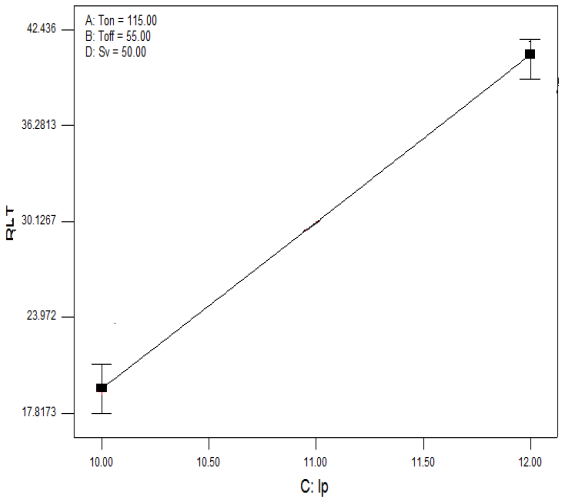

(c) I_p (A)

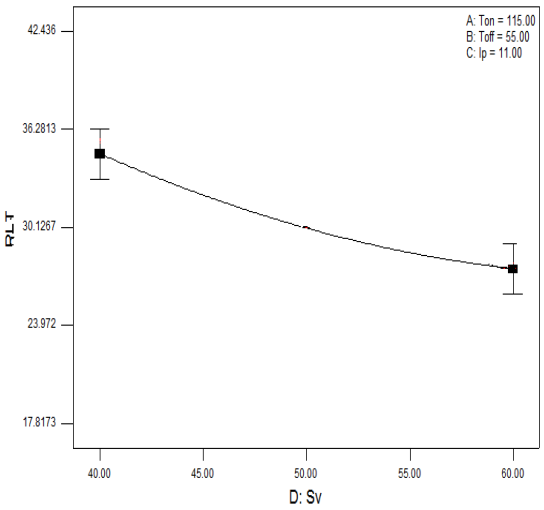

(d) S_v (V)

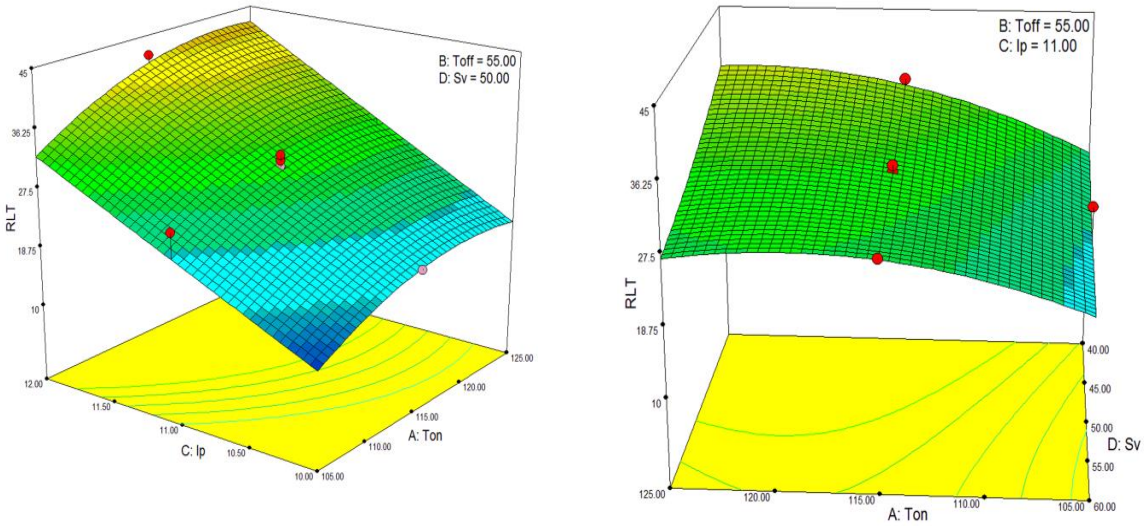

(e) T_{on} (µs) and I_p (A) (f) T_{on} (µs) and S_v (V)

Figure 6.1. Effect of process parameters on recast layer thickness while machining Inconel-690

(b) ***ANOVA analysis of micro-hardness***

From the ANOVA Table 6.3, it is observed that the factors such as pulse-on time, pulse-off time, peak current, and servo voltage influence the hardness of machined surfaces.

Table 6.3 ANOVA results of MH for Inconel-690

Source	SS	DF	MS	F	P
Model	3845.28	14	274.662976	64.93432235	< 0.0001
A-T_{on}	323.682	1	323.6816056	76.52303934	< 0.0001
B- T_{off}	113.854	1	113.85405	26.91675337	0.0001
C-I_p	2905	1	2904.998272	686.7838433	< 0.0001
D-S_v	251.852	1	251.8516056	59.54138261	< 0.0001
AB	3.58156	1	3.58155625	0.846731989	0.3720

AC	1.42206	1	1.42205625	0.336194781	0.5706
AD	0.11731	1	0.11730625	0.027732904	0.8700
BC	4.37856	1	4.37855625	1.035154381	0.3251
BD	15.5433	1	15.54330625	3.674663667	0.0745
CD	3.45031	1	3.45030625	0.81570258	0.3807
A^2	24.3159	1	24.31590463	5.748633516	0.0300
B^2	0.1799	1	0.179904625	0.04253207	0.8394
C^2	24.3159	1	24.31590463	5.748633516	0.0300
D^2	0.493632	1	0.493631898	0.11670176	0.7374
Residual	63.44787	15	4.229858202		
Lack of Fit	55.77454	10	5.577453969	3.634309711	0.0835
Pure Error	7.673333	5	1.534666667		
Cor. Total	3908.73	29			

A prediction model has been developed using ANOVA and is given by Equation (6.2) in coded form. The R-squared, adjusted R-squared and predicted R-squared values are 98.37 %, 96.86 % and 88.95 % respectively for this model.

$$MH = 141.159 - 4.241A + 2.51B - 12.7C + 3.74D + 0.47AB - 0.3AC - 0.086AD - 0.52BC - 0.99BD - 0.46CD + 3.06A^2 + 0.26B^2 + 3.06C^2 - 0.44D^2 \quad (6.2)$$

Hardness of bulk material (zero recast layer thickness) is higher for nickel based super alloys as compared to that of recast layer. This is due to the fact that recast layer is composed of elements like Cu, Zn, oxides and salts. Therefore hardness and RLT are inversely related.

The effects of various process parameters and their interactions on hardness are shown in Figure 6.2 (a) to (d). It can be observed from the Figure 6.2 (a) that the hardness decreases as pulse-on time increases. At higher pulse-on time discharge energy is more causing the cutting speed to increase. RLT increases with increase in cutting speed thereby decreasing the hardness of machined surface. The behavior with pulse-off time is opposite to that of pulse-on time as shown in Figure 6.2 (b). As the discharge energy is directly proportional to the current, at the high peak current, the cutting speed, melting of metal is more. Therefore the RLT increases thereby hardness decreases as shown in Figure 6.2 (c). At low value of servo voltage, cutting speed is high due to the reasons explained earlier. As a result, RLT increases thereby decreasing the hardness as shown in Figure 6.2 (d).

The recast-layers of the machined samples were measured using the inbuilt measuring software of scanning electron microscope. Two specimens are chosen, one at lowest RLT from Table 6.1, corresponding to Experiment number 20 (T_{on}=105 µs, T_{off} = 60 µs, I_p = 10 A, S_v = 60 V) and another at highest RLT corresponding to Experiment number 25 (T_{on} = 125 µs, T_{off} = 50 µs, I_p = 12 A, S_v = 40 V) shown in Figure 6.3.

Micro cracks, voids can also be observed on the WEDMed surfaces (Figure 6.4). A pool of molten metal in the form of debris, which is not flushed away by di-electric fluid, deposits on the machined surface as shown in Figure 6.4. A pool of molten metal increases RLT and it cannot be completely eliminated during WEDM process. RLT can be minimized upto certain level by choosing the optimal machining conditions. Also, circulation of dielectric fluid with sufficient pressure will flush most of the molten metal and debris thereby reducing the RLT. The recast layer thickness, was observed in the range of 10 - 50 µm. Hardness of Inconel-690 base material is 221 HV. However, hardness of the machined surface was found to lie in the range 122 - 171 HV due to the variation of the RLT at different conditions. The reduction in hardness can be attributed to the presence of Zn, Cu, oxides and salts in the recast layer.

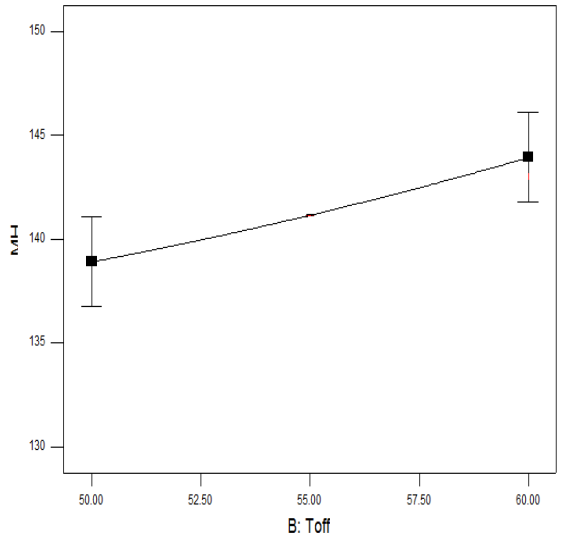

(a) T_{on} (µs)

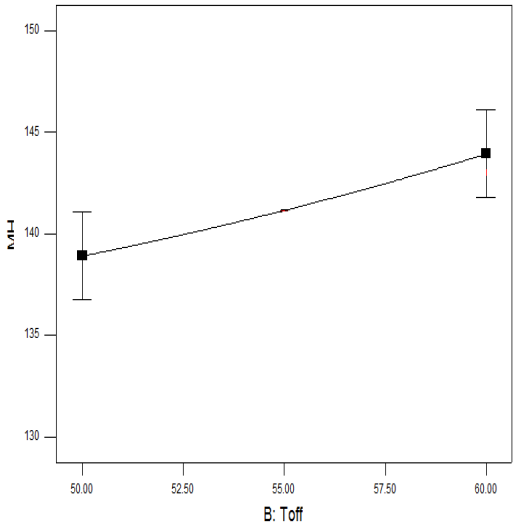

(b) T_{off} (µs)

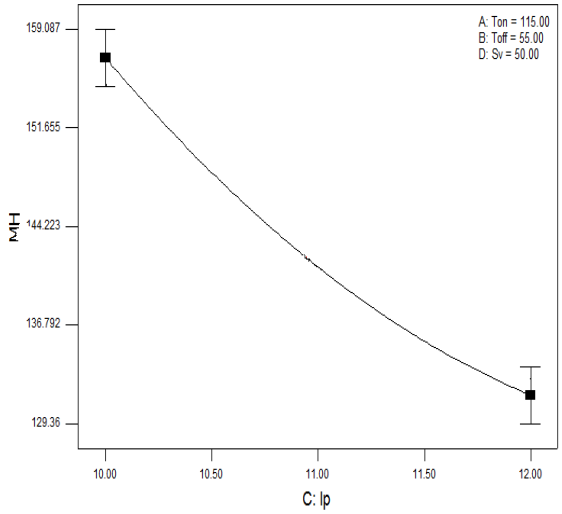

(c) I_p (A)

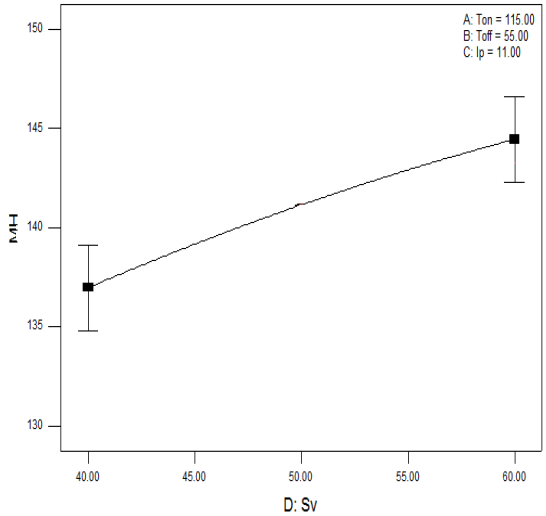

(d) S_v (V)

Figure 6.2. Effect of process parameters on micro-hardness while machining Inconel-690

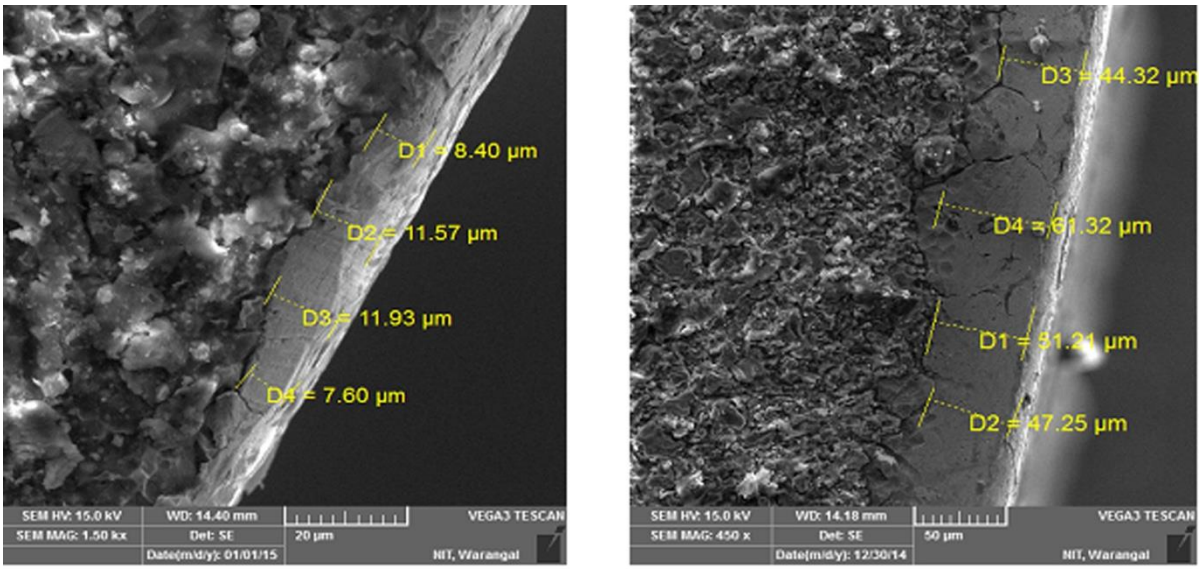

(a) T_{on}=105 µs, T_{off} =60 µs,I_p=10 A, S_v=60 V (b) T_{on}=125 µs, T_{off} =50 µs,I_p =12 A, S_v=40 V

Figure 6.3. SEM images showing the recast layer thicknesses at different conditions

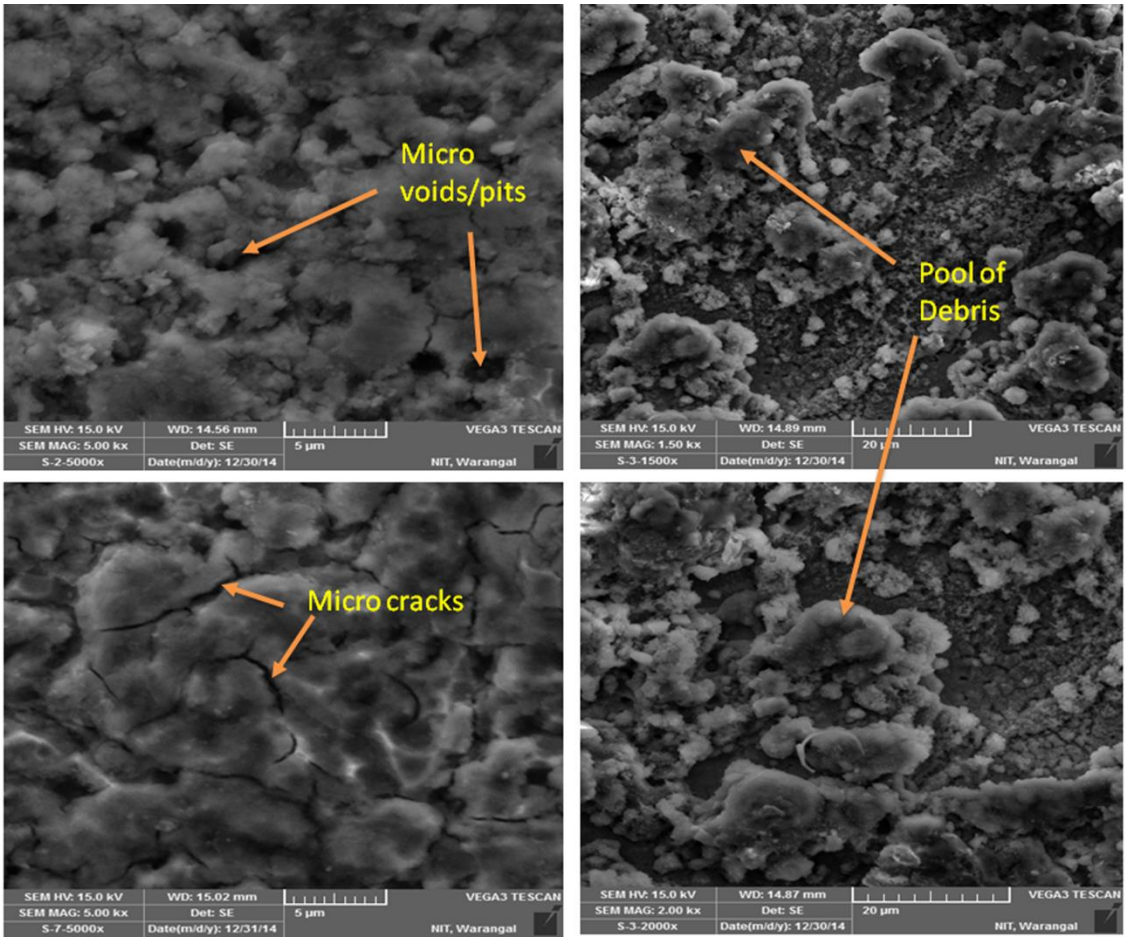

Figure 6.4. SEM images showing micro cracks, voids and debris of molten metal

6.2.2. EDS analysis

Energy Dispersive X-ray Spectroscopy or EDS coupled with SEM, is used for compositional analysis and chemical characterization. Surface layers of the WEDMed specimens have been analysed using EDS. Figure 6.5 (a) and (b) show the EDS spectra of machined surfaces corresponding to experiment number 20 (T_{on} = 105 µs, T_{off} = 60 µs, I_p = 10 A, S_v = 60 V) and experiment number 25 (T_{on} = 125 µs, T_{off} = 50 µs, I_p = 12 A, S_v = 40 V) respectively. Though, the bulk material does not have zinc and has very less percentage of copper, the WEDMed surfaces were found to be contained these elements in appreciable quantities. The quantities of these elements corresponding to experiment number 20 and 25 are found to be 4.12 % Zn and 0.94 % Cu and also 8.26 % Zn and 1.51 % Cu respectively. These elements are migrated from the wire electrode while machining. Migration of Zn and Cu leads to soften the machined surfaces. Hence hardness of the machined surface is lesser than that of the bulk material. Hardness of the machined surfaces are presented in Table 6.1.

6.3. Modeling of RLT and MH for Nimonic-263

Similar experimental procedure has been followed for the Nimonic-263 material, a nickel based super alloy of size 120 mm × 110 mm × 18.5 mm also. The influence of WEDM process parameters such as pulse-on time, pulse-off time, peak current and servo voltage on the micro-hardness and recast layer of Nimonic-263 machined surfaces have been studied. Predictive mathematical models for RLT and MH are also developed.

6.3.1. Results and analysis

Experiments are conducted as per the RSM plan as presented in Table 6.4 along with the measured responses. ANOVA has been conducted for RLT, SR and MH to study the significance of parameters and their interaction effects on the responses. Prediction models are generated using RSM and the adequacies of these models are expressed in terms of R-squared values.

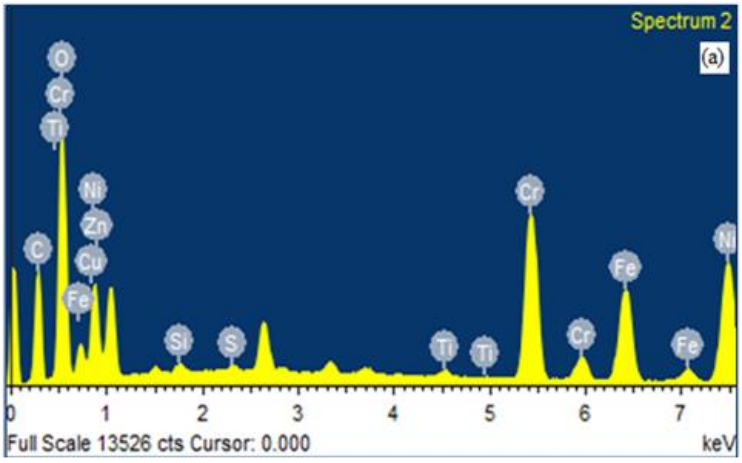

Element	Weight%	Atomic%
C K	23.14	42.92
O K	26.69	37.17
Si K	0.3	0.24
S K	0.2	0.14
Ti K	0.35	0.16
Cr K	13.2	5.66
Fe K	10.37	4.14
Ni K	20.69	7.85
Cu K	0.94	0.33
Zn K	4.12	1.4
Totals	100	

(a) T_{on} = 105 µs, T_{off} = 60 µs, I_p = 10 A, S_v = 60 V

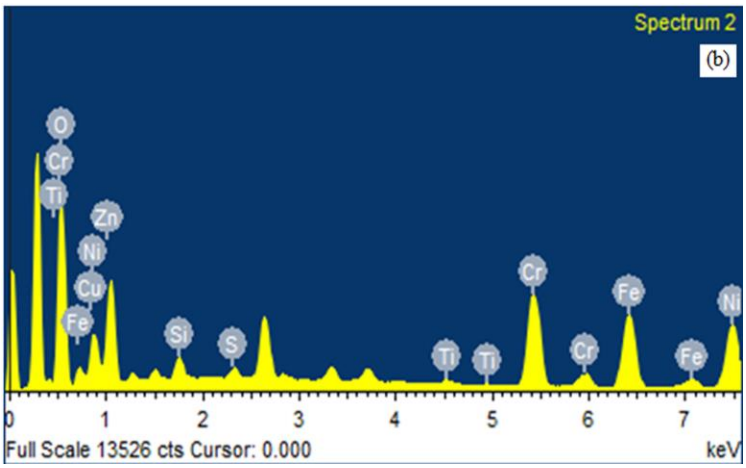

Element	Weight%	Atomic%
O K	30.06	59.62
Si K	1.8	2.04
S K	0.85	0.84
Ti K	0.52	0.34
Cr K	15.8	9.64
Fe K	17.6	10
Ni K	23.6	12.75
Cu K	1.51	0.75
Zn K	8.26	4.01
Totals	100	

(b) T_{on} = 125 µs, T_{off} = 50 µs, I_p = 12 A, S_v = 40 V

Figure 6.5. EDS images at different conditions

Table 6.4 Experimental plan and results for Nimonic-263

S. No	T_{on} (µs)	T_{off} (µs)	I_p (A)	S_v (V)	RLT (µm)	MH (HV)
1	125	60	12	60	26.05	259.1
2	125	60	10	60	10.21	320.9
3	115	55	11	40	24.88	267.6

4	115	55	11	50	19.09	287.7
5	105	60	12	60	15.75	309.1
6	125	55	11	50	25.19	260
7	125	50	10	40	15.49	313
8	115	55	12	50	28.49	245
9	115	50	11	50	19.87	247.4
10	105	50	10	40	12.33	318.1
11	115	55	10	50	11.89	315
12	105	60	10	60	8.8	335.9
13	125	50	10	60	10.954	327.1
14	115	55	11	50	18.57	298
15	125	50	12	40	37.79	232.2
16	105	60	10	40	9.5	330.2
17	125	60	12	40	36.31	238
18	105	55	11	50	14.27	313
19	115	55	11	60	17.68	299.5
20	115	60	11	50	18.36	298.1
21	125	60	10	40	13.99	314.6
22	105	50	12	40	25.38	259.8

23	125	50	12	60	26.67	248.3
24	105	60	12	40	22	281.6
25	105	50	10	60	8.99	332.5
26	105	50	12	60	22.39	273.2

(a) ***ANOVA analysis of RLT***

It is observed from the ANOVA results of RLT that the factors influencing the RLT are pulse-on time, pulse-off time, peak current, servo voltage and the interaction effects of pulse-on time and current, pulse-on time and servo voltage, and current and servo voltage as shown in Figures 6.6 (a) - (g).

Table 6.5 ANOVA results of RLT for Nimonic-263

Source	**SSquares**	**DF**	**MS**	**F**	**P**
Model	1553.01	10	155.301	65.56155	< 0.0001
A-T_{on}	222.2113	1	222.2113	93.80828	< 0.0001
B-T_{off}	19.8324	1	19.8324	8.372407	0.0111
C-I_p	1068.391	1	1068.391	451.0297	< 0.0001
D-S_v	139.8684	1	139.8684	59.04656	< 0.0001
AB	4.726276	1	4.726276	1.995235	0.1782
AC	57.28976	1	57.28976	24.18533	0.0002

AD	16.84282	1	16.84282	7.110329	0.0176
BC	2.937796	1	2.937796	1.240214	0.2830
BD	0.062001	1	0.062001	0.026174	0.8736
CD	20.84836	1	20.84836	8.8013	0.0096
Residual	35.53172	15	2.368781		
Lack of Fit	35.39652	14	2.528323	18.70061	0.1795
Pure Error	0.1352	1	0.1352		
Cor Total	1588.542	25			

The factors for which the P value is less than 0.05, will influence the model. A mathematical predictive model has been developed using ANOVA. The predictive model of coded form is given in Equation (6.3). For this model R-square, adjusted R-square and predicted R-square values are 97.76 %, 96.27 % and 91.34 % respectively.

$$RLT = 19.27 + 3.51A - 1.05B + 7.7C - 2.79D + 0.54AB + 1.89AC - 1.03AD - 0.43BC + 0.062BD - 1.14CD \quad (6.3)$$

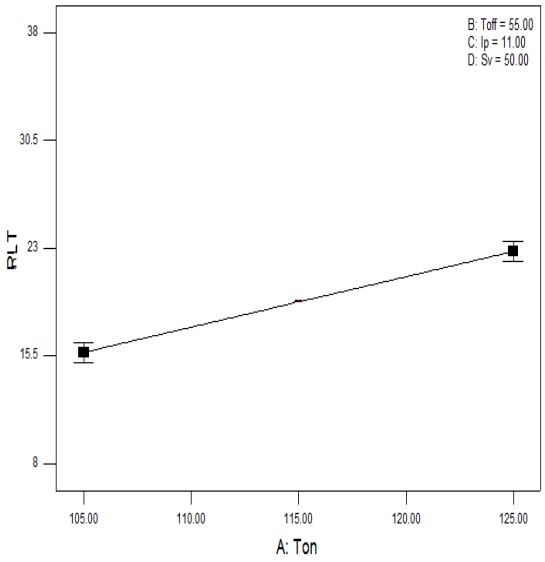

(a) T_{on}

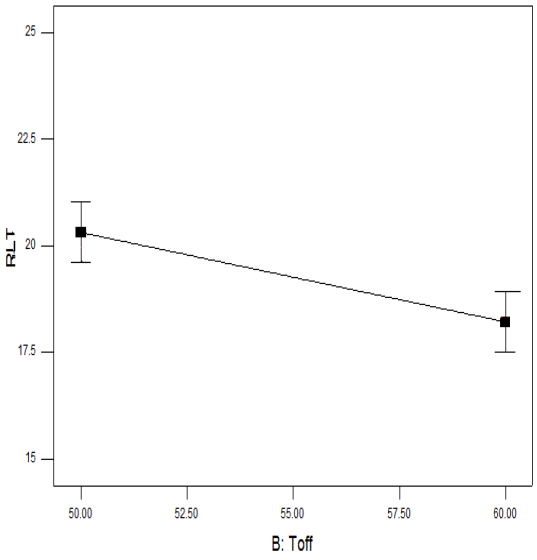

(b) T_{off}

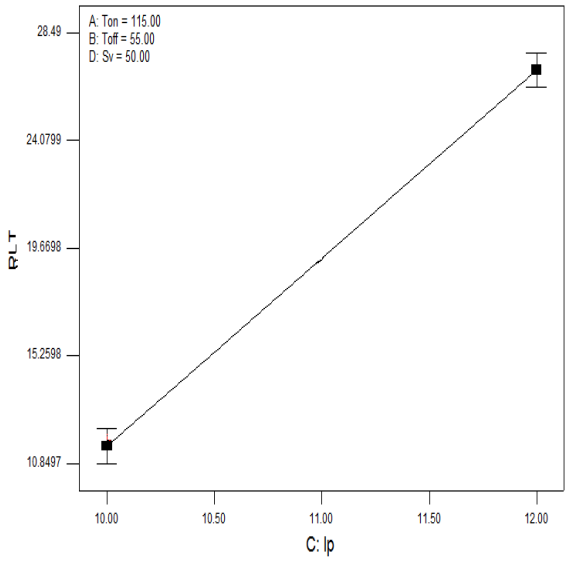

(c) I_p

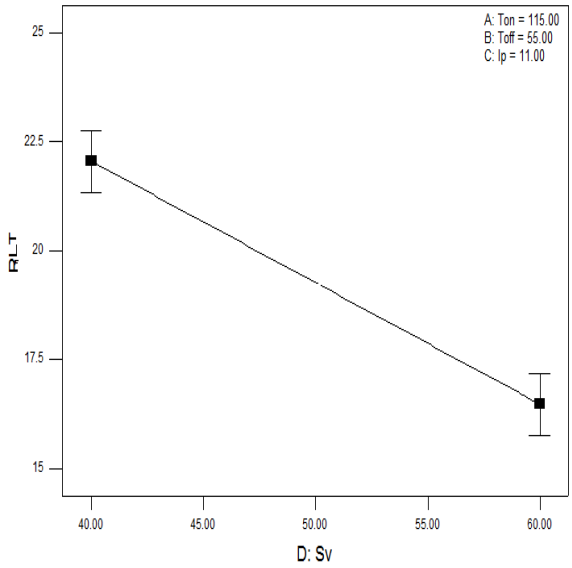

(d) S_v

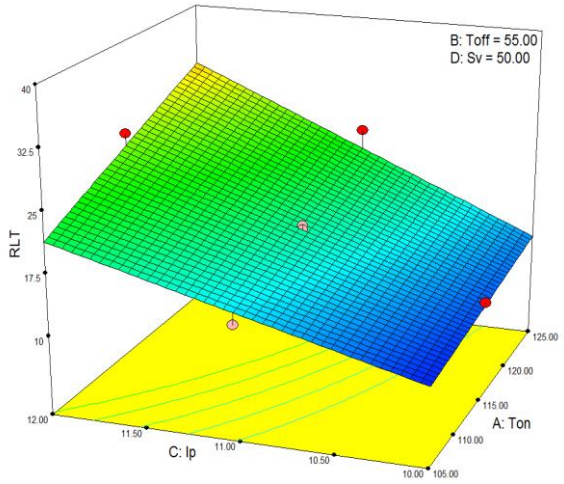

(e) T_{on} and I_p

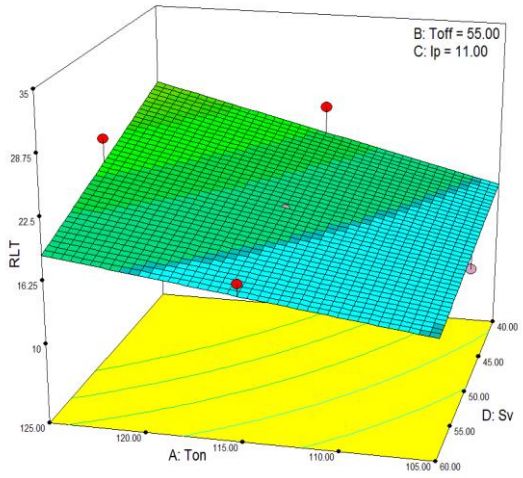

(f) T_{on} and S_v

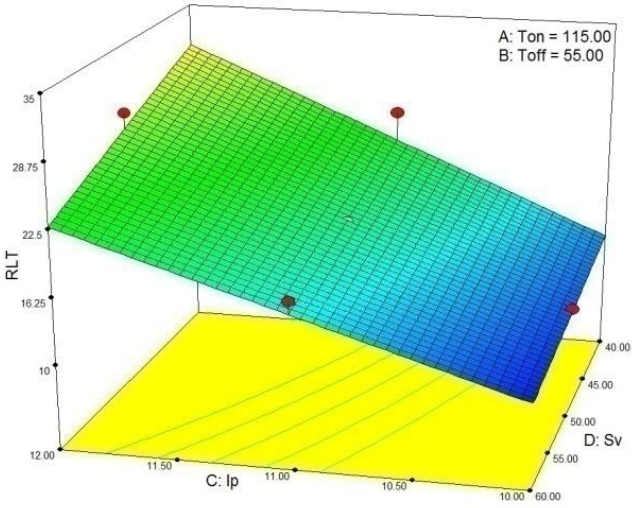

(g) I_p and S_v

Figure 6.6. Effect of process parameters on recast layer thickness while machining Nimonic-263

Effect of various process parameters (Figure 6.6) on RLT in machining of Nimonic-263 are as similar as thst of machining in Inconel-690 and are explained in 6.2. The interaction effects on RLT are also shown in Figure 6.6 (e) to (g).

(b) ***ANOVA analysis of micro-hardness***

From the ANOVA Table 6.6, it is observed that the factors such as pulse-on time, pulse-off time, peak current, and servo voltage influence the hardness of machined surfaces.

Table 6.6 ANOVA results of MH for Nimonic-263

Source	SSquares	DF	MS	F	P
Model	23929.8	14	1709.27	27.4674	< 0.0001
A-T_{on}	858.361	1	858.361	13.7936	0.0034
B-T_{off}	228.98	1	228.98	3.67964	0.0814
C-I_p	19503.1	1	19503.1	313.409	< 0.0001
D-S_v	1854.41	1	1854.41	29.7997	0.0002
AB	12.4256	1	12.4256	0.19968	0.6637
AC	43.8906	1	43.8906	0.70531	0.4189
AD	108.681	1	108.681	1.74647	0.2131
BC	0.05063	1	0.05063	0.00081	0.9778
BD	3.90063	1	3.90063	0.06268	0.8069
CD	33.3506	1	33.3506	0.53594	0.4794
A^2	65.1882	1	65.1882	1.04755	0.3281
B^2	148.107	1	148.107	2.38004	0.1512
C^2	610.935	1	610.935	9.81753	0.0095
D^2	0.76134	1	0.76134	0.01223	0.9139
Residual	684.518	11	62.2289		
Lack of Fit	653.313	10	65.3313	2.09362	0.4948
Pure Error	31.205	1	31.205		
Cor. Total	24614.3	25			

From the ANOVA Table 6.6, it is observed that pulse-on time, peak current and servo voltage are influencing the hardness model. A prediction model has been developed using ANOVA. The predictive model of coded form is given in Equation (6.4). The R-square, adjusted R-square and predicted R-square values are 93.26 %, 87.03 % and 74.02 % respectively for this model.

$$MH = 281.63 - 13.34A + 7.55B - 31.17C + 8.36D - 3.83AB - 6.56AC + 3.96BC + 2.35CD + 8.61A^2 - 5.14B^2 + 2.11C^2 + 5.66D^2 \quad (6.4)$$

The effect of various process parameters and interaction effects on hardness are shown in Figure 6.7 (a) to (c). Effect of various process parameters (Figure 6.6) on RLT in machining of Nimonic-263 are as similar as that of machining in Inconel-690 and are explained in 6.2. The recast-layer of the machined samples was measured using the inbuilt measuring software of scanning electron microscope.

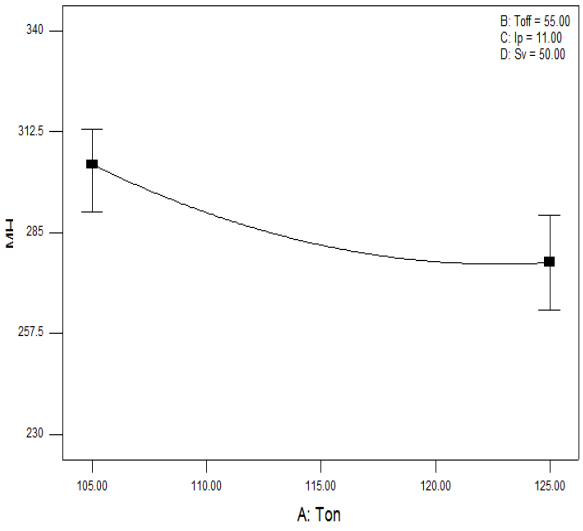

(a) T_{on}

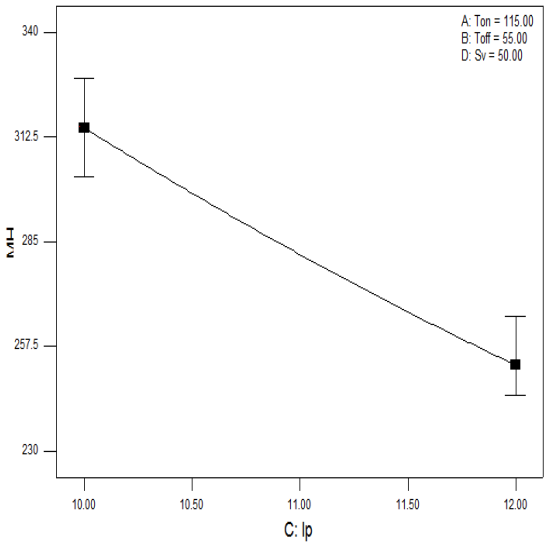

(b) I_p

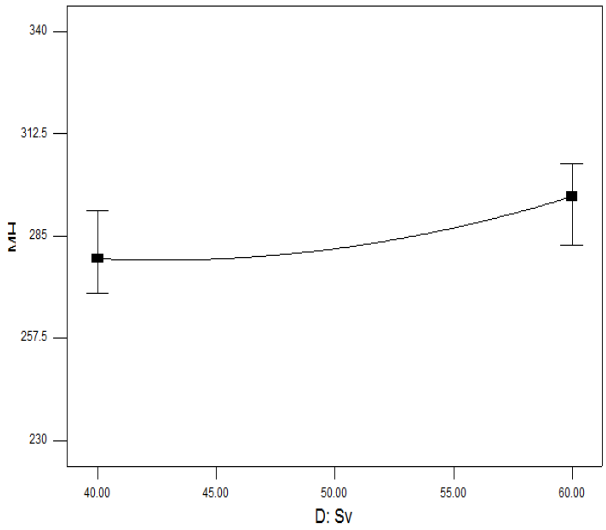

(c) S_v

Figure 6.7. Effect of process parameters on micro hardness while machining Nimonic-263

6.4. Summary

Nickel based super alloys are gaining importance day by day due to their superior properties like high hardness at elevated temperatures, low thermal conductivity and high resistance to corrosion. Machining of these alloys with conventional machining processes is very difficult due to these properties. Inconel-690 and Nimonic-263 which are nickel based alloys can be machined using WEDM process. Recast layers will be formed on the surfaces of these machined components, this leads to decrease in hardness as compared to base materials. However, the machined components should meet their functional requirements like retaining the hardness at high temperatures. Avoiding the rejection rate of machined surface based on the functional criteria is a challenging task especially in a machining process like WEDM due to its stochastic nature. In the present work an attempt is made to investigate the influence of WEDM process parameters on recast layer thickness and hardness of the machined surfaces of Inconel-690 and Nimonic-263. Summary of the observations include:

- Recast layer thickness of machined components is increasing with increase of pulse-on time and peak current, whereas, it is decreasing with increase of servo voltage.
- Hardness of the machined surface is lower than that of the base material.
- Hardness of the machined surface is affected by pulse-on time, peak current, servo voltage, interaction of pulse-on time and servo voltage and interaction of peak current and pulse-off time.
- Micro-cracks are observed on the machined surfaces.
- Some amount of zinc is embodied to the machined surface while machining.

Also, predictive models for recast layer thickness and hardness are developed with respect to WEDM process parameters for the first time and are very much useful to the industry.

CHAPTER 7

CONCLUSIONS AND SCOPE FOR FUTURE WORK

7.1. Conclusions

Nickel-based super alloys are a special class of materials with an exceptional combination of high temperature strength, toughness, and resistance to degradation in corrosive or oxidizing environments. These materials are extremely hard to shape using traditional machining methods due to rapid work hardening. Therefore, modern machining methods are to be employed to process such materials. WEDM is known for machining complex shapes with lesser energy requirements. Since adequate WEDM studies are not reported on these materials, generation of machining data using WEDM on these materials assumes a great importance from the industry viewpoint. In the present study, performance of WEDM process is assessed in terms of MRR, SR, RLT, MH and form errors such as circularity and cylindricity of the machined surfaces for Inconel-690 and Nimonic-263 materials.

Surface roughness affects several functional attributes of parts, such as friction, wear and tear, light reflection, heat transmission, ability of distributing and holding a lubricant and coating. Hence, assessment of surface roughness of the parts is important from the quality viewpoint. Further, in order to meet the customer requirement in terms of due date, the manufacturer always tries to maximize the MRR. Increasing the MRR is also important from the viewpoint of machining economics. Depending upon the requirements of the industry, these responses are to be optimized either individually or simultaneously. Since the accuracy of cuckoo search algorithm (CSA) heavily depends upon the initial solution and its location from the target value, it may involve large number of generations. In order to overcome these drawbacks, a modified cuckoo search (MCS) algorithm has been proposed in this work. The two-stage initialization concept ensures the identification of initial solution set very nearer to the final target value. Therefore, the proposed MCS algorithm is more accurate and faster when compared to CSA. Before applying the proposed method on actual WEDM data, it has been successfully tested on standard benchmark problems for its robustness in yielding the accurate results. The results for the WEDM data using the proposed MCS algorithm were found to be better than that of the

CSA.Confirmation tests were also conducted at optimal parameter sets and the deviations between the predicted values and experimental values are less than 5 %.Therefore, the proposed MCS algorithm can also be applied for optimization problems in other fields. Non-dominating sorting principle has also been applied on the proposed MCS to generate Pareto optimal solutions. The Pareto solutions will give the alternate solutions to the manufacturer so as to select the best solution based on the requirement. The machining data generated for the first time for Inconel-690 and Nimonic-263 in this work provides the industry some useful information on general behavior of WEDM. Based on this data, industry can carry out focused work to meet the specific needs.

In order to meet the desired functional and assembly requirements, engineering components need to have tighter dimensional and geometrical tolerances. Majority of the engineering components have circular and cylindrical features in them. These components are used for different applications such as rotating devices, transmission systems, injection moulds, bearings and engine cylinders etc. Producing straight cuts is easier as compared to machining of axisymmetric components. The difficulties are further amplified while machining such features on super alloys with the stochastic nature of WEDM process. Although most of the WEDM literature is focused on responses such as MRR, SR, Kerf, WWR etc. Studies on geometrical errors of axisymmetric components are not yet reported. Therefore attempts are made to model the geometrical errors in order to accurately predict these errors to reduce the rejection rate of the components during inspection. Neural network technique was used to develop the predictive models and the models are trained, validated and tested with different data sets. Deviations between experimental and predicted circularity and also cylindricity errors are estimated for all the data sets. Since the regression coefficient values are above 96 % for all the data sets, correlations between experimental and predicted circularity and cylindricity errors are strong. It was found from the results of confirmation test data sets that the average deviation of circularity error from experimental value to the predicted value is 5.08 %.The average deviation of cylindricity error between the experimental and the predicted values was found to be 4.87 %. Since all the deviations of the circularity and cylindricity errors are in acceptable range, the models developed in this work can be applied for accurate prediction of the circularity and cylindricity errors. The machining data generated on geometric errors for the first time in the

present work for Inconel-690 and also Nimonic-263 using WEDM process will be useful to the industry.

Mechanical properties of any material after machining will vary due to the machining phenomena of sudden heating and cooling. It is difficult to retain the base material properties after machining. In WEDM process, a huge amount of heat is generated is used to melt the workpiece. A portion of the melted workpiece material is removed by a dielectric circulation system. The remaining molten material will rapidly re-solidify to form a layer known as the recast layer. This recast layer thickness affects the surface integrity aspects such as hardness and other surface properties of the materials. Prediction models for recast layer thickness and hardness are developed with respect to WEDM process parameters for the first time and are very much useful to the industry. The re-cast layer thickness values of machined components are increasing with increase of pulse-on time and peak current, whereas, RLT is decreasing with decrease of servo voltage. Pulse-on time, peak current, servo voltage, interaction of pulse-on time and servo voltage and interaction of peak current and pulse-off time affect the hardness of the machined surface. Hardness of the machined surface was found to be lower than that of the base material for both the work materials chosen. The reduction in hardness values of machined surfaces can be attributed to the migration of Zn and Cu from the wire electrode to the workpiece and formation of oxides and carbides while machining as revealed by the EDS studies. Micro-cracks are also observed on the machined surfaces. The machining data generated on surface integrity for the first time for Inconel-690 and Nimonic-263 in this work provides the industry some useful information on general behavior of WEDM.

7.2. Scope for future work

The proposed cuckoo search algorithm with two stage initialization is generic in nature and therefore can be extended to other optimization problems. The principle of two stage initialization can also be applied to other evolutionary algorithms. Generation of machine data for different super alloys can be carried out in the similar lines. Further work may be directed to optimize more than two WEDM responses simultaneously by using non dominated sorting principle. Other form errors such as conicity, straightness etc. may also be studied on WEDMed parts.

REFERECES

1 American Society of Mechanical Engineers (1994) Dimensioning and Tolerancing. ASME Y14.5M

2 Antar M T, Soo S L, Aspinwall D K, Jones D, Perez R, (2011) Productivity and workpiece surface integrity when WEDM aerospace alloys using coated wires. Procedia Engineering 19: 3-8

3 Aravind S N, Sowmya S, Yuvaraj K P, (2012) Optimization Of Metal Removal Rate And Surface Roughness On Wire Edm Using Taguchi Method. In: IEEE-International Conference On Advances In Engineering, Science And Management. IEEE; 2012: 155-159

4 Balasubramanian S, Ganapathy S, (2011) Grey Relational Analysis to determine optimum process parameters for Wire Electro Discharge Machining (WEDM). Int J Eng Sci Technol 3(1): 95-101

5 Benardos P G, Vosniakos G C, (2002) Prediction of surface roughness in CNC face milling using neural networks and Taguchi's design of experiments. Robot Comput Integr Manuf 18(5): 343-354

6 Carl Sommer, Steeve Sommer, (2005) The complete EDM Handbook, Advance Publishers Inc., USA

7 Carpinetti L C R, Chetwynd D G, (1994) A new strategy for inspecting roundness features. Prec Eng. 16(4): 283-289

8 Carr K, Ferreira P, (1995) Verification of form tolerances Part II: Cylindricity and straightness of a median line. Preci Eng 17(2): 144-156

9 Çaydas U, Hasçalik A, (2008) A study on surface roughness in abrasive waterjet machining process using artificial neural networks and regression analysis method. J mater proces technol 202(1): 574-582

10 Çaydas U, Hasçalik A, Ekici S, (2009) An adaptive neuro-fuzzy inference system (ANFIS) model for wire-EDM. Expert Systems with Applications 36(3): 6135-6139

11 Chandrasekaran K, Simon S P, (2012) Multi-objective scheduling problem: Hybrid approach using fuzzy assisted cuckoo search algorithm. Swarm Evol Comput 5:1-16

12 Chang H, Lin T W, (1993) Evaluation of circularity tolerance using Monte Carlo simulation for coordinate measuring machine. Int J Prod Rese 31: 2079-2086

13 Chen H C, Lin J C, Yang Y K, Tsai C H, (2010) Optimization of wire electrical discharge machining for pure tungsten using a neural network integrated simulated annealing approach. Expert Systems with Applications 37(10): 7147-7153

14 Chen M C, (2002) Roundness measurements for discontinuous perimeters via machine visions. Computers in Industry 47(2): 185-197

15 Chen M C, Tsai D M, Tseng H Y, (1999) A stochastic optimization approach for roundness measurement, Pattern Recognition Letters, 20, 707-719.

16 Chetwynd D G, (1985) Applications of linear programming to engineering metrology. Proc Inst Mech Eng Part B J Eng Manuf 199(2): 93-100

17 Chiang K T, Chang F P, (2006) Optimization of the WEDM process of particle-reinforced material with multiple performance characteristics using grey relational analysis. J Mater Process Technol 180(1): 96-101

18 Choudhury S K, Bartarya G, (2003) Role of temperature and surface finish in predicting tool wear using neural network and design of experiments. Int J Machine Tools Manuf 43(7): 747-753

19 Cusanelli G, Hessler-Wyser A, Bobard F, Demellayer R, Perez R, Flukiger R, (2004) Microstructure at submicron scale of the white layer produced by EDM technique. J Mater Process Technol 149(1): 289-295

20 Das M K, Kumar K, Barman T K, Sahoo P, (2014) Optimization of surface roughness in WEDM process using Artificial Bee Colony algorithm, Int J App Eng Resea 9(26): 8748-8751

21 Datta S, Mahapatra S S, (2010) Modeling, Simulation and parametric optimization of wire EDM process using response surface methodology coupled with grey-Taguchi technique. Int J Adv Manuf Technol 2(5): 162-1183

22 Deb K, Optimization for engineering design: Algorithms and examples. 2nd Edition. PHI Learning Private Limited; 2013.

23 Deng G, Wang G, Duan J, (2003) A new algorithm for evaluating form error: the valid characteristic point method with the rapidly contracted constraint zone, J Mater Proces Technol 139(1): 247-252

24 Devillers O, Preparata F, (2000) Evaluating the cylindricity of a nominally cylindrical point set. ACM-SIAM Sympos. Discrete Algorithms, Jan 2000, San Francisco, United

States.

25 Devillers O, Ramos P, (2002) Computing roundness is easy if the data set is almost round. Int J Computational Geometry and Applications, 12: 229-248

26 DiBitonto D D, Eubank P T, Patel M R, Barrufet M A, (1989) Theoretical models of the electrical discharge machining process-I: a simple cathode erosion model, J Appl Phys 66(9): 4095-4103

27 Ding Y, Zhu L, Ding H, (2007) A unified approach for circularity and spatial straightness evaluation using semi-definite programming. Int. J. Machine Tools Manuf, 47(10): 1646-1650

28 Ebrahimi M, Rezaei E, Vaseghi B, Danesh M, (2006) Rotor resistance identification using neural networks for induction motor drives in the case of insensitivity to load variations. Iranian J Scie Technol: Transaction B Eng 30(B2): 223-236

29 El Ela A A, Abido M A, Spea S R, (2010) Optimal power flow using differential evolution algorithm. Electr Power Syst Res 80(7): 878-885

30 Esme U, Sagbas A, Kahraman F, (2009) Prediction of surface roughness in wire electrical discharge machining using design of experiments and neural networks. Iranian J Sci Technol Transaction B: Eng 33(B3): 231-240

31 Fausett L, (1994) Fundamentals of neural networks: architectures, algorithms, and applications. Prentice-Hall, Inc., USA

32 Fuller JE, (1996) Electrical Discharging Machining. ASME Machining Handbook 16:557-564

33 Gandomi A H, Yang X S, Alavi A H, (2013) Cuckoo search algorithm: A metaheuristic approach to solve structural optimization problems. Eng Comput 29(1): 17-35

34 Gauri S K, Chakraborty S, (2009) Multi-response optimisation of WEDM process using principal component analysis. Int J Adv Manuf Technol 41(7-8): 741-748

35 Gauri S K, Chakraborty S, (2009) Optimisation of multiple responses for WEDM processes using weighted principal components. Int J Adv Manuf Technol 40(11-12): 1102-1110.

36 Gauri S K, Chakraborty S, (2010) A study on the performance of some multi-response optimization methods of WEDM processes, Int J Adv Manuf Technol 49(1-4): 155-166

37 Ghodsiyeh D, Golshan A, Shirvanehdeh J A, (2013) Review on current research trends in wire electrical discharge machining (WEDM). Indian J Scie Technol 6(2): 4128-4140

38 Goswami A, Kumar J, (2014) Investigation of surface integrity, material removal rate and wire wear ratio for WEDM of Nimonic 80A alloy using GRA and Taguchi method. Eng Scie Technol 17(4): 173-184

39 Guiqin L, Fanhui K, Wenle L, Qingfeng Y, Minglun F, (2007) The Neural-Fuzzy modeling and Genetic Optimization in WEDM. IEEE International Conference In Control and Automation (ICCA 2007): 1440-1443

40 Guitrau E B, The EDM Handbook, Hanser Gardner Publications, Cincinnati, OH, 1997

41 Guven O, Esme U, Kaya I E, Kazancoglu Y, Kulekci M K, Boga C, (2010) Comparative modeling of wire electrical discharge machining (WEDM) process using Back propagation (BPN) and general regression neural networks (GRNN). Mater Technol 44(3): 147-152

42 Han F, Jiang J, Yu D, (2007) Influence of machining parameters on surface roughness in finish cut of WEDM. Int J Adv Manuf Technol 34(5-6): 538-546

43 Hasçalik A, Çaydas U, (2007) Electrical discharge machining of titanium alloy (Ti-6Al-4V). Appl Surface Scie 253(22): 9007-9016

44 Herrmann K, Hardness Testing: Principles and Applications, ASM International, USA, 2011.

45 Ho K H, Newman S T, Rahimifard S, Allen A D, (2004) State of the art in wire electrical discharge machining (WEDM). Int J Machine Tools Manuf 44(12): 1247-1259

46 Iqbal A K M, Khan A A, (2010) Influence of process parameters on Electrical discharge machined job surface integrity. American J Eng Appl Sci 3(2): 396-402

47 Jabbaripour B, Sadeghi M H, Faridvand Sh, Shabgard M R, (2012) Investigating the effects of EDM parameters on surface integrity, MRR and TWR in machining of Ti-6Al-4V. Mach Scie Technol: An Int. J 16(3): 419-444

48 Jain V K (2005) Advanced Machining Processes. Allied Publishers Pvt. Limited, New Delhi

49 Jangra K K, Kumar V, Kumar V, (2014) An experimental and comparative study on rough and trim cutting operation in WEDM of hard to machine materials. Procedia Materials Science 5: 1603-1612

50 Joghataie A, Amiri B, (2005) Modeling structure-actuator systems by neural networks. Iranian J Scie Technol Transaction B: Eng 29(B3): 323-332

51 Kaiser M J, Morin T L, (1994) Centers, out-of-roundness measures and mathematical programming. Comp Industrial Eng, 26(1): 35-54

52 Kansal H K, Singh S, Kumar P, (2005) Parametric optimization of powder mixed electrical discharge machining by response surface methodology. J Mater Process Technol 169(3): 427-436

53 Khan A A, Ali M B M, Shaffiar N B M, (2006) Relationship of surface roughness with current and voltage during wire EDM. J Appl Scie 6(10): 2317-2320

54 Khan N J, Khan Z A, Siddiquee A N, Chanda A K, (2014) Investigations on the effect of wire EDM process parameters on surface integrity of HSLA: A multi-performance characteristics optimization. Prod Manuf Res 2(1): 501-518

55 Kim N H, Kim S W, (1996) Geometrical tolerances: improved linear approximation of least squares evaluation of circularity by minimum variance. Int. J Machine Tools Manuf 36(3): 355-366

56 Konda R, Rajurkar K P, Bishu R R, Guha A, Parson M, (1999) Design of experiments to study and optimize process performance. Int J Quality & Relia Manag 16(1): 56-71

57 Kovvur Y, Ramaswami H, Anand R B, Anand S, (2008) Minimum zone form evaluation using Particle swarm optimization. Int. J. Systems Technologies and Appli 4(1-2): 79-96

58 Kumar A, Kumar V, Kumar J, (2012) Prediction of surface roughness in wire electric discharge machining (WEDM) process based on response surface methodology. Int J Eng Technol 2(4): 708-719

59 Kumar K, Agarwal S, (2012) Multi-objective parametric optimization on machining with wire electric discharge machining. Int J Adv Manuf Technol 62(5-8): 617-633

60 Kumar V, Jangra K, (2016) An experimental study on trim cutting operation using powder mixed dielectric WEDM of Nimonic-90. Int J Ind Eng Computations 7(1): 135-146

61 Kuriakose S, Mohan K, Shunmugam M S, (2003) Data mining applied to wire-EDM process. J Mater Proces Technol 142(1): 182-189

62 Lai H Y, Jywe W Y, Liu C H (2000) Precision modeling of form errors for cylindricity evaluation using genetic algorithms. Preci Eng 24(4): 310-319

63 Lai J Y, Chen I H, (1996) Minimum zone evaluation of circles and cylinders, Int. J. Machine Tools Manuf 36(4): 435-451

64 Lai K, Wang J, (1988) A computational geometry approach to geometric tolerancing, Proc. 16th North Amer. Manuf. Res. Conf., University of Illinois, 376-379

65 Lee W M, Liao Y S, (2003) Self-tuning fuzzy control with a grey prediction for wire rupture prevention in WEDM, Int J Adv Manuf Technol 22(7-8): 481-490

66 Lei X, Song H, Xue Y, Li J, Zhou J, Duan M, (2011) Method of cylindricity error evaluation using Geometry Optimization Searching Algorithm. Measurement 44(9): 1556-1563

67 Li L, Guo Y B, Wei X T, Li W, (2013) Surface integrity characteristics in wire-EDM of inconel 718 at different discharge energy. Procedia CIRP 6: 221 - 226

68 Li X, Shi Z, (2009) The relationship between the minimum zone circle and the maximum inscribed circle and the minimum circumscribed circle. Preci Eng 33(3): 284-290.

69 Liao P, Yu SY (2001) A calculating method of circle radius using genetic algorithms, Metrology Transaction China, 20(7): 87-89

70 Liao Y S, Huang J T, Su H C, (1997) A study on the machining-parameters optimization of wire electrical discharge machining. J Mater Proces Technol 71(3): 487-493

71 Liao Y S, Yan M T, Chang C C ,(2002) A neural network approach for the on-line estimation of workpiece height in WEDM. J mater proces technol 121(2): 252-258

72 Lin S S, Varghese P, (1995) A comparative analysis of CMM form fitting algorithms. Manuf Rev 8: 47-58

73 Lok Y K, Lee T C, (1997) Processing of advanced ceramics using the wire-cut EDM process. J Mater Proces Technol 63(1): 839-843

74 Mahapatra S S, Patnaik A, (2007) Optimization of wire electrical discharge machining (WEDM) process parameters using Taguchi method. Int J Adv Manuf Technol 34(9-10): 911-925

75 Manna A, Bhattacharayya B, (2005) Influence of machining parameters on the machinability of particulate reinforced Al/SiC–MMC. Int J Adv Manuf Technol 25(9): 67-75

76 Manna A, Bhattacharayya B, (2006) Taguchi and Gauss elimination method: A dual response approach for parametric optimization of CNC wire cut EDM of PRAlSiCMMC. Int J Adv Manuf Technol 28(1-2): 67-75

77 Ming W, Hou J, Zhang Z, Huang H, Xu Z, Zhang G, Huang Y, (2015) Integrated ANN-LWPA for cutting parameter optimization in WEDM. Int J Adv Manuf Technol 1-18

78 Montgomery D C, (2005) Design and Analysis of Experiments. 6th edition, John Wiley & Sons, Inc., USA

79 Mukherjee R, Chakraborty S, Samanta S, (2012) Selection of wire electrical discharge machining process parameters using non-traditional optimization algorithms. Appl Soft

Comput 12(8): 2506-2516

80 Murthy T S R, (1982) A compararison of different algorithms for cylindricity evaluation. lnt J Mach Tool Des Res 22(4): 283-292

81 Murthy T S R, Abdin S Z, (1980) Minimum zone evaluation of surfaces. Int. J Machine Tool Des Re 20(2): 123-136

82 Muthu Kumar V, Suresh Babu A, Venkatasamy R, Raajenthiren M (2010), Optimization of the WEDM Parameters on Machining Incoloy800 Super alloy with Multiple Quality Characteristics,Int J Eng Scie Technol 2(5): 162-183

83 Muthukumar V, Babu A S, Venkatasamy R, Kumar N S, (2015) An Accelerated Particle Swarm optimization algorithm on parametric optimization of WEDM of Die-Steel. J Insti Engineers : Series C 96(1): 49-56

84 Nash S G, Sofer A, (1996) Linear and Nonlinear Programming. McGraw-Hill, New York.

85 Newton T R, Melkote S N, Watkins T R, Trejo R M, Reister L, (2009) Investigation of the effect of process parameters on the formation and characteristics of recast layer in wire-EDM of Inconel 718. Mater Scie Eng A 513: 208-215

86 Pasam V K, Battula S B, Madar Valli P, Swapna M, (2010) Optimizing Surface finish in WEDM using the Taguchi parameter design method, J Braz Soci Mechan Scie Eng 32(2): 107-113

87 Patel M R, Barrufet M A, Eubank P T, DiBitonto D D, (1989) Theoretical models of the electrical discharge machining process-II: the anode erosion model. J Appl Phy 66(9): 4104-4111

88 Patowari P K, Saha P, Mishra P K, (2010) Artificial neural network model in surface modification by EDM using tungsten-copper powder metallurgy sintered electrodes. Int J Adv Manuf Technol 51(5-8): 627-638

89 Pawar P J (2011) Multi-objective optimization of wire electric discharge machining process using shuffled frog leaping algorithm. Int J Manuf Technol Indust Eng 1(1): 43-47

90 Portman V T, Rubenchik Y L, Shuster V G, (2002) Statistical approach to assessments of geometrical accuracy. CIRP Ann - Manuf Technol 51(1): 463-466

91 Prasad D V S S S V, Krishna A G, (2009) Empirical modeling and optimization of wire electrical discharge machining. Int J Adv Manuf Technol 43(9-10): 914-925

92 Qui H, Li Y, Cheng K, Li Yan, (2000) A practical evaluation approach towards from deviation for two-dimensional contours based on coordinate measurement data. Int J

Machine Tools Manuf 40(2): 259-275

93 Radhakrishnan S, Ventura J A, Ramaswamy S E, (1998) The minimax cylinder estimation problem. J manuf syst 17(2): 97-106

94 Rajabioun R (2011) Cuckoo optimization algorithm. Appl Soft Comput 11(8): 5508-5518

95 Rajurkar K P, Pandit S M, (1984) Quantitative expressions for some aspects of surface integrity of electro discharge machined components. J Manuf Scie Eng 106(2): 171-177

96 Ramakrishnan R, Karunamoorthy L, (2006) Multi response optimization of wire EDM operations using robust design of experiments. Int J Adv Manuf Technol 29(1-2): 105-112

97 Ramakrishnana R, Karunamoorthy L, (2008) Modeling and multi-response optimization of inconel 718 on machining of CNC WEDM process. J Mater Proces Technol 207(1): 343-349

98 Rao M S, Venkaiah N, (2015) Parametric optimization in machining of Nimonic-263 alloy using RSM and particle swarm optimization. Procedia Mater Scie 10: 70-79

99 Rao R V, (2011) Advanced Modeling and Optimization of Manufacturing Processes, International Research and Development, Springer-Verlag, London

100 Rao R V, Pawar P J, (2009) Modelling and optimization of process parameters of wire electrical discharge machining. Proc Inst Mech Eng Part B J Eng Manuf Eng 223(11): 1431-1440

101 Rao R V, Pawar P J, (2010) Process parameters modeling and optimization of wire electrical discharge machining. Adv Prod Eng Mater 5(3): 139-150

102 Sadeghi M, Razavi H, Esmaeilzadeh A, Kolahan F, (2011) Optimization of cutting conditions in WEDM process using regression modelling and Tabu-search algorithm. Proc Inst Mech Eng Part B J Eng Manuf Eng 225(10): 1825-1834

103 Saha P, Singha A, Pal S K, Saha P, (2008) Soft computing models based prediction of cutting speed and surface roughness in wire electro-discharge machining of tungsten carbide cobalt composite. Int J Adv Manuf Technol 39(1): 74-84

104 Samuel G L, Shunmugam M S, (2000) Evaluation circularity from coordinate and form data using computational geometric techniques. Preci Eng 24(3): 251-263

105 Sarkar S, Mitra S, Bhattacharyya B, (2006) Parametric optimisation of wire electrical discharge machining of γ titanium aluminide alloy through an artificial neural network model. Int J Adv Manuf Technol 27(5-6): 501-508

106 Sarkar S, Sekh M, Mitra S, Bhattacharyya B. (2008) Modeling and optimization of wire

electrical discharge machining of γ-TiAl in trim cutting operation. J Mater Proces Technol 205(1): 376-387

107 Sarkheyli A, Zain A M, Sharif S, (2015) A multi-performance prediction model based on ANFIS and new modified-GA for machining processes. J Intelligent Manuf 26(4): 703-715

108 Satishkumar D, Kanthababu M, Vajjiravelu V, Anburaj R, Sundarrajan N T, Arul H, (2011) Investigation of wire electrical discharge machining characteristics of Al6063/SiCp composites. Int J Adv Manuf Technol 56(9-12): 975-986

109 Scott D, Boyina S, Rajurkar K P, (1991) Analysis and optimization of parameter combinations in wire electrical discharge machining. Int J Prod Res 29(11): 2189-2207

110 Shah A, Mufti N A, Rakwal D, Bamberg E, (2011) Material removal rate, kerf, and surface roughness of tungsten carbide machined with wire electrical discharge machining. J Mater Eng Perf 20(1): 71-76

111 Shahali H, Yazdi M R S, Mohammadi A, Iimanian E, (2012) Optimization of surface roughness and thickness of white layer in wire electrical discharge machining of DIN 1.4542 stainless steel using micro-genetic algorithm and signal to noise ratio techniques. Proc Inst Mech Eng Part B J Eng Manuf Eng 226(5): 803-812

112 Shakarji C M, Clement A, (2004) Reference algorithms for Chebyshev and one-sided data fitting for coordinate metrology. CIRP Annals-Manuf Technol 53(1): 439-442

113 Shandilya P, Jain P K, Jain N K, (2012) Parametric optimization during wire electrical discharge machining using response surface methodology. Procedia Engineerin 38: 2371 – 2377

114 Shandilya P, Jain P K, Jain N K, (2013) RSM and ANN Modeling Approaches For Predicting Average Cutting Speed During WEDM of SiC p/6061 Al MMC. Procedia Eng 64: 767-774

115 Shandilya P, Jain P K, Jain N K, (2013) Study on wire electric discharge machining based on response surface methodology and genetic algorithm. Adv Mater Rese 622: 1280-1284

116 Sharma N, Ahuja N, Gupta S, Singh A, Sharma R, (2014) Modeling and parametric investigation of WEDM for D-2 tool steel using RSM and GA. Appl Mechan Mater 592: 511-515

117 Sharma N, Khanna R, Gupta R D, Sharma R, (2013) Modeling and multi response optimization on WEDM for HSLA by RSM. Int J Adv Manuf Technol 67(9-12): 2269-

2281.

118 Sharma R, Rajagopal K, Anand S, (2000) A genetic algorithm based approach for robust evaluation of form tolerances. J Manuf Syst 19(1): 46-57

119 Shunmugam M S, (1986) On assessment of geometric errors. Int J Prod Res 24 (2): 413-425

120 Shunmugam M S, Venkaiah N (2010) Establishing circle and circular-cylinder references using computational geometric techniques. Int J Adv Manuf Technol 51(1-4): 261-275

121 Singh H, Garg R, (2009) Effects of process parameters on material removal rate in WEDM. J Achievements Mater Manuf Eng 32(1): 70-74

122 Singh H, Khanna R, (2011) Parametric optimization of cryogenic-treated D-3 for cutting rate in wire electrical discharge machining, J Eng Technol 1(2): 59-64

123 Singh M K (2010) Unconventional Manufacturing Process. New Age International, New Delhi

124 Somashekhar K P, Ramachandran N, Mathew J, (2010) Optimization of material removal rate in micro-EDM using artificial neural network and genetic algorithms. Mater Manuf Process 25(6): 467-475

125 Soni J S, Chakraverti G, (1996) Experimental investigation on migration of material during EDM of die steel (T215 Cr12). J Mater Process Technol 56(1): 439-451

126 Spedding T A, Wang Z Q, (1997) Parametric optimization and surface characterization of wire electrical discharge machining process. Preci Eng 20(1): 5-15

127 Sun T H, (2009) Applying particle swarm optimization algorithm to roundness measurement. Expert Syst Appl 36(2): 3428-3438

128 Tarng Y S, Ma S C, Chung L K, (1995) Determination of optimal cutting parameters in wire electrical discharge machining. Int J Machine Tools Manuf 35(12): 1693-1701

129 Tharian B K, Kuriachen B, Paul J, Paul V E, (2015) Surface roughness optimization of wire electrical discharge machining using ABC algorithm. Appl Mechanics Mater 766-767: 902-907

130 Thomas S M, Chan Y T, (1989) A simple approach for the estimation of circular arc center and its radius. Computer Vision, Graphics and Image Processing 45(3): 362-370

131 Tosun N, (2003) The effect of the cutting parameters on performance of WEDM. KSME Int J 17(6): 816-824

132 Tosun N, Cogun C, (2003), An investigation on wire wear in WEDM. J Mater Proces Technol 134(3): 273-278

133 Tosun N, Pihtili H, (2003) The effect of cutting parameters on wire crater sizes in wire EDM. Int J Adv Manuf Technol 21(10-11): 857-865

134 Tsai T C, Horng J T, Liu N M, Chou C C, Chiang K T, (2008) The effect of heterogeneous second phase on the machinability evaluation of spheroidal graphite cast irons in the WEDM process. Mater Design, 29(9): 1762-1767

135 Tsukada T, Kanada T and Liu S (1998) The development of computer-aided centering and leveling system for cylindrical form measurement, Preci Eng 10(1): 13-18

136 Tzeng C J, Yang Y K, Hsieh M H, Jeng M C, (2011) Optimization of wire electrical discharge machining of pure tungsten using neural network and response surface methodology. Proc Inst Mech Eng Part B J Eng Manuf 225: 841-852

137 Valian E, Tavakoli S, Mohanna S, Haghi A, (2013) Improved cuckoo search for reliability optimization problems. Comput Ind Eng 64(1): 459-468

138 Venkaiah N, Shunmugam M S, (2007) Evaluation of form data using computational geometric techniques-Part I: Circularity error, Int J Mach Tools Manuf 47(7): 1229-1236

139 Vundavilli P R, Kumar J P, Priyatham C S, (2012) Parameter optimization of wire electric discharge machining process using GA and PSO. IEEE-International Conference On Advances In Engineering, Science And Management (ICAESM -2012) March 30, 31,180-185

140 Wen X, Xia Q, Zhao Y, (2006) An effective genetic algorithm for circularity error unified evaluation. Int J Mach Tools Manuf 46(14): 1770-1777

141 Whitehouse D J, (2002) Surfaces and their Measurement. Hermens Penton Ltd., London

142 Wolf P R, Ghilani C D, (1997) Adjustment Computations, Statistics and Least Squares in Surveying and GIS. John Wiley & Sons Inc, New York

143 Xu C S, (2012) Working principle and performance of wire electrical discharge machining. Adv Mater Res 507: 7147-7153

144 Yang R T, Tzeng C J, Yang Y K, Hsieh M H, (2012) Optimization of wire electrical discharge machining process parameters for cutting tungsten. Int J Adv Manuf Technol 60(1-4): 135-147

145 Yang X S, Deb S, (2009) Cuckoo search via Levy flights. In: 2009 World Congress on Nature and Biologically Inspired Computing, NABIC 2009 - Proceedings. 2009: 210-214

146 Yang X S, Deb S, (2010) Engineering optimisation by Cuckoo search. Int J Math Model Numer Optim 1(4): 330-343

147 Yu P H, Lee H K, Lin Y X, Qin S J, Yan B H, Huang F Y, (2011) Machining characteristics of polycrystalline silicon by wire electrical discharge machining. Mater Manuf Proces 26(12): 1443-1450

148 Zhang X, Jiang X, Scott P J, (2011) A reliable method of minimum zone evaluation of cylindricity and conicity from coordinate measurement data. Preci Eng 35(3): 484-489

149 Zhang, G., Zhang, Z., Guo, J., Ming, W., Li, M., & Huang, Y. (2013). Modeling and optimization of medium-speed WEDM process parameters for machining SKD11. Materials and Manufacturing Processes, 28(10), 1124-1132.

150 Zhu L M, Ding H, Xiong Y L, (2003) A steepest descent algorithm for circularity evaluation. Computer-Aided Design 35(3): 255-265

Visible Research Output

International Journals:

1. Sreenivasa Rao M and Venkaiah N, 2015. "Parametric Optimization in Machining of Nimonic-263 alloy using RSM and Particle Swarm Optimization". ***Procedia Materials Science,* 10: 70-79.**
2. Sreenivasa Rao M and Venkaiah N, "Modeling of circularity error while machining Inconel-690 using WEDM", ***International Journal of Applied Engineering Research,* 11: 3999-4006**
3. Sreenivasa Rao M and Venkaiah N, "A modified cuckoo search algorithm to optimize Wire-EDM process while machining Inconel-690", ***Journal of the Brazilian Society of Mechanical Sciences and Engineering* (Accepted with minor modifications).**
4. Sreenivasa Rao M and Venkaiah N, "Experimental investigations on surface integrity issues of Inconel-690 during WEDM process", ***Proceedings of the iMechE, Part B: Journal of Engineering Manufacture* (1st review completed).**
5. Sreenivasa Rao M and Venkaiah N, "Multi-response optimization of WEDM process in machining of Nimonic-263 super alloy", ***International Journal of Materials and Product Technology*: Inder Science (1st review completed).**
6. Sreenivasa Rao M and Venkaiah N, "Modeling of Cylindricity Error while Machining Nimonic-263 using WEDM", ***Indian Journal of Engineering & Materials Sciences* (Under review).**
7. Sreenivasa Rao M and Venkaiah N, "Application of differential evolution algorithm for parametric optimization of WEDM while machining Nimonic-263 alloy" ***International Journal of Advancements in Mechanical and Aeronautical Engineering,* 2(2): 57-61.**
8. Sreenivasa Rao M, Venkaiah N, 2013. "*Review on Wire-Cut EDM Process*", ***International Journal of Advanced Trends in Computer Science and Engineering,* 2(6): 12-17.**